INFLUENZA A VIRUS FITNESS IS LINKED WITH ANTIGENIC CHANGES IN THE HEMAGGLUTININ AND NEURAMINIDASE PROTEINS

by
Harrison Robert Powell

A dissertation submitted to Johns Hopkins University in conformity with the

requirements for the degree of Doctor of Philosophy

Baltimore, Maryland
April 2020

Abstract

Influenza virus remains a public health burden. Each year millions of people are infected and potentially thousands succumb to illness. In recent years the efficacy of the live-attenuated influenza vaccine (LAIV) has been substantially lower than the traditional inactivated influenza virus (IIV) vaccine, primarily due to the vaccine components' inability to efficiently replicate in the human nasal epithelium. The influenza Hemagglutinin (HA) receptor lies at the heart of this issue. When LAIVs are grown in eggs for production, The HA receptor of LAIV is mutated resulting amino acid changes involving critical residues in and around the HA receptor binding site. These HA receptor mutations lead to a dramatic change in the receptor-ligand binding profile, decreased replication at higher temperatures, decreased host innate immune responses to the virus and a reduced ability to infect cells present in the human nasal epithelium. All of these side effects of egg adaptation can decrease LAIV effectiveness and will persist until the process of manufacturing vaccine is significantly changed.

In recent years, the neuraminidase (NA) of human H3N2 viruses gained an n-linked glycosylation site which affected the function and antigenicity of the protein. This n-linked glycosylation on the human H3N2 NA is situated directly over the active site of the NA protein. The research herein demonstrates that this n-linked glycosylation decreases enzymatic activity by nearly 50%, decreases infectious virus production in viral growth assays, and inhibited the binding of active site-specific anti-NA antibodies. This fitness trade off, enzymatic activity and viral replication for immune evasion, is now seen in virtually all human H3N2 viruses. The once promising universal vaccine epitope found in the active site of human H3N2 NAs is now rendered useless by this universal H3N2 NA glycosylation. This dissertation serves to further our understanding of vaccine

efficacy and influenza virus evolution. Together these studies demonstrate that the HA and NA proteins of the LAIV and seasonal human influenza A viruses are major determinants of virus fitness and live vaccine efficacy.

Thesis Readers

Adviser: Andrew Pekosz, PhD	Molecular and Microbiology Immunology – JHSPH
Sabra Klein, PhD	Molecular and Microbiology Immunology – JHSPH
William Wright, PhD	Biochemistry and Molecular Biology – JHSPH
Carolyn Machamer, PhD	BCMB – SOM

Alternates

Gary Ketner, PhD	Molecular and Microbiology Immunology – JHSPH
Catherine Sutcliffe, PhD	Epidemiology – JHSPH

Acknowledgements

I would like to thank Dr. Andrew Pekosz for the guidance, support and advice he's given me during my time in his lab. When I joined Andy's lab, I had very limited knowledge in virology or microbiology. For the past four years Andy has taught me an incredible amount of virology, worked with me in designing experiments and guided me through problems and challenges. I can't thank him enough for his mentorship during these years and being a champion of my professional development. The lab members along the years in Andy's lab have also been so helpful to me in personal and professional development. Katherine Fenstermacher (dad mom) and Katy Shaw-Saliba (mom mom) adopted me as a son on day one and continue to be great friends to this day. Additionally, the labs of Dr. Sabra Klein and Dr. Kim Davis have been tremendously supportive in their feedback in tuning presentations and experiments as well. It takes a lot of time and effort to take a finding and develop it into a project and manuscript, and their feedback and support has been invaluable.

I'd also like to thank the various members of my thesis committee and oral exam committee for their support and mentorship. Dr. Carolyn Machamer, Dr. William Wright, Dr. Gary Ketner, Dr. Sabra Klein and Dr. John Nicholas guided this dissertation for the past few years and helped me refine experiments, focus on important questions and develop strong narratives about results. Gail O'Connor has also been a crucial person in graduating. Gail is tireless in assisting me and other PhD candidates in hitting deadlines, submitting paperwork and getting everything in order for graduation. I'd like to thank Gail for her support over the years in helping me graduate, because I wouldn't have been able to do this without her.

Coming to Baltimore and not knowing a single person, I've made a lot of friends along the way. To name a few- Jim, Brendan and Payam have been the boyos since day 1. Roommates and friends for life, love you guys like brothers. Matt, Adrianna, Ian and all the other Baltimore friends. Thank you for being my friend and bringing me into the group. Tom and Cody, you guys are ok too.

To my amazing girlfriend Becca- the last few months of any thesis submission is stressful and I couldn't have done it without you. We've had date nights, movie nights and walks around the city just to relax and clear our minds. Even if we can't agree on what sports teams to support, your care and support have been crucial to my success. You are an amazing person and I'm so happy I met you. I can't wait until you're finishing up your PhD and I can offer the support and help as much as you've given to me. A special shout out to your cats Loki and Odin, as much as they can be a menace in the early hours of the morning, they feel like part of my family now and I'm grateful you let me you help adopt Odin this year.

And finally, I want to thank my family for their love and support at home in Massachusetts. Mom, Dad and Steve (and Sam and Ollie!) none of this would have been possible without you. Your love and support and constant checking in about how I'm doing in Baltimore and asking about my research has helped me at every step of the way. The care packages and stuffing my bags with food and treats when I head back to Baltimore always help Mom!

Table of Contents

Abstract ii
Thesis Readers iii
Acknowledgements iv
Table of Contents vi
List of Tables xi
List of Figures xii
List of Abbreviations xiv

CHAPTER 1: Introduction 1

Background 2
General Influenza Virus Biology 2
Influenza Entry into Host Cells 3
Influenza Genome Replication and Transcription 4
Influenza Particle Assembly 5
Influenza A Hemagglutinin Protein 8
Influenza A Neuraminidase Protein 10
Balanced Activity of Influenza HA and NA Proteins 12
Traditional Inactivated and Live Influenza Vaccines 14
Figures 19

Egg Adaptation Associated Receptor Changes in Live Attenuated Influenza Virus Decrease Viral Replication in Human Nasal Epithelial Cell Cultures 21

Abstract 22
Introduction 23
Materials and Methods 25
Cell Lines and Primary Cells 25
Plasmids 25
Recombinant Virus Production 26
Virus seed and working stocks 27

Partially Purifying Virus Particles 27
Labeling Partially Purified Virus Particles 28
Consortium for Functional Glycomics Glycan Array 28
Low-MOI Infections 28
Basolateral IFN-λ Analysis 29
Plaque Assay 29
$TCID_{50}$ 30
Flow Cytometry 30
Primary Antibodies 31
Secondary Antibodies 31
Statistical Analysis 31
Results 31
Discussion 36
Figures and Tables 40

CHAPTER 3: Novel Neuraminidase glycosylation genotype in clade 3c.2a H3N2 2014-2015 isolates impacts viral growth on human nasal epithelial cells and neuraminidase function 57

Abstract 58
Introduction 59
Materials and Methods 61
Cell Lines and Primary Cells 61
Plasmids 61
Transient Transfection for NA-Flag expressing cells 61
SDS-PAGE and Western Blotting 62
Immunoprecipitation and PNGase F treatment 62
Primary Antibodies 63
Secondary Antibodies 63
Influenza H3N2 Database Sequence Analysis 63
Virus Isolation 64
Virus Working Stock Generation 64

Plaque Assay 65
Low-MOI Infections 65
$TCID_{50}$ 66
NA-*Star* Assay 66
Enzyme Linked Lectin Assay 66
Statistical Analysis 68
Results 68
Discussion 71
Figures and Tables 75

CHAPTER 4: A neuraminidase glycosylation in H3N2 clade 3c.2a impacts virus growth on human nasal epithelial cells, neuraminidase activity, and inhibitory antibody binding 82

Abstract 83
Introduction 84
Materials and Methods 86
Cell Lines and Primary Cells 86
Plasmids 87
Recombinant Virus Production 88
Plaque Assay 89
Virus Seed and Working Stocks 90
Low-MOI Infections 90
$TCID_{50}$ 91
Transient Transfection for NA-Flag expressing cells 91
NA Antibodies 91
Secondary Antibodies 92
Human Serum 92
Flow Cytometry 92
Partially Purifying Virus Particles 93
PNGase, SDS-PAGE and Western Blotting 93
NA-*Star* Assay 94
Enzyme Linked Lectin Assay 94

NA-Fluor Assay 96
NA Neutralizing Antibody Assay 96
NA Neutralizing Antibody Virus Replication Assay 96
Statistical Analysis 97
Results 97
Discussion 103
Figures and Tables 108

CHAPTER 5: Novel HA and NA Glycosylations of H3N2 viruses Impacts Fitness but not HA/NA Balance 118

Abstract 119
Introduction 120
Materials and Methods 121
Structural Analysis 121
Cell Lines and Primary Cells 121
Plasmids 122
Recombinant Virus Production 123
Virus Working Stock Generation 123
Partially Purifying Virus Particles 124
Labeling Partially Purified Virus Particles 124
Consortium for Functional Glycomics Glycan Array 124
Low-MOI Infections 125
$TCID_{50}$ 125
Plaque Assay 126
Statistical Analysis 126
Results 126
Discussion 129
Figures and Tables 133

CHAPTER 6: General Discussion 139

Advisory Committee on Immunization Practices Has Recently Reversed Ruling in 2016-17 Which Advised Against LAIV Vaccination 140

LAIV Replication Deficiencies Impact Vaccine Effectiveness 143
Utilizing a Dual HA LAIV to Balance Egg Growth and Antigenic Stability 145
Utilizing a Cell Based Approach to Manufacturing LAIV 146
Temperature Sensitivity of Egg Adapted HA protein..... 148
PB1-F2 Protein Emergence with 245 NA Gly+ Isolates..... 149
Identifying the Mechanism that 245 NA Glycosylation Impacts Viral Replication..... 151
Addressing the Ability of 245 NA Gly +/- Proteins to Cleave Sialic Acid from Respiratory Mucins 152
Addressing Recent NA Protein Specificity for Sialic Acid Containing Ligands..... 153
Neuraminidase Immunity Can Still be Utilized as a Universal Vaccine..... 154
Identifying Antigenic Epitopes of H3N2 neuraminidase protein and NA Immunity... 155
Neuraminidase Immunity and Antigenic Sin 157
Evaluate NA Antibodies Contribution to Antibody Dependent Cellular Cytotoxicity (ADCC) 158
Conclusion..... 159
References..... 161
Curriculum Vitae..... 207

List of Tables

Table 2.1: WT HA A/Victoria/361/2011 CFG synthetic glycan array binding data 46

Table 2.2: EA HA A/Victoria/361/2011 CFG synthetic glycan array binding data 47

Table 2.3: 2,3 EA HA A/Victoria/361/2011 CFG synthetic glycan array binding data 48

Table 2.4: Synthetic glycan array structure ID 56

Table 3.1: Amino acid differences between A/Bethesda/55/2015 (245 NA Gly+) and A/Columbia/41/2014 (245 NA Gly-) used for isolate characterization 81

Table 4.1: Enzyme kinetics of 245 NA Gly- and 245 NA Gly+ viruses 116

Table 4.2: Serum samples and 50% NAI values in ELLA Assay 117

Table 5.1: HA 158 Gly- CFG synthetic glycan array binding data 137

Table 5.2: 158 Gly+ HA CFG synthetic glycan array binding data 138

List of Figures

Figure 1.1: IAV Particle 19

Figure 1.2: IAV Life Cycle 20

Figure 2.1: 3D modeling of A/Victoria/361/2011 HA proteins 40

Figure 2.2: Glycan array analysis of recombinant LAIV's with different HA proteins 42

Figure 2.3: Replication of recombinant H3N2 LAIV viruses in MDCK cell cultures 43

Figure 2.4: Replication of recombinant H3N2 LAIV viruses in hNEC cultures 44

Figure 2.5: Tropism of LAIV in hNEC Cultures 45

Figure 3.1: Emergence of 245 NA Gly+ genotype in human isolates and utilization of the putative 245 NA Glycosylation site. 75

Figure 3.2: Replication of clinical isolate H3N2 viruses with or without 245 NA glycosylation in MDCK, MDCK-SIAT1, or hNEC cultures 78

Figure 3.3: Neuraminidase activity of H3N2 clinical isolates that differ in 245 NA glycosylation status 79

Figure 4.1: Replication of recombinant H3N2 viruses in MDCK-SIAT1, MDCK or hNEC cultures with or without 245 NA glycosylation 108

Figure 4.2: Binding of neuraminidase inhibitory antibodies to cells expressing NA Gly+/- proteins 110

Figure 4.3: Effect of 245 NA glycosylation on neuraminidase activity 111

Figure 4.4: Effect of inhibitory antibodies and human serum on NA enzymatic function ELLA and NA Star. 114

Figure 4.5: Effect of neuraminidase activity inhibiting antibodies on virus growth 115

Figure 5.1: Structure of A/Bethesda/55/2015 HA trimer with or without 158-160 glycosylation used in recombinant virus preparation 133
Figure 5.2: Glycan array analysis of two recombinant H3N2 viruses with different HA proteins 134
Figure 5.3: Replication of recombinant H3N2 viruses in MDCK cell cultures 136

List of Abbreviations

Abbreviation	Meaning
2,3 EA	2,3 Egg Adapted
ACIP	Advisory Committee on Immunization Practices
ADCC	Antibody Dependent Cellular Cytotoxicity
CD4	Cluster of Differentiation 4 (T cells)
CDC	Center for Disease Control
CEIRS	Centers of Excellence for Influenza Research and Surveillance
CFG	Center for Functional Glycomics
CM	Complete Media
CVV	Candidate Vaccine Virus
EA	Egg Adapted
ELLA	Enzyme Linked Lectin Assay
ER	Endoplasmic Reticulum
Gly	Glycosylation, i.e. 245 Gly+ means this protein has a glycosylation
HA	Hemagglutinin
HEK293T	Human Embryonic Kidney 293T
hNEC	Human Nasal Epithelial Cells
HPI	Hours Post Infection
IAV	Influenza A Virus
IFN	Interferon
IgA	Immunoglobulin A
IgG	Immunoglobulin G
IM	Infection Media
L.O.D.	Limit of Detection
LAIV	Live, Attenuated Influenza Virus
M	Matrix Gene
M1	Matrix Protein 1
M2	Matrix Protein 2
MDCK	Madin-Darby Canine Kidney
MDCK-SIAT1	Madin-Darby Canine Kidney sialyltransferase-1
MOI	Multiplicity of Infection
mRNA	Messenger Ribonucleic Acid
NA	Neuraminidase
NEP	Nuclear Export Protein
NP	Nucleoprotein
NS	Non-Structural Gene
NS1	Non-Structural Protein 1
NS2	Non-Structural Protein 1 (NEP)
PA	Polymerase Acidic
PB1	Polymerase Basic 1
PB2	Polymerase Basic 2
PBS	Phosphate Buffered Saline
PBS+	Phosphate Buffered Saline with Calcium and Magnesium
PDB	Protein Data Bank

RNA	Ribonucleic Acid
RT-PCR	Reverse Transcriptase Polymerase Chain Reaction
SD	Standard Deviation
SEM	Standard Error of Mean
TCID50	Tissue Culture Infectious Dose 50
vRNA	Viral Messenger Ribonucleic Acid
vRNP	Viral Ribonucleoprotein
WHO	World Health Organization
WT	Wild Type

CHAPTER 1: Introduction

Background

General Influenza Virus Biology

Influenza viruses are members of the Orthomyxoviridae family of viruses; a family that to date includes four genera of influenza viruses (A, B, C and D)[1, 2]. Influenza A viruses (IAV), the focus of this dissertation, are a major public health concern primary because of hospitalizations, economic loss and death due to IAV infection [3].

The influenza A genome consists of eight separate, self-replicating segments. The genome is a negative sense single stranded ribonucleic acid (RNA) genome. Each segment encodes for at least one protein, and some segments (matrix, non-structural, polymerase basic 1) encode for multiple spice variants. Together, the IAV genome encodes for 10-14 proteins depending on the specific subtype [1, 4-8]. The IAV particle is enveloped, with the membrane being derived from the host cell during viral budding. IAV particles are either spherical or membranous depending on the subtype. The IAV viral envelope is studded with viral proteins, two of which are heavily glycosylated. These proteins, hemagglutinin (HA), neuraminidase (NA) and matrix protein 2 (M2) function in entry, attachment and uncoating of the genome. Within the viral envelope, IAV matrix protein 1 (M1) coats the luminal surface of the viral lipid membrane (Figure 1.1) [9-14]. The core of the virion contains the eight self-replicating segments. Each viral genomic segment is coated in viral nucleoprotein (NP) and is anchored at the 5' and 3' end by the polymerase complex (vRNP). The IAV polymerase complex is a heterotrimer complex consisting of the polymerase acidic (PA), polymerase basic 1 (PB1) and polymerase basic 2 (PB2) (Figure 1.1) [15-20]. Each polymerase unit in complex with a viral genomic segment replicates independently of other segments. The viral non-

structural protein 2 (NS2) is found within the viral particle as well, and facilitates movement of the vRNP into and out of the host cell nucleus [19].

Influenza Entry into Host Cells

IAV primarily infects airway epithelial cells [21, 22]. The receptor for IAV, the HA protein, binds to sialic acid on host cells to initiate infection. Sialic acid is the last sugar present on host cell N-linked glycans suitable for HA receptor binding and entry. Sialic acid is the common name for a group of nine carbon sugars named neuraminic acid. The most common neuraminic acid, and the accepted HA receptor ligand is N-acetyl neuraminic acid (Neu5Ac). In all species infected by IAV, the HA receptor binds to two major types of Neu5Ac, “α2,6 SA” or “α2,3 SA”. Where α2,6 or α2,3 refers to the Neu5Ac carbon-carbon linkage to the penultimate sugar in the glycan, typically galactose [23]. The α2,6 vs α2,3 for Neu5ac linkages dictate IAV host tropism. Human IAVs canonically use the α2,6 sialic acid receptor ligand and avian influenza viruses canonically use the α2,3 sialic acid receptor ligand [21, 22, 24, 25]. The type of sialic acid linkage is an important barrier to infection for human or avian IAVs. Additionally, as discussed later, IAV HA using an α2,6 vs α2,3 Neu5ac linkage is an important consideration when human vaccine candidate viruses are passaged through embryonated hen’s eggs during vaccine manufacturing.

Once the HA receptor binds the sialic acid, the virus particle enters the host cell through the endocytic pathway or through the micropinocytosis pathway [26-28]. Within the endosome, the pH of endocytic vesicles drops to a pH of 5 to 5.5 [11, 26, 27, 29]. This pH lowering event is critical to the IAV particle to initiate a number of downstream effects. Influenza HA protein is a type I fusion protein with the fusion peptide (a hydrophobic peptide capable of inserting into the host cell membrane) buried within the

HA structure [27, 30-33]. Once the pH of the endosome lowers, the HA protein undergoes a conformational change which exposes the fusion peptide of the HA protein. This allows the viral membrane and the host endosome to fuse. Additionally, the low pH environment of the endosome allows the viral M2 protein to acidify the inside of the viral particle. This allows the release of vRNPs into the cytoplasm by releasing vRNPs that are bound to viral M1 within the viral protein [14, 28, 34-36]. Once the viral membrane has fused with the host endocytic vesicle and the vRNPs have released from the viral particle, the vRNPs are free to move about the host cell and initiate genome replication, transcription and ultimately translation of viral proteins (Figure 1.2).

Influenza Genome Replication and Transcription

After vRNP complexes are released into the host cell cytoplasm, the vRNP complex must enter the nucleus to replicate and transcribe the genomic material. This is accomplished by utilizing the host cell importins which bind to nuclear import signals present on the viral nucleoprotein [37-39]. All eight segments of IAV enter the nucleus and begin transcription and replication of the genome.

Influenza A genome replication is performed via a copy RNA intermediate. The polymerase complex accomplishes this partly due to the 5’ and 3’ end of each segment and numerous secondary structures to self-prime polymerase activity and induce production of copy vRNA. Recent studies have shown that adenine triphosphate and guanine triphosphate bound to the vRNA in the vRNP complex and initiate transcription of the copy RNA as sort of a priming event [1, 37, 40, 41]. As copy RNA is being transcribed, it binds to free nucleoprotein within the nucleus and the polymerase complex to form a new vRNP complex [1, 15, 37]. At this point, the copy RNA bound to vRNP can initiate transcription of vRNA, which will be packaged in the viral particles.

The IAV polymerase complex is an RNA dependent RNA polymerase with no functional proof reading exonuclease mechanism, meaning that in approximately every 10,000 nucleotides transcribed one will be an incorrect base pair [42, 43]. Considering the IAV genome is approximately 13,200 nucleotides in total, each progeny virion will, on average, have one incorrectly copied nucleotide. While a considerable amount of these mutations could be deleterious, synonymous or occurring outside the open reading frame of each segment, a small amount of mutations will incur a fitness benefit to the virus. Furthermore, an infected cell can product over one million infectious particles, it's clear that the process of error prone genome replication allows IAV to quickly adapt to new hosts and immune pressure by continually altering the amino acid sequence of all eight segments at random [7, 42, 43]. The vRNP complex exits the nucleus via binding to another viral protein, NEP, which facilitates recruitment of host cell exportins. Once free of the nucleus, vRNPs are moved to the plasma membrane via microtubules, where they are packaged in a budding influenza virus [7].

Influenza Particle Assembly

Freshly transcribed viral mRNAs are produced and exported from the nucleus, undergoing splicing if necessary, and then bind free ribosomal units found in the host cell cytoplasm. Influenza A viral mRNAs are similar to host mRNAs in structure (containing both a 5' cap and 3' poly A tail) and as such the translation of protein is similar to translating host cell proteins. Out of the eight segments in IAV, five are synthesized in the cytoplasm by free ribosomes and will traffic in the cytoplasm and into the nucleus of the cell. The other three proteins, NA, HA and M2 are transmembrane proteins and require a different mechanism of translation. When a viral mRNA encoding an influenza transmembrane protein binds a free ribosomal subunit, the ribosome-

mRNA complex is directed to the cellular endoplasmic reticulum (ER) as is the case for normal cellular transmembrane proteins. This targeting event is directed by the transmembrane domain, a sequence of hydrophobic amino acids, in the case of NA and M2 [7, 44]. The HA protein has a cleaved signal peptide that facilitates trafficking to the ER [7, 44]. Peptide synthesis occurs through a translocon protein in the ER membrane, allowing the growing peptide chain for HA, NA and M2 to enter the lumen of the ER [7].

Within the lumen of the ER a variety of post translational processing events take place for the three transmembrane proteins. The HA and NA contain a number of N-linked glycans, which are added by host cell oligosaccharyltransferases to the amino acid sequence N-X-T/S in the viral protein. Where X can be any amino acid besides proline. These N-glycosylations are added as a high mannose residue in the ER of the host cell and modified as the protein travels through the Golgi complex of the cell [45, 46], typical of normal n-linked glycosylations. Additionally, the HA and NA proteins exists at homotrimer and homotetramer proteins, respectively, on the influenza viral envelope. These are assembled within the ER and cysteine disulfide exist between monomers of each protein and within individual protein chains to hold the tertiary and quaternary structures together. The M2 protein of IAV does not have canonical N-linked glycosylation sites but does contain cysteine disulfide bonds [1, 7, 47, 48].

To assemble the influenza A particle, all components must meet at the apical plasma membrane. In the cytoplasm, vRNP complexes are trafficked to the apical plasma membrane via the host cell exocytic pathway. At the apical surface, M1 binds the host plasma membrane to vRNP complexes [1, 7, 49-51].

Hemagglutinin, NA and M2 proteins are embedded within the apical plasma membrane and congregate within lipid rafts and Influenza particles are rich in cholesterol [52-54]. On the viral surface, the distribution of HA and NA is not completely random. Clusters of NA proteins surrounded by HA or single NA proteins surrounded by HA proteins have been observed. The significance of such is not completely understood but might allow the virus to efficiently move through mucin rich respiratory epithelial tracts [55-57]. In order to complete the influenza particle, cytoplasmic vRNPs must reach the apical surface and interact with the cytoplasmic tail of these three transmembrane influenza proteins. Particle formation and viral budding is orchestrated through the M2 ion channel protein, partly because M2 is a membrane bending protein. M2 contains an alpha helix with hydrophobic amino acids that extend into the hydrophobic core of the plasma membrane lipid bilayer [58, 59]. Membrane bending leads to membrane scission, and particle formation.

As the influenza particle is formed and released from the cell, the neuraminidase protein is required for complete viral release. Influenza HA proteins bind sialic acid present on both host and cell proteins, and without NA activity the viral particle will not effectively bud from the cell, resulting in numerous viral particles stuck to the cell surface. Neuraminidase activity removes sialic acid ligands from both host and viral glycoproteins preventing the HA protein from binding to viral particles and host cell glycoproteins [60, 61]. In the presence of NA inhibitor or mutant NA function, influenza viral particles are formed but not released from the cell surface which effectively stops viral spread throughout tissue [62, 63]. In the human nasal epithelium, the site of seasonal influenza viral replication, viral movement from cell to cell involves

neuraminidase cleaving decoy sialic acid receptors from mucins and viral particles traveling through respiratory mucins. When the viral particle reaches another epithelial cell, the viral life cycle is initiated once again.

Influenza A Hemagglutinin Protein

The IAV HA exists in nature in a at least 18 different antigenically distinct groups. In humans the H3 and H1 groups currently cause seasonal illness, with H2 and an antigenically distinct additional H1 virus previously circulating. Hemagglutinin molecules are further divided into clades. Influenza HA clades are proteins with minor changes in sequence related to a common ancestor, clades are typically noted for their antigenic difference or sequence differences from one another [7, 64].

Hemagglutinin is not only a defining protein to classify influenza virus, it is the receptor for influenza virus and facilitates viral entry via binding to sialic acid present on host cells. The HA protein is a type 1 transmembrane protein, meaning the N terminus of the protein is on the outside of the viral particle and the C terminus is on the inside of the viral particle. There are two distinct regions of the HA molecule which will be discussed, the stalk region which contains the fusion peptide and the head region which contains the receptor binding domain [65, 66]. The head region is the immunodominant region of the HA, and the vast majority of humoral immunity produced during infection is directed against the HA [65, 66].

The HA protein is synthesized in ribosomes bound to the ER of the host cell. Proteolytic cleavage of the stalk is necessary for infection, HA function and freeing the fusion peptide to function [67-69]. For the seasonal human influenza virus, serine proteases (specially tryptase-like proteases) cleave the HA to proteolytically activate it. This cleavage event occurs either intracellularly or through membrane bound tryptases

[67-69]. H3N2 influenza HA has been shown to use tryptases secreted by respiratory epithelial cells, which to a certain extent dictates host cell tropism [69, 70].

During processing and export of the HA protein to the cellular surface a number of glycosylations are added to n-linked glycosylation sites in the HA protein. For the currently circulating H3N2 viruses in 2017-2018, there are seven to eight N-linked glycosylation sites depending on clade of HA [71, 72]. The majority of these glycosylation sites are present in the head of the HA molecule. When the H3N2 virus first emerged in the human population in 1968 there were seven n-linked glycosylations sites on the HA protein [7, 64]. However, only two sites were present in the head of HA. The other five potential glycosylation sites were present in the stalk region of the protein [71, 72]. As the HA protein evolves as viruses move from species to species, glycosylation sites are moved around the HA molecule as immune pressure mounts. This allows the influenza HA protein to continuously evade host immunity by shielding the immunodominant HA head region via N-linked glycosylation.

Sialic acid is the receptor for IAV, and it exists in two types. Viruses that circulate in avian populations such as migratory birds and domestic poultry bind to a sialic acid molecule in the α2,3 conformation. This nomenclature refers to the linkage of the 2^{nd} carbon on sialic acid to the penultimate sugar in the carbohydrate chain, usually galactose. Viruses that circulate in humans bind to sialic acid in the α2,6 linkage, with sialic acid covalently linked to the 6^{th} carbon which is typically galactose. This is an important barrier in transmission and determining host range. Swine influenza viruses utilize both α2,6 and α2,3 sialic acid, highlighting their importance as a vehicle to mix

human and avian influenza viruses [73-77]. Human seasonal influenza viruses prefer to bind α2,6 sialic acid. [78].

In recent years the composition of glycan attached to the sialic acid has come under focus. The Center for Functional Glycomics (CFG) routinely conducts arrays with influenza viruses to determine the sialic acid preference and type of glycan preferred by the influenza HA. There are a number of studies showing that the length, type and even shape of the glycan can dictate HA receptor preferences [79, 80]. Furthermore, two influenza viruses with a similar sialic acid binding preference can show dramatically different preferences for the underlying sugars in carbohydrate chains, suggesting that other molecules in the glycan play a role in dictating viral receptor preference [81, 82].

Influenza A Neuraminidase Protein

Neuraminidase is a mushroom shaped homotetramer viral glycoprotein, of which 9 antigenically distinct groups exist in nature. Neuraminidase is a type 2 transmembrane protein, meaning the C terminus of the peptide is on the outside of the viral particle, and the N terminus of the peptide is within the viral particle. Neuraminidase is a sialidase by nature, meaning it removes sialic acid by cleaving the linkage between sialic acid and the penultimate sugar on a carbohydrate chain [61, 83, 84]. This allows the viral particle to travel through respiratory mucins and prevents the HA receptor from binding to mucins and not the target cell. As the viral particle is being released from the infected cell, NA removes sialic acid from both host and viral glycoproteins. This prevents the HA receptor from binding to other viral particles in the vicinity or re-infecting the cell it just budded from [1, 61].

The head region of NA, which contains the catalytic enzyme region, extends outward from the virion surface. The catalytic site of neuraminidase is highly conserved

across all influenza A NA subtypes and influenza B. There are two groups of amino acids necessary for NA function. Amino acids that coordinate sialic acid in the enzyme pocket (119E, 156R, 178S, 198D/N, 222I, 227E, 274H, 277E, 294N, 425E) orient sialic acid inside the active site for the catalytic residues (118R, 151D, 152R, 224R, 276E, 292R, 371R, 406Y) to perform the enzymatic reaction [83, 84]. Most circulating human NAs are able to effectively remove either α2,3 or α2,6 sialic acid from glycoproteins, so the stringent specificity seen in comparing avian and human HA receptor preference is not seen in NA proteins. However, both N1 and N2 show an increased reactivity towards α2,3 sialic acid vs α2,6 sialic acid. Human N2 NA is roughly 3 times more active against α2,3 vs α2,6 sialic acid [61, 85-87]. This suggests that removal of sialic acid attached to mucins (α2,3 linkage) is critical for viral fitness. In certain experiments, scanning mutagenesis revealed that changing residues involved with enzymatic function or coordinating the sialic acid substrate results in a significantly decreased enzyme function and viral replication [88, 89]. These conserved residues in all influenza A and B NA proteins protein allow for pan-NA inhibitors and monoclonal antibodies to target any accessibly residues within this sequence. Viral isolates that show resistance to chemical inhibitors of NA function typically show a decreased NA activity and/or viral fitness [88, 89]. One prominent example of this is resistance seen in pre-2009 pandemic H1N1 viruses. These isolates had substantial resistance to oseltamivir, a common NA inhibitor. These isolates with this NA mutation, H274Y, had decreased replication phenotype and a decreased enzymatic activity, highlighting the trade off in being able to resist inhibitors but occurring a significant fitness disadvantage [90]. Compensatory

mutations occurred in both the HA and NA restored some aspect of viral fitness, however this resistant strain was replaced with the pandemic 2009 H1N1 event [90, 91].

Human N2 neuraminidase proteins contain between 8 and 9 N-linked glycosylation sites and there are no predicted o-linked glycosylation sequences similar to the HA protein [61, 84]. Neuraminidase glycosylations occur in the stalk to stabilize the protein and the head of the protein, which are likely shielding antigenic sites [92, 93]. The NA protein is a complex molecule and has recently re-entered the spotlight as an important antigen in developing universal influenza vaccines [26, 94-96]. Understanding how the NA protein evolves year to year will become as important as understanding HA mutations when designing vaccines, studying virus evolution and predicting pandemics.

Balanced Activity of Influenza HA and NA Proteins

Influenza virus fitness is a general term relating to the ability to infect, reproduce and spread virus to different hosts. One crucial part of this process the functional balance between the HA and NA proteins. Both influenza proteins interact with the same host molecule, sialic acid. As such, balancing the activity of each protein to this ligand is important in infectivity and release of progeny virions [97-99]. In broad strokes, an influenza particle with a balance HA/NA interaction will be able to travel through respiratory mucins, bind to target receptor, release from the cell at the end of the viral life cycle and infect other respiratory epithelial cells [56, 97, 100]. If the HA receptor activity is too strong in relation to NA activity, the HA protein could potentially bind too strongly to respiratory mucins and not reach the target cell or not be able to bud effectively from the cell if infection is successful [98]. Alternatively, too strong of an NA protein activity in relation to the HA protein could lead to destruction of the IAV receptor

blocking initiation of infection and entry into the host cell [97-99]. There are numerous factors of the HA and NA protein that dictate this fine balance.

Numerous experiments about HA and NA function have shown that completely blocking the function of either protein results in an unfit virus. Modifying the receptor binding site of HA, creating a functional but “dead” HA protein, produces viruses which cannot infect cells [101]. On the NA side of the spectrum, numerous studies have shown that modifying the NA protein or inhibiting activity via small molecular inhibitors prevents the viral particle from infecting mucin covered epithelial cells or budding progeny virions from the apical surface of the infected cell [102]. Small molecule inhibitors of NA function (e.g., Oseltamivir and Zanamivir) inhibit NA function and prevent the virus from releasing effectively from the cell surface. Scanning electron microscopy of oseltamivir treated influenza virus infections show numerous particles on the infected cell surface, because the NA protein is not de-sialating host and viral proteins on the cell surface, causing the HA protein to bind to sialic acid ligands on the infected cell and other viral particles [103].

While these experiments show that a complete lack of either HA or NA activity effectively inhibit the influenza virus life cycle, there are numerous studies that show the HA/NA balance is more nuanced. For example, expressing NA alone or in combination with a functionally dead HA protein in a virus like particle (VLP) dramatically reduces the activity of the NA protein resulting in a 50 fold reduction in activity when testing activity with a bound substrate [104]. However, when NA is expressed alone enzymatic activity with soluble substrate is not perceptively affected. This indicates that HA plays a role in

anchoring the particle to a substrate or improving NA function via an unknown mechanism.

Pandemic events offer additional insights into the delicate HA/NA balance required for viral fitness. In many cases when an avian HA and NA, such as the pandemic 2009 H1N1 event or H5N1 isolated outbreaks, enter a human population dramatic changes in the HA and NA occur. Avian viruses use the α2,3 linkage of sialic acid and human viruses use a α2,6 sialic acid. Avian HA receptors often mutate to more efficiently use the α2,6 sialic acid receptor ligands. The NA protein also changes when viruses undergo species jumps. Highly pathogenic avian influenza viruses (i.e. H7N9 or H5N1) often have stalk deletions in the NA protein when comparing the wild aquatic bird virus isolates to domestic poultry isolates [105]. This suggests that the position of the NA enzyme due to stalk length is also critically important in determining virulence and fitness of influenza viruses. This short stalk found in avian H5N1 influenza prevents transmission between ferrets [106].

What isn't clear is how minor changes to the HA and NA proteins that occur in seasonal human influenza impact the balanced activity of HA and NA function. Human seasonal HA proteins are under constant immune pressure, and many of the antigenic epitopes that mutate season to season are near the receptor binding site of the HA protein [107, 108]. Similarly, the NA protein in recent H3N2 isolates has undergone significant changes [109]. Studying how these individual mutations impact HA and NA balance of human seasonal influenza viruses is crucial to understanding influenza virus evolution and viral fitness.

Traditional Inactivated and Live Influenza Vaccines

To prepare seasonal vaccinations, the WHO identifies candidate vaccine strains at the tail end of the one influenza season in preparation for the next influenza season. Typically conducted in February for the northern hemisphere and September in the southern hemisphere, vaccine strain selection is done at least 6 months before the start of the next season [110]. This is the first important issue with the current influenza vaccine preparation. Due to the high mutation rate of influenza and constant immune pressure from the human population, choosing a vaccine strain six months ahead of the influenza season is essentially a guessing game. There have been numerous accounts where the chosen vaccine strain no longer represents the dominant circulating virus strain the following influenza season [111-113].

Vaccine preparation has not been significantly modified in the past few decades. The HA and NA protein from circulating strains for each subtype (H3N2, H1N1 and one to two influenza B strains) are combined with a helper virus, A/Puerto Rico/8/34. The internal segments from the helper virus are adapted for egg growth and allow sufficient replication of the virus eggs, whereas human viruses potentially have issues replicated in eggs. Combining viruses can be done via classical reassortment, which is done by culturing both viruses together and selecting the right reassortment, or via reverse genetics where cells are transfected with the correct DNA plasmids [114, 115]. The resulting candidate vaccine virus (CVV) contains the HA and NA of the chosen vaccine strain and the internal segments (PA, PB1, PB2, NP, NS and M). This vaccine virus is theoretically antigenically similar to the circulating viruses and should result in a high amount of influenza virus vaccine prepared in eggs.

This high growth reassortment virus is then passaged in eggs repeatedly during vaccine preparation. Herein lies more issues with the current vaccine preparation technique. First, there have been instances where the HA and NA protein could not grow efficiently in eggs. During the 2002-03 season a H3N2 strain was identified as the dominant circulating strain and selected for the following year's influenza vaccine. This strain could not efficiently grow in eggs and as a result the previous year's strain was re-used. In this particular season, 2003-04, there was a very poor vaccine efficacy and nearly 85% of the isolated strains were not antigenically similar to the vaccine strain. Most of the viruses sequenced that year were a good match with the preferred vaccine strain that wasn't used due to poor growth in eggs [116]. An additional issue with growing influenza viruses in embryonated hen's eggs is that hen's eggs contain different sialic acid receptors compared to the human nasal epithelium. CVVs are selected for a high growth phenotype which is necessary to produce large amount of vaccine antigen. These CVVs uniformly contain egg associated mutations in the HA protein as a result. Egg associated HA mutations are typically in or around the receptor binding site of the HA protein and the result of the human isolated virus, which uses a human α2,6 sialic acid receptor, growing in an avian cell culture system which only expressed the avian receptor α2,3 sialic acid [115, 117-121]. The issue with receptor switching and associated mutations is that a number of the amino acids that change during receptor switching and egg adaptation are located in antigenic sites [76, 115, 117, 122-124]. The problem arises when the vaccine virus, which effectively grows in eggs, is no longer antigenically matched to the selected virus strain and circulating virus strains. This was the case in the 2012-13 year where the H3N2 vaccine component A/Victoria/361/2011

gained three amino acid changes (H156Q G186V and S219Y) during egg adaptation. This vaccine strain was ineffective at protecting vaccine recipients from infection and as a result this mismatch led to a poor vaccine efficacy for the H3N2 component [118]. As severe influenza seasons are continuously occurring, updating our vaccine technology or moving towards a universal vaccine will be necessary to keep pace with IAV.

In addition to the inactivated vaccine there is another live virus vaccine option currently available, the live attenuated influenza virus vaccine (LAIV). The LAIV strain is a live attenuated virus capable of infecting vaccine recipients and mimicking a mild natural infection. LAIV is produced via a reverse genetics process where the LAIV internal segments, which confer the temperature sensitive phenotype, are combined with the circulating HA and NA chosen for that vaccine season. Currently, LAIV is manufactured by MedImmune and indicated for individuals between 2 and 49 years of age. LAIV was first created by serially passaging a master donor virus, A/Ann Arbor/6/1960 in cooler and cooler temperatures [125-127]. This cold adapted virus can replicate at room temperature (25ºC), shows poor growth at physiological temperature (37ºC) and is attenuated *in vivo* replication [125, 128]. There are 6 known amino acid changes in the polymerase proteins (PA, PB1 and PB2) and one in the M2 matrix protein that contribute to this attenuation phenotype [128, 129]. The LAIV is thought to induce a strong mucosal immune response, stimulating production of nasal IgA and systemic IgG[130, 131] Additionally, unlike the inactivated flu shot, the LAIV can induce a CD4 T cell response which aids in protection against subsequent infection. Mucosal IgA, an adaptive T cell response as well as stimulating production of interferons mimicking natural infection are all reasons why LAIV is an attractive vaccine platform for

robust influenza protection [132, 133]. The LAIV vaccine has been marketed towards children and has proven safe in both immunocompetent and slightly immunocompromised child recipients, with minor virus shedding noted in both groups of children [134, 135]. LAIV has been heralded as an excellent vaccine to mimic natural infection and provide a multifaceted immune response. However, the process of producing the vaccine as well as year to year variation in strain selection impacts the vaccine production.

Many of the issues seen in the IIV (i.e., the flu shot) are amplified when considering the LAIV. In order to be an effective vaccine, LAIV must sufficiently replicate when administered to the nasal epithelium. Receptor switching that occurs during egg propagation leads to the LAIV HA receptor adopting a preference for α2,3 sialic acid, the avian receptor. LAIV must replicate in the human nasal epithelium which expresses high levels of the human α2,6 sialic acid receptor. Therefore, the egg adapted LAIV could potentially be over attenuated by utilizing an HA receptor which has a preference for the avian receptor, not the human receptor. Furthermore, as discussed before, egg adaptation can lead to an antigenic mismatch between the vaccine virus and circulating human viruses. In theory, LAIV is a superior vaccine candidate when indicated. However, the potential for an antigenic mismatch LAIV that doesn't replicate efficiently in the human nasal epithelium could lead to a severely poor performing vaccine platform.

Figures

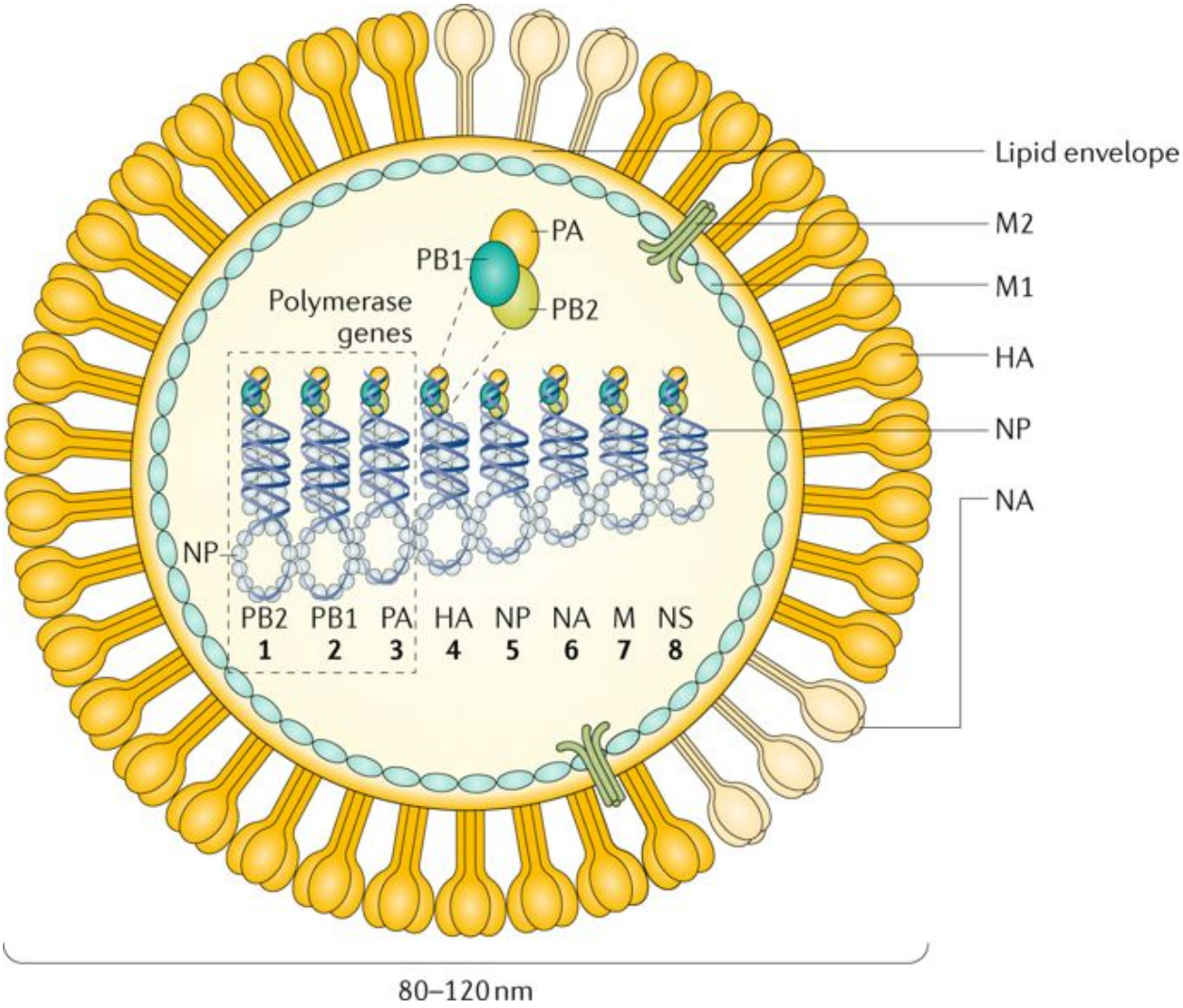

Figure 1.1: IAV Particle

Influenza particle illustrating 8 segment negative sense RNA genome. Each genomic segment is covered in NP protein with a polymerase complex (PA, PB1, PB2) attached to each viral genome segment. Luminal side of viral membrane is coated in Matrix protein M1. Influenza HA and NA glycoproteins decorate outer surface of viral particle. M2 Ion channel embedded in viral envelope. Abbreviations: PB2 Polymerase Basic 2, PB1 Polymerase Basic 1, PA Polymerase Acidic, HA Hemagglutinin, NP Nucleoprotein, NA Neuraminidase, M Matrix, NS Non-Structural. M1 Matrix Protein 1, M2 Matrix Protein 2. [136]

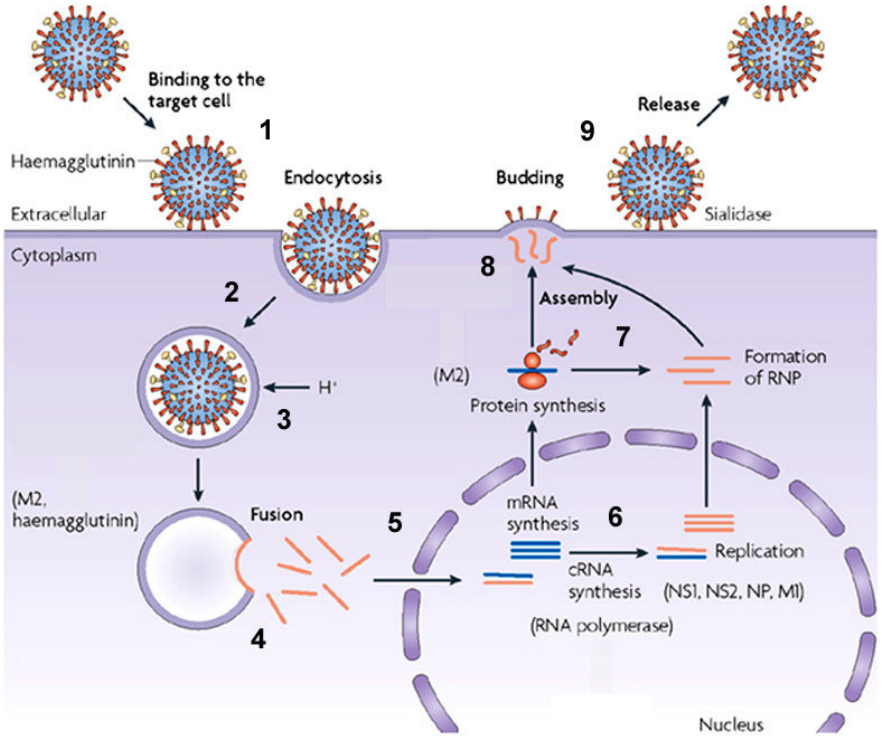

Figure 1.2: IAV Life Cycle

(1) Influenza particle attaches to host cell receptor containing sialic acid. (2) endocytosis of influenza particle. (3) After endocytosis acidification of endosome. (4) Fusion of viral membrane and host endosome membrane. M2 ion channel activity acidifies viral particle causing release of viral genome. (5) Viral genome enters nucleus through nuclear import signals. (6) Viral mRNA synthesized and viral genome replicated in nucleus. Viral mRNA leaves nucleus for translation. (7) Viral proteins translated by host cell ribosomes. vRNP complexes assembled with viral RNA genome and polymerase units. (8) Viral particle is assembled at apical surface of cellular membrane. (9) Viral particle is released due to NA activity. Image adapted from [137]

Egg Adaptation Associated Receptor Changes in Live Attenuated Influenza Virus Decrease Viral Replication in Human Nasal Epithelial Cell Cultures

Harrison Powell, Hsuan Liu, and Andrew Pekosz

Abstract

Live Attenuated Influenza Virus (LAIV) is administered as a live virus vaccine to the nasal epithelium. LAIV, which is propagated in eggs, must replicate in the nasal epithelium to induce a protective antibody titer and cellular immune reponse. Candidate vaccine strains are selected based on their ability to replicate to a high titer in eggs as well as maintaining similar antigenicity to parental viral strains. However, the process of egg propagation necessary for vaccine production can lead to mutations which alter the antigenicity of the hemagglutinin (HA) gene and receptor tropism. In the 2012-2013 northern hemisphere vaccine the H3N2 vaccine component contained three egg adaptation associated amino acid mutations in the HA gene. These mutations, H156Q, G186V and S219Y decreased vaccine efficacy for that season. Ferret anti-sera raised against the vaccine strains failed to completely neutralize circulating H3N2 viruses isolated in the 2013-2014 season. LAIVs were created using the wild-type (WT) parental HA of A/Victoria/361/2011 (WT HA LAIV), the egg adapted HA (EA HA) from the vaccine strain and an egg adapted virus with additional HA receptor amino acid changes to promote α2,3 sialic acid binding (2,3 EA HA). The WT HA LAIV preferred more α2,6 sialic (i.e., the human IAV receptor ligand) compared to the EA HA and 2,3 EA HA LAIV which both demonstrated an increased preference for α2,3 sialic acid (i.e., the avian receptor ligand). On immortalized MDCKs, the WT HA and EA HA LAIV showed similar replication at 32ºC but at 37ºC the EA HA replicated significantly less. The 2,3 EA HA LAIV replicated poorly at both temperatures. This phenotypic difference was also observed on primary human nasal epithelial cells (hNECs); the WT HA LAIV, however, induced the higher amount of IFN-λ at both 32ºC and 37ºC compared with the other viruses. Finally, the WT HA LAIV infected the greatest percentage of hNEC cells

compared to both the EA and 2,3 EA HA LAIV including a significantly higher amount of ciliated epithelial cells. These results together suggest that egg adaptation of LAIV significantly impacts virus fitness in the human nasal epithelium, and possibly result in decreased vaccine efficacy overall.

Introduction

Influenza A virus (IAV) is a member of the *Orthomyxoviridae* family of viruses. Each year IAVs infect between 10 and 20% of the world population, cause thousands of deaths and result in millions in economic loss [3]. As such, yearly vaccination is necessary to decrease the burden of influenza disease. There are several options available for annual influenza vaccination, one of which is the live, attenuated influenza virus (LAIV) vaccine. The LAIV is a cold-adapted, attenuated IAV. The LAIV strain used in the United States was first created by serially passaging of a seasonal H2N2 virus, A/Ann Arbor/6/1960 [125-128]. By repeatedly passaging this virus in cooler and cooler temperatures, the resulting virus was capable of growth at lower temperature (25ºC), but attenuated at 37ºC and 39ºC in animal models [138]. The attenuation phenotype of LAIV results in a virus that is capable of growing in the upper airway of humans, but has restricted, attenuated growth in the lower airway. Previous studies have mapped the temperature attenuation phenotype to mutations in polymerase complex (PA, PB2, PB1 and NP) as well as the matrix protein M2 [128, 129]. The mutations result in inefficient viral RNA synthesis, defective particle formation, deficient replication, and a reduced incorporation of the viral matrix M1 protein into progeny virions [138-140]. LAIV produces the same amount of viral particles at 37ºC compared to a matched wild type (WT) virus, but the ratio of infective particles to total particles is significant lower [132].

The LAIV vaccine is a 6:2 reassortment virus created by combining hemagglutinin (HA) and neuraminidase (NA) segments from circulating seasonal influenza viruses with the LAIV internal segments. This recombinant LAIV is an attenuated replication competent antigenically similar to circulating. This results in a virus that can replicate and mimic mild disease in the upper airway, stimulate an innate, humoral and cellular immune response but cannot efficiently replicate in the lower airway and cause significant disease symptoms [141, 142].

One often overlooked aspect of the LAIV vaccine is the process of manufacturing the vaccine in embryonated hens' eggs. Both the IIV and LAIV are grown in eggs, partially purified, then administered in their respective vaccine formulation [143, 144]. During egg propagation and selection of a candidate vaccine virus (CVV), the viral HA receptor accrues a number of amino acid mutation in the HA protein [122, 124]. Most of these amino changes are in the receptor binding site located in the head of HA and the receptor binding residues in HA often overlap with antigenic regions of the HA head. These amino acid changes are necessary for the CVV to replicate to high enough titers to provide a substantial amount of vaccine antigen [123, 124]. There are many noted issues with egg propagated viruses undergoing drastic antigenic changes. One notable instance was in the 2012/13 season where the H3N2 vaccine component (A/Victoria/361/2011) was antigenically mismatched from circulating viruses that season [118]. The issue lies with the intended function of LAIV, which is to replicate and mimic a natural and mild influenza infection. The virus must replicate in the human nasal epithelium to induce a robust mucosal and systemic humoral and cellular immune response. While LAIV's are historically tested for replication competence in

immortalized cells, very little research has been conducted on the ability of H3N2 LAIVs to replicate in human nasal epithelial cells and how egg adaption of the LAIV HA receptor impacts LAIV fitness and efficacy.

In this study we found that egg adaptation of the H3N2 LAIV vaccine strain for the 2012-13 season results in sialic acid receptor changes, decreased replication efficiency on human nasal epithelial cells (hNECs), decreased innate immune induction and a decreased efficiency of infecting human nasal epithelial cells. Switching receptor preference by producing the LAIV vaccine in eggs could potentially have a dramatic effect on the replication and efficiency of the LAIV vaccine platform when administered to humans.

Materials and Methods

Cell Lines and Primary Cells

Madin-Darby Canine Kidney Cells (MDCK) and human embryonic kidney cells 293T (HEK293T) were maintained in complete medium (CM) consisting of Dulbecco's Modified Eagle Medium (DMEM) supplemented with 10% fetal bovine serum, 100U/ml penicillin/streptomycin (Life Technologies) and 2mM Glutamax (Gibco). Human nasal epithelial cells (hNEC) were isolated from non-diseased donor tissue following endoscopic sinus surgery. Cells were grown, differentiated and maintained at the air liquid interface as previously described [129, 138, 145]. hNEC differentiation medium and maintenance medium was prepared as previously described [138, 142, 146]. hNEC cultures were used for low MOI growth curves only when fully differentiated. All cells were maintained at 37ºC in a humidified incubator supplemented with 5% CO_2. hNEC cultures were acclimated to 32ºC for 48 hours before infection for 32ºC infections.

Plasmids

The plasmid pHH21 was used to generate full length influenza hemagglutinin (HA) or neuraminidase (NA) plasmids for recombinant virus production. LAIV internal segments from the cold adapted A/Ann Arbor/6/1960 was used as previously described [129, 132, 138]. Briefly, viral RNA was isolated from the 2012/2013 H3N2 northern hemisphere wild type strain A/Victoria/361/2011 with a Qiagen mini-vRNA isolation kit. Gene specific primers with cloning sites for H3N2 neuraminidase or hemagglutinin were used to create cDNA via a one-step RT-PCR reaction (SuperScript III-Platinum Taq mix, ThermoFisher Scientific). The cDNA products were cut with appropriate restriction enzymes, column purified (QIAquick PCR Purification kit) and ligated with restriction enzyme cut-pHH21 using T4-ligase (New England Biolabs, NEB). To create the mutated EA and 2,3 EA plasmids, site directed mutagenesis was performed on the WT plasmid (Agilent). Three mutations were performed on the WT plasmid (H156Q, G186V and S219Y) to create the EA plasmid, per the available IVR-165 sequence [147]. To create the 2,3 EA plasmid, two further amino acid mutations were introduced via site directed mutagenesis (I226Q and S228G). All plasmids were maxi prepped and sanger sequence verified before use in recombinant virus production.

Recombinant Virus Production

Recombinant H3N2 LAIV viruses were generated using the 12-plasmids reverse genetics system as previously described [148, 149]. Briefly HEK293T cells were plated at 50% confluency 1 day before transfection in complete media. On the day of transfection, media was replaced with serum free Opti-MEM. HEK293Ts were then transfected with eight plasmids encoding full length influenza segments in the pHH21 vector (PB2, PB1, PA, HA, NP, NA, M, NS) and four plasmids encoding the influenza replication proteins in the pcDNA3.1 vector (PB2, PB1, PA and NP). At one day post

transfection 5µg/ml N-acetyl trypsin was added to the transfection reaction. MDCK cells were over-laid four hours post trypsin treatment. Every 24 hours post MDCK-overlay virus containing supernatant was sampled for virus production. Fresh Opti-MEM with 5µg/ml N-acetyl trypsin was added when a sample was taken. Virus from the transfected cell supernatants was plaque purified as described below, sequenced, and used to generate seed stocks by infecting MDCK cells at a MOI of 0.001. Working stocks were generated from sequence confirmed seed stocks by infecting MDCK cells at a MOI of .001 as described below.

Virus seed and working stocks

For generation of recombinant virus seed stocks, 250ul of plaque picked virus was added to confluent MDCK cells plated in 6 well plates and infected for 1hr as previously described [145, 150]. The plaque pick inoculum was removed and infection media (IM) was added. Infection medium (IM), consisted of DMEM with .3% BSA (Sigma), 100U/ml pen/strep (Life Technologies), 2mM Glutamax (Gibco) and 5µg/ml N-acetyl trypsin((Sigma)). Cells were placed in a 32ºC incubator and monitored daily for CPE. Seed stock was harvested between 3 and 5 days or when CPE reached approximately 75-80%. Seed stocks were then sequenced, and infectious virus titer determined via TCID50. Working stocks for each LAIV was done by infecting confluent MDCK cells in a T75 flask at a MOI of .001 for 1 hour at 32ºC. The inoculum was removed, and IM was added. Flasks were incubated at 32ºC for infection. Cells were monitored daily for CPE and working stock harvested when CPE reached approximately 75-80%. Working stocks were sequenced verified and infectious virus determined via TCID50 as described below.

Partially Purifying Virus Particles

Virus was partially purified by ultracentrifugation over a sucrose cushion for glycan array. Approximately 150ml of virus was grown for partially purifying. Clarified virus working stock supernatant was overlaid onto a 25% sucrose-NTE (100nM NaCl (ThermoFisher Scientific), 10mM Tris-HCl (Promega) and 1mM EDTA (Sigma)) buffer pH of 7.5. Virus was centrifuged at 27,000 RPM in a SW-28 rotor in a Beckman Coulter Optima L90-K UltraCentrifuge for 2 hours. After the first ultracentrifugation, the supernatant was removed. The virus pellet was re-suspended in PBS. Pellet was further concentrated by ultracentrifugation in an SW-28ti rotor at 23,000 RPM for 1hr. The pellet was resuspended in PBS for use in labelling and glycan array

Labeling Partially Purified Virus Particles

Partially purified virus particles were labeled with Alexa Fluor 488 Succinimidyl Ester per the manufacturer's instructions (Thermofisher Scientific).

Consortium for Functional Glycomics Glycan Array

To assess HA receptor specificity partially purified, whole virus particle labeled with fluorescent dye was allowed to bind to Consortium for Functional Glycomics Array version 5. synthetic glycan chip as previously described [79-82]. Labeled virus was allowed to bind to array chip for 1 hr. at room temperature, then excess was aspirated. Slides were washed three times before fluorescence analysis. The array chip was scanned with GenePix 4300A Microarray scanner then data was analyzed with GenePix Pro Microarray Analysis Software and processed via Excel spreadsheets as previously described [79-82]. Only sialic acid containing ligands were considered for analysis.

Low-MOI Infections

Low-MOI growth curves were performed at a MOI of .001 in MDCK cells and .01 in hNEC cultures. MDCK cell infections were performed as described above. After the infection, the inoculum was removed and the MDCK cells were washed three times with

PBS+. After washing IM was added and the cells were placed at 32ºC. At the indicated times post inoculation, IM was removed from the MDCK cells and frozen at -80ºC. Fresh IM was then added. For low-MOI growth curves in the presence of monoclonal antibodies, the indicated antibodies were added to the IM after the virus was allowed to attach to cells. In low-MOI hNEC growth curves, hNECs were acclimated to 32ºC or 37ºC for 48hrs before infection. The apical surface was washed three times with PBS and the basolateral media was changed at time of infection. hNEC cultures were inoculated at a MOI of .015. hNEC cultures were then placed in a 32ºC incubator for 2 hours. After inoculation, the hNECs were washed three times with PBS. At the indicated times, 100ul of IM without N-acetyl trypsin was added to the apical surface of the hNECs. The hNECs were then incubated for 5 minutes at 32ºC and the IM was harvested and frozen at -80ºC. Basolateral media was changed every 24hrs post infection for the duration of the experiment.

Basolateral IFN-λ Analysis

Secreted IFN-λ was quantified from basolateral samples taken during low MOI hNEC infections taken 24 hours post infection. The DIY Human IFN-λ I/II/III (IL-29/28A/28B) ELISA (PBL Assay Science) was used according to manufacturers' instructions. Samples were diluted 1:4 to stay within working range of the assay. Values of IFN-λ were adjusted by subtracting mock infected and plotted as picograms/ml.

Plaque Assay

MDCK cells were grown in complete medium to 100% confluency in 6-well plates. Complete medium was removed, cells were washed twice with PBS containing 2mm calcium magnesium (PBS+) and 400uL of inoculum was added. Cells were incubated at 32ºC for 1hour with rocking every 15 minutes. After 1hr, the virus inoculum

was removed and phenol-red free DMEM supplemented with3% BSA (Sigma), 100U/ml pen/strep (Life Technologies), 2mM Glutamax (Gibco) and 5μg/ml N-acetyl trypsin (Sigma) and 1% agarose was added. Cells were incubated at 32ºC for 3-5 days and then fixed with 4% formaldehyde. After removing the agarose, cells were stained with napthol-blue black. Plaque size was analyzed in Image J [151]. For recombinant virus production, virus plaques were picked with a pipette instead of fixing with formaldehyde and placed in IM and stored at -80ºC for later seed stock generation.

$TCID_{50}$

MDCK cells were seeded in a 96 well plate 2 days before assay and grown to 100% confluence. Cells were washed twice with PBS+ then 180uL of IM was added to each well. Ten-fold serial dilutions of virus was created and then 20uL of the virus dilution was added to the MDCK cells. Cells were incubated for 6 days at 32ºC then fixed with 2% formaldehyde. After fixing, cells were stained with napthol blue-black, washed and virus titer was calculated.

Flow Cytometry

hNECs were infected for 14 hours with the indicated LAIV at 32ºC. After infection, apical and basolateral surfaces were washed with PBS- twice. Cells were then detached with 1X TrypLE (Life Technologies) for 15 minutes at 37ºC. After, cells were pelleted by centrifugation. Cells were washed again with PBS- and fixed with 2% paraformaldehyde (Affymetrix) at room temperature for 15 minutes. Cells were permeabilized with .2% Tween-20 for 15 minutes at room temperature. After, cells were then incubated with blocking buffer (1% 2º species serum, .3% BSA in 1X PBS-). After blocking, cells were incubated with indicated primary antibodies, washed twice, then incubated with secondary antibodies. Each washing step was done with FACS buffer

which consisted of 0.3% BSA (Sigma) in 1X PBS-. Cells were analyzed on a BD-LSR II and data analyzed with FlowJo V10.5.3 software.

Primary Antibodies

Primary antibodies against human beta tubulin IV (Novus Bio, clone OTI3F1) Alexa Fluor 488 was used at a concentration of 0.5µg/ml to identify ciliated cells in hNEC cultures. Goat anti-Aichi H3N2 anti-serum (BEI resources) was used to identify infected cells in hNEC cultures. Serum was diluted 1:500 for use in Flow Cytometry. Rabbit anti-M1 (Genetex, cat # GTX125928) was used at a concentration of 0.5µg/ml to identify infected cells in hNEC cultures via IF microscopy.

Secondary Antibodies

Secondary antibodies were used to detect binding of primary unconjugated monoclonal antibodies or poly clonal serum. Donkey anti-Goat IgG Alexa Fluor 647 was diluted to 0.5µg/ml in flow cytometry buffer (ThermoFisher Scientific) for Flow cytometry analysis. Goat anti-Rabbit IgG Alexa Fluor 647 was used at a concentration of 0.5µg/ml in blocking buffer (ThermoFisher Scientific) for IF microscopy.

Statistical Analysis

Statistical analysis was performed using Graph Pad Prism Software (GraphPad v8.4.2). Viral growth was analyzed using two-way anova with a Bonferroni post test correction. Differences were considered significant if $p < .05$. Plaque size and infectivity in hNECs was analyzed using an unpaired t-Test. Differences were considered significant if $p < .05$.

Results

Egg-associated amino acid mutations that occur to human influenza isolates typically alter the sialic acid binding preference, due to amino acid changes in the receptor binding site (RBS) [116, 123, 124, 152-154]. To study the effect that egg

adaptation has on receptor specificity, virus replication and innate immune responses were analyzed against a panel of three recombinant LAIVs. All three HA proteins were based off of the 2012-13 northern hemisphere isolate chosen for the H3N2 vaccine component, A/Victoria/361/2011. The WT HA was cloned from the WT A/Victoria/361/2011 HA sequence. Using the WT HA, three amino acids modifications were introduced according to the EA vaccine virus, IVR-165 [147]. These amino acid mutations were H156Q, G186V and S219Y and have been previously shown to shift sialic acid binding from the human α2,6 receptor to the avian α2,3 receptor [122]. Two additional amino acid changes were introduced into the EA HA gene to make the 2,3 EA HA which we believed would bind only α2,3 sialic acid. These amino acid changes, I226Q and S228G, have been shown to shift sialic acid binding preference from α2,6 to α2,3 sialic acid in other H3 proteins [74]. This third HA protein, 2,3 EA, should theoretically have the highest amount of α2,3 sialic acid binding out of all three HA proteins used. The 3D structure with highlighted amino acid changes and RBS of each protein is shown for the WT (Fig 2.1A), EA (Fig 2.1B) and 2,3 EA (Fig 2.1C). After cloning and sequence verification, the HA proteins were combined with the neuraminidase of A/Victoria/361/2011 and the six internal segments of the cold adapted A/Ann Arbor/6/64 H2N2 strain.

These receptor variant H3N2 LAIVs were first characterized for their sialic acid binding preference using a synthetic glycan array available from the Consortium for Functional Glycomics (v5.3 array) [155]. This array contains 156 glycans that contain the human α2,6 sialic acid receptor ligand, the avian α2,3 sialic acid receptor ligands, a mixture of each, or the non-traditional 2,8 sialic acid linkage. From this array, the sialic

acid ligand preference as well as subtle preferences in sugar groups within the ligand were determined. The WT HA LAIV, having an identical HA sequence to the circulating human clinical isolate, bound to a number of α2,6 and α2,3 sialic acid ligands (Fig 2.2A, Table 2.1). Out of the top 20 highest binding glycans, 12 glycans contained the human α2,6 sialic acid ligand. Seventeen out of the 20 of the highest binding glycans contain galactose (Gal) as the penultimate sugar (Table 2.1). The EA HA LAIV, having an HA protein that has an amino acid sequence of a highly egg passaged virus, also bound to a mixture of α2,6 and α2,3 sialic acid containing ligands. However, out of the top 20 highest binding glycans, only 8 out of 20 contained the human α2,6 sialic acid ligand (Fig 2.2B, Table 2.2). There was not a significant switch in preference for other sugars in the carbohydrate chain, as 17 out of these 20 highest binding ligands contain galactose, similar to the WT HA. For the 2,3 EA out of the top 20 highest binding ligands, 7 out of 20 contained the human α2,6 sialic acid receptor ligand (Fig 2.2C, Table 2.3). The penultimate sugar for every top 20 binder was galactose for the 2,3 EA. However, 8/20 contained a fucose molecules attached to the synthetic glycan. From our glycan array analysis, we concluded that the amino acid differences between the different HA proteins did alter the glycan binding preference of each HA, but did not significantly alter the preference for other sugars in the carbohydrate ligand. The preference for fucosylated ligands of the 2,3 EA HA is interesting, but the relevance of such is unknown. Full information about all 156 sialic acid ligands used in the array can be found in Table 2.4 [155].

After determining the receptor preferences of the three LAIVs, we next tested how these receptor changes impacted viral replication in immortalized cells. Madin-

Darby Canine Kidney are routinely used immortalized cells that express both α2,3 and α2,6 sialic acid [156]. We studied viral replication using these cells at two different temperatures. First at 32ºC, the average temperature of the upper airway and the permissive temperature to LAIV replication, both the WT and EA LAIV replicated similarly with no significant difference in replication kinetics or peak virus titer. However, the 2,3 EA HA LAIV replicated poorly at this temperature, suggesting that some aspect of HA function is impacted by the additions of I226Q S228G (Fig 2.3A). At 37ºC, the temperature of the lower airway and the non-permissive attenuating temperature for LAIV, the WT HA LAIV produced the highest amount of infectious virus compared to the EA HA LAIV and the 2,3 EA HA LAIV (Fig 2.3B). Plaque appearance, morphology and size was then assessed using MDCK cells at 32ºC. Both the WT and EA LAIV produced clear, distinct plaques (Fig 2.3C) of similar size (Fig 2.3D). However, the 2,3 EA LAIV produced significantly smaller plaques compared to the WT HA LAIV (FIG 2.3C, D).

Because MDCK cells do not accurately represent nasal epithelium where LAIV (FluMist) is administered, virus replication was then tested on primary hNEC cultures. We have previously shown that hNEC cultures are an excellent model of the normal nasal epithelium and allow phenotypes to show that aren't found on MDCK cells [129, 138, 145]. We studied viral replication at both 32ºC and 37º on hNECs. The WT HA LAIV yielded a significantly higher infectious virus compared to both the EA HA LAIV and the 2,3 EA HA LAIV at both 32ºC (Fig 2.4A) and 37ºC (Fig 2.4B). In addition to low MOI growth curves, basolateral supernatant from hNEC cultures was tested for presence of interferon lambda I/II/III (IFN-λ) every 24hrs post infection. Previous studies have shown that hNECs secrete IFN-λ during infection with IAVs [142]. Correlating with

infectious virus production, the WT HA LAIV induced the highest amount of IFN-λ at 32ºC (Fig 2.4C) and 37ºC (Fig 2.4D) compared to the EA HA LAIV and 2,3 EA HA LAIV.

Human nasal epithelial cell cultures are a heterogenous mixture of cells containing ciliated epithelial cells, mucus secreting goblet cells, basal cells and other supporting cells in a pseudostratified epithelium [146, 157-162]. There is a considerable amount of information about differential sialic acid receptor expression on the various cells in hNEC cultures. Ciliated cells tend to express more α2,6 sialic acid than α2,3 sialic acid, and other cells in hNEC cultures tend to express more α2,3 sialic acid than α2,6 sialic acid [25, 75]. Using our different HA containing LAIVs with experimentally determined receptor differences, we next wanted to assess whether there was a difference in cellular tropism in hNEC culture and if this could explain the replication differences found. Human nasal epithelial cell cultures were infected with an equal amount of virus at a high MOI of 3 for 14 hours (Fig 2.5A) and then dissociated and stained for markers of cell lineage (Beta Tubulin IV, ciliated cells) and a marker of infection (H3 Anti-Serum) (Fig 2.5B). Gating strategy shown for one replicate (Fig 2.5C). We found that there was no extreme difference in cellular tropism due to receptor preference shifting. The WT HA LAIV infected a higher percentage of ciliated epithelial cells compared to both the EA HA LAIV and 2,3 EA HA LAIV (Fig 5B). However, the EA HA LAIV and WT HA LAIV infected a similar amount of non-ciliated epithelial cells suggesting that the EA amino acid changes reduce infectivity of the virus without altering cellular tropism in hNEC cultures. Overall, the WT HA infected a higher percentage of cells compared to both the EA and 2,3 EA HA LAIV (Fig 5B), likely driven by consistently infecting more ciliated epithelial cells. As expected, based on the

previous results, the 2,3 EA HA LAIV showed the least infectivity across any cell type present in hNEC cultures. These results combined with poor replication seen in MDCKs (Fig 3A-B) and hNECs (Fig 4A-B), suggest that the 2,3 EA HA LAIV has a poor HA receptor and cannot efficiently infect or replicate in either MDCKs or hNECs in culture.

Discussion

With the recent issues of the LAIV vaccine in the United States [163], this study was designed to understand how egg adaptation and the associated HA receptor amino acid mutations impact receptor specificity, viral fitness, innate immune induction and cellular tropism of an H3N2 LAIV vaccine strain. We demonstrated that egg adaptation during vaccine manufacturing significantly changes the function of the HA protein via a recombinant virus approach. Using three different HA proteins with varying amino acid mutations introduced to alter the receptor specificity (Fig 1), we tested the hypothesis that egg adaptation and altering receptor preference would decrease vaccine efficacy. Human H3N2 WT viruses typically bind to a high amount of the human α2,6 sialic acid receptor ligand [25, 75, 164-167]. There is still an appreciable α2,3 sialic acid binding of the WT HA used in this study, as many human viruses bind both α2,6 and α2,3 sialic acid [168, 169]. As expected, the EA HA receptor increased binding to the avian α2,3 receptor. Using the EA HA protein and introducing two additional amino acid mutations to further reduce recognition of α2,6 sialic acid, we showed that this 2,3 EA HA virus preferred α2,3 sialic acid over the human α2,6 sialic acid receptor ligand (Fig 2). While these results were expected and back up previous glycan array studies using A/Victoria/361/2011, they verified our hypothesis that altering HA receptor binding site amino acids would alter receptor binding preferences [122]. In addition to α2,3 vs α2,6 preference we found notable differences in the preference for penultimate sugars and

other sugar groups in the receptor ligands. Further studies into the significance of such findings is necessary, but these data suggest that HA receptor preference involves more than α2,3 or α2,6 sialic acid. We then took these viruses and conducted a number of virus fitness and cellular tropism studies to connect receptor preference differences with LAIV fitness.

On immortalized MDCK cells, both the WT and EA virus produced a similar amount of infectious virus in a low MOI growth curve at 32ºC, while both were significantly better than the 2,3 EA HA LAIV (Fig 3). At 37ºC, the WT HA LAIV produced the highest amount of infectious virus titer compared to the EA HA LAIV and 2,3 EA HA LAIV, suggesting that HA egg associated amino acid changes were contributing to the attenuation phenotype of LAIV at 37ºC. In our hNEC studies we showed that egg adaptation of the A/Victoria/361/2011 HA decreased replication at both 32ºC and 37ºC (temperature of the upper and lower respiratory tract respectively) as well as significantly decreased IFN-λ production at both 32ºC and 37ºC (Fig 4). We then found that the WT HA LAIV infected more hNECs than either the EA HA or 2,3 EA HA LAIV (Fig 5). These results suggest that the receptor changes that resulted in differential recognition of sialic acid (Fig 2) impact the ability of EA and 2,3 EA HA LAIV to infect cells in hNEC cultures. A decreased ability to infect receptor binding differences can, in part, explain the lack of infectious virus production of the EA and 2,3 EA HA LAIV in low MOI growth curves. However, further studies into the glycan composition in hNEC cultures is necessary to prove this hypothesis. At the current time, it is unknown which ligands present in the CFG synthetic glycan array 5.3 are physiologically relevant in human infections and hNEC cultures. Taken together, these results suggest that egg

adapting the HA of LAIV further attenuates the LAIV and could significantly decrease vaccine effectiveness.

The LAIV vaccine has always been heralded as superior vaccine compared to the traditional IIV. This is in part due to the fact that the LAIV induces formation of mucosal IgG and IgA antibodies, a broad T cell response and significantly more heterologous protection compared to the IIV. [170-173]. However, many H3N2 isolates that are passaged through eggs for vaccine manufacturing contain the G186V mutation, as seen in the A/Victoria/361/2011 strain used in this study [122, 124]. While this residue isn't considered an important antigenic site, it likely assists HA recognition of α2,3 sialic acid and thus contributes to the phenotypes shown here in this study [174, 175].

Because LAIV has been in use in the US and around the world, the "dogma" for IAV LAIV has always been any H3N2 or H1N1 HA and NA combination could be combined with the LAIV internal gene segment plasmids to produce an antigenic attenuated virus that protects recipients from that season's circulating influenza viruses. In 2016, the Advisory Committee on Immunization Practices (ACIP) issued a statement which resulted in the LAIV not being used for the 2016-2017 season. This was due to an ineffective H1N1 component in the previous 2015-2016 season [163]. The H1N1 component of LAIV was an antigenically similar but not identical strain to that used in the IIV. In 2015/16 IIV had much greater efficacy compared to LAIV indicating that the efficacy issues in LAIV were due to viral replication issues. Since then, the H1 HA used for the 2015/16 season has demonstrated very poor replication competency in MDCKs and human cell lines, suggesting that some aspect of egg adaptation or combining that

particular H1 HA with the LAIV internal segments is significantly decreasing viral fitness [176]. While the LAIV has been re-recommended by ACIP starting in the 2018/19 season, it's impossible to predict if a chosen vaccine strain could have the same replication issues as seen in 2015/16 H1N1 LAIV vaccine strain. LAIV is still an attractive vaccine platform even with many potential pitfalls of replication competency. Live, attenuated vaccines continue to be used to induce a robust and broadly effective immunity for many different viral infections. However, more focused research on stabilizing the HA protein during egg passaging or using an alternative substrate to grow vaccine stocks could solve antigenic mismatch and replication issues seen in LAIV.

Figures and Tables

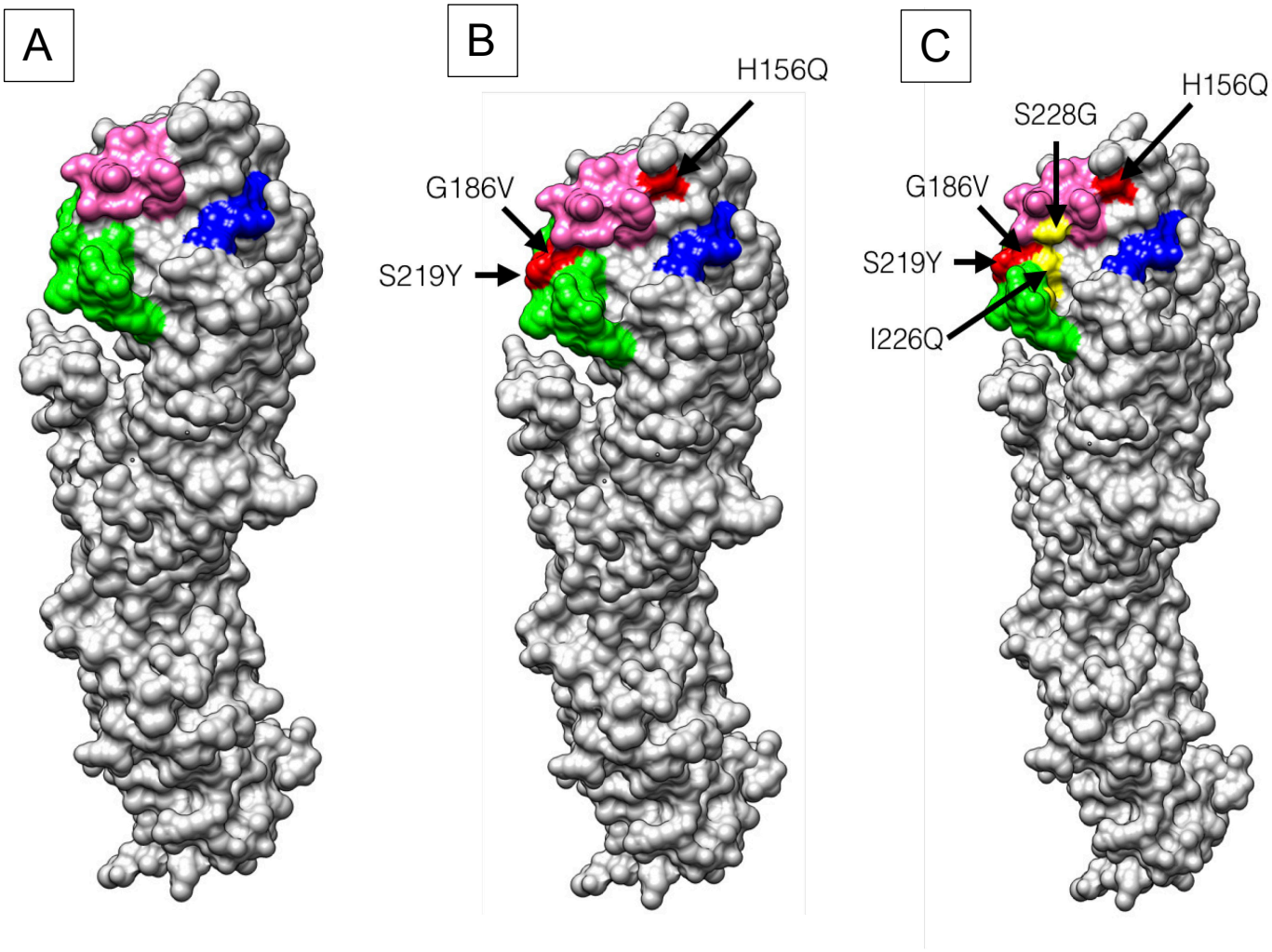

Figure 2.1: 3D modeling of A/Victoria/361/2011 HA proteins

WT A/Victoria/361/2011 HA monomer protein adapted from Protein Data Bank A/Victoria/361/2011 HA (Code 4WE9). Sialic acid binding pocket residues highlighted [174, 175, 177-179] 190 Helix in pink, 130 loop in blue and 220 loop in green. (B) Model of EA A/Victoria/361/2011 HA. Egg adaptation of A/Victoria/361/2011 during vaccine manufacturing resulted in three amino acid changes, highlighted on the structure (H156Q, G186V and S219Y). (C) Model of 2,3 EA HA. Two additional amino acid changes were added to the EA HA to shift sialic acid binding preference to α2,3 sialic acid (I226Q and S228G).

A

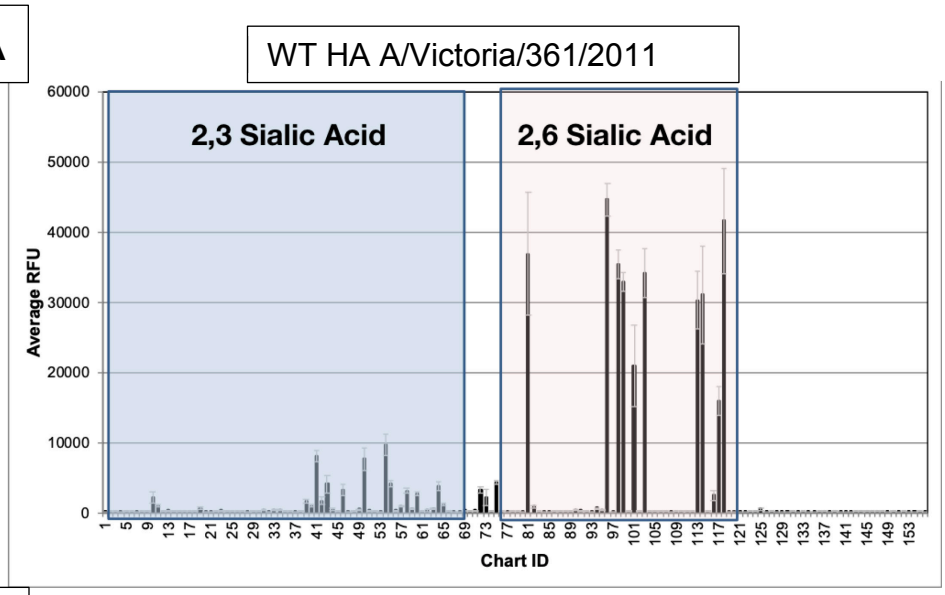
WT HA A/Victoria/361/2011
2,3 Sialic Acid
2,6 Sialic Acid
Average RFU
Chart ID

B

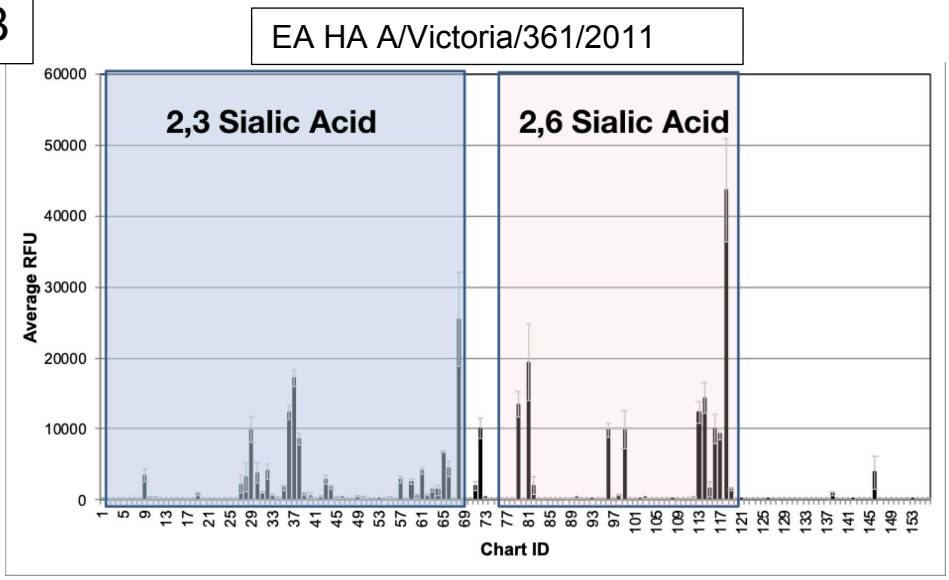
EA HA A/Victoria/361/2011
2,3 Sialic Acid
2,6 Sialic Acid
Average RFU
Chart ID

C

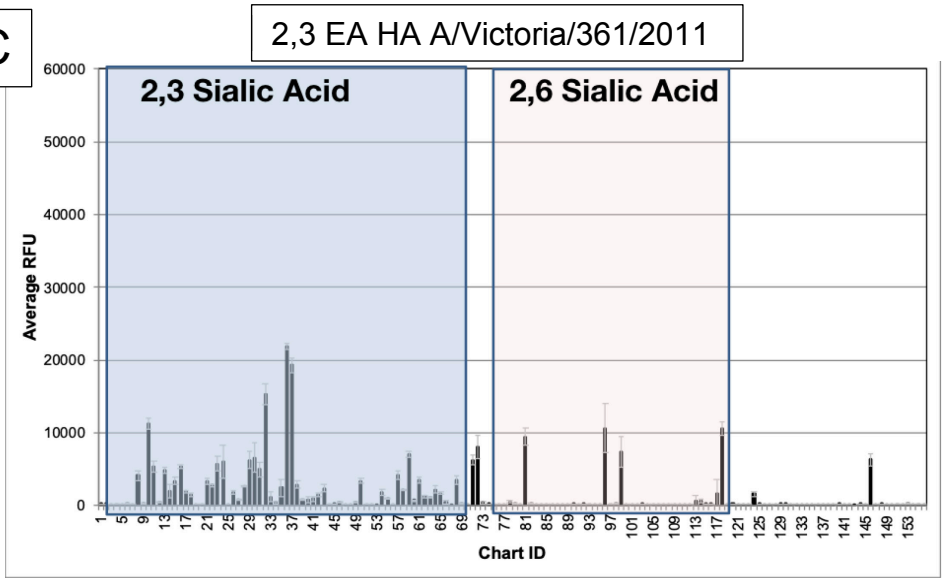
2,3 EA HA A/Victoria/361/2011
2,3 Sialic Acid
2,6 Sialic Acid
Average RFU
Chart ID

Figure 2.2: Glycan array analysis of recombinant LAIV's with different HA proteins

WT HA LAIV (**A**), EA HA (**B**) and 2,3 EA HA (**C**) were subjected to glycan array analysis. Y axis indicates raw RFU, X axis indicates specific glycan. See Tables 1-4 for information regarding chemical structure and glycan ID. α2,3 Sialic acid containing ligands in blue box (glycans 2-68) and α2,6 sialic acid containing glycans in off white box (glycans 75-118).

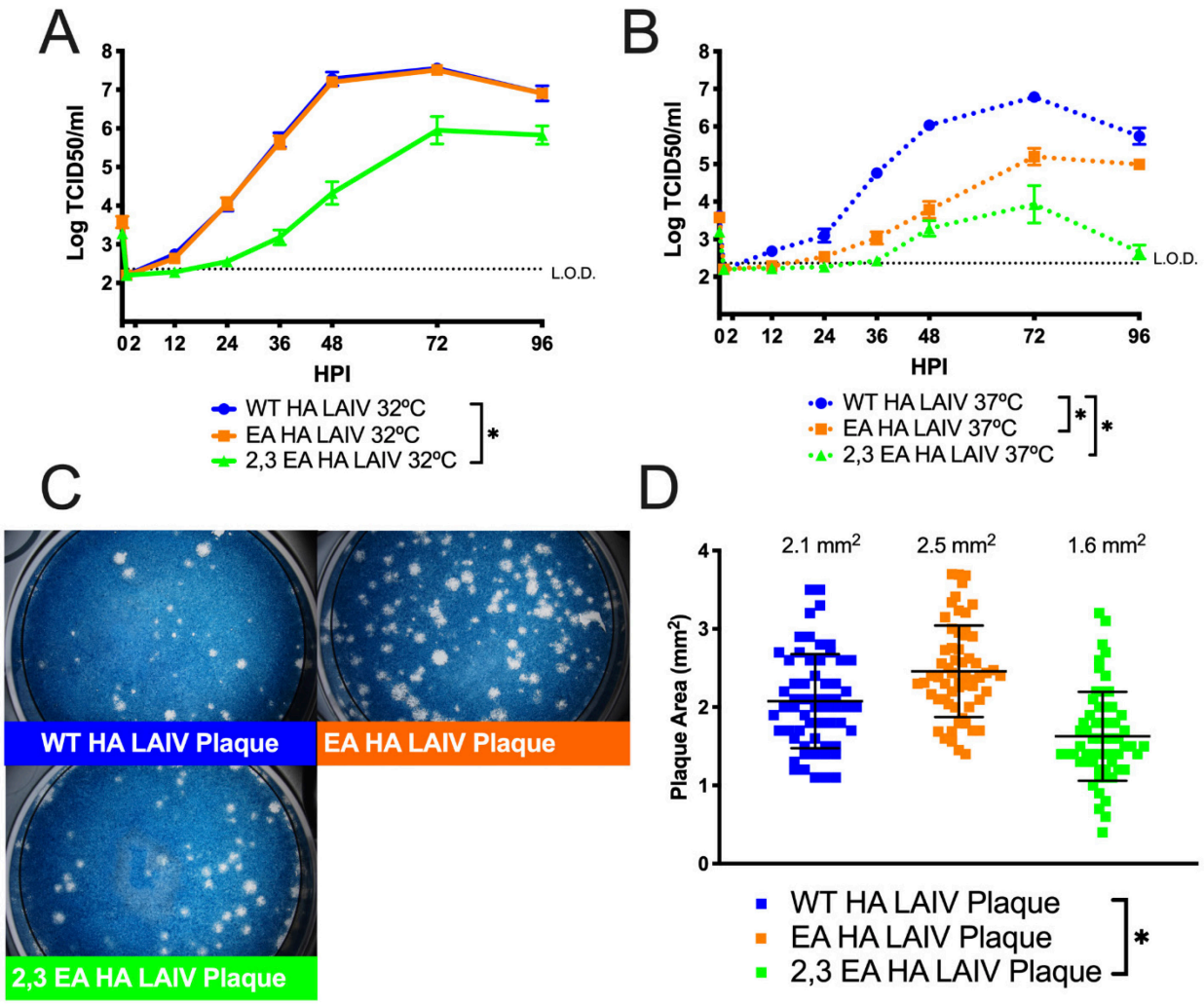

Figure 2.3: Replication of recombinant H3N2 LAIV viruses in MDCK cell cultures

Low MOI growth curves with MDCK at 32ºC (**A**) or MDCK at 37ºC (**B**) with the indicated recombinant viruses. Hours post infection (HPI) on X axis, Log of TCID50/ml on Y axis. Data are pooled from 3 independent experiments with four replicates per virus per experiment (total n = 12 wells per virus timepoint). Data were analyzed with *p<.05 and two-way repeated measures ANOVA with Bonferroni multiple comparison posttest. The limit of detection (L.O.D.) is indicated with a dotted line at log 2.37 TCID50/ml. Error bars in A and B are SEM, error bars in D are SD. (**C**) Plaque assay performed with recombinant LAIV expressing WT, EA or 2,3 EA HA proteins. (**D**) Quantification of plaque area from 30-50 individual plaques per virus from 3 independent experiments. *p<.05 unpaired T test.

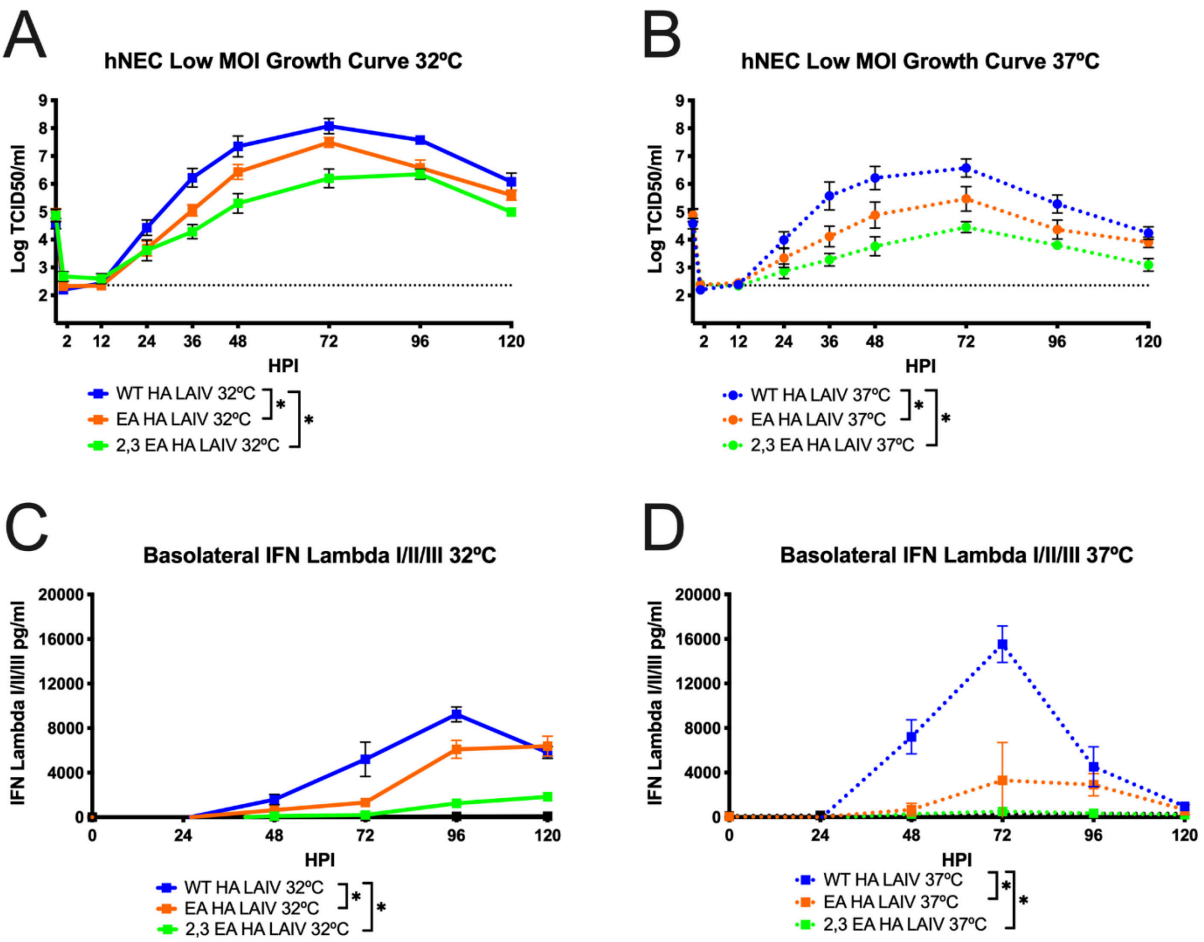

Figure 2.4: Replication of recombinant H3N2 LAIV viruses in hNEC cultures

Low MOI growth curves with hNECs at 32ºC (**A**) or hNECs at 37ºC (**B**) with the indicated recombinant viruses. Hours post infection (HPI) on X axis, Log of TCID50/ml on Y axis. Data are pooled from 2 independent experiments with four replicates per virus per experiment (total n = 8 wells per virus timepoint). Data were analyzed with *p<.05 and two-way repeated measures ANOVA with Bonferroni multiple comparison posttest. The limit of detection (L.O.D.) is indicated with a dotted line at log 2.37 TCID50/ml. Error bars in A-D are SEM. (**C**) and (**D**) Quantification of IFN-λ I/II/III at 32ºC (C) and 37ºC (D) secreted in the basolateral media of hNEC cultures. Y axis pg/ml X axis hours post infection (HPI). Data were analyzed with *p<.05 and two-way repeated measures ANOVA with Bonferroni multiple comparison posttest.

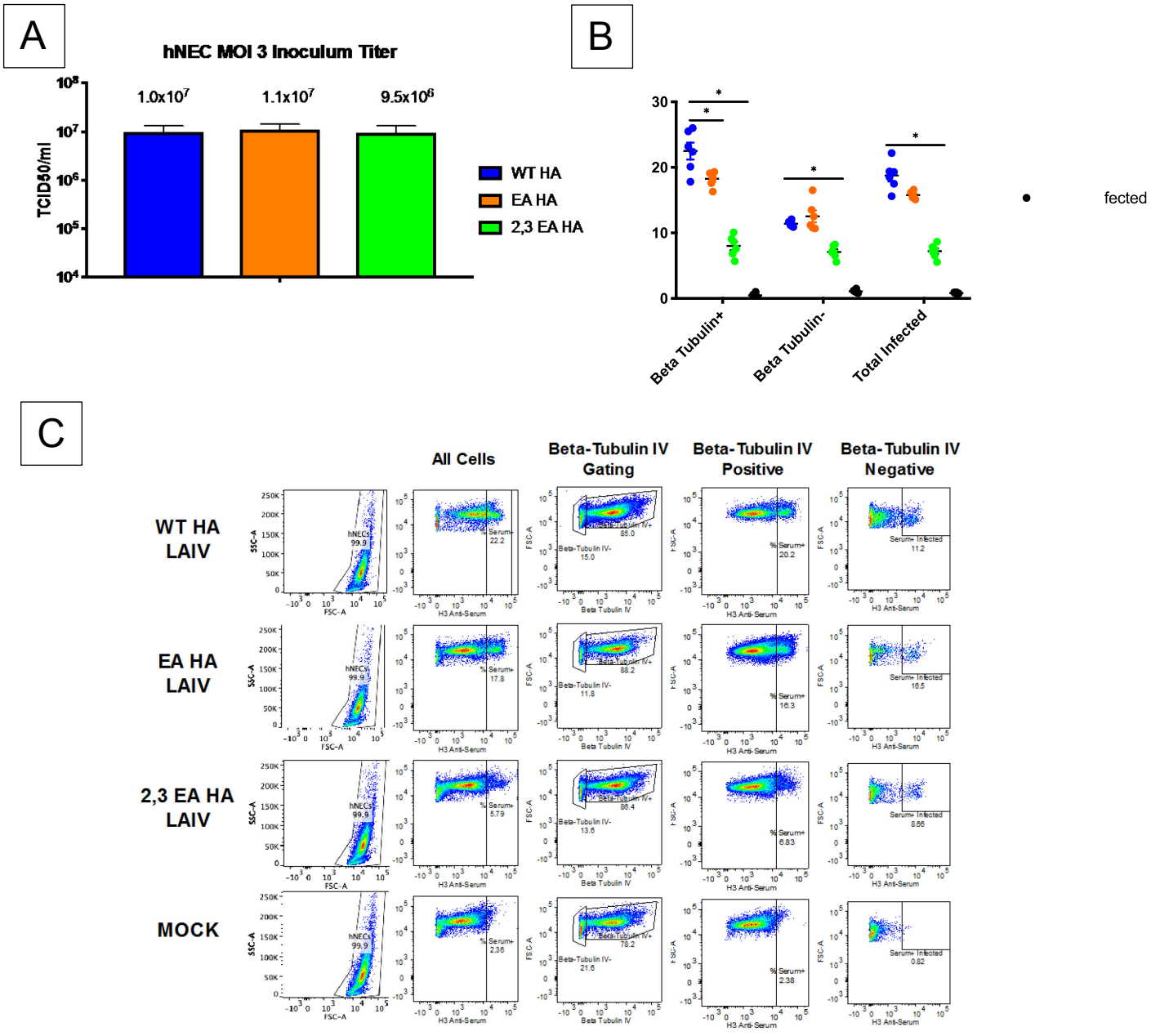

Figure 2.5: Tropism of LAIV in hNEC Cultures

hNEC infected with a high MOI of three and virus tropism was determined via flow cytometry.**(A)** TCID50 values of infection inoculum to verify similar titers used between three LAIVs. **(B)** Quantification of infection of total cells, Beta-Tubulin IV+ (ciliated epithelial cells) and Beta-Tubulin IV- (everything else in hNEC culture). **(C)** Gating strategy is shown for identifying lineages within heterogenous cell culture. Data are pooled from 3 independent experiments with 2 replicates per virus per experiment (total n = 6 hNEC wells tropism analysis). Data were analyzed with *p<.05 unpaired T test in B. Data was compared from WT HA LAIV percent infected to either EA or 2,3 EA HA. Mock is shown for background fluorescence in B and C. Error bars in B are SEM. Acquisition of data on BD LSR II flow cytometer and analysis done with FlowJo 10.5.3 software and GraphPad Prism8.

Sample ID	Average RFU	α2,3 or α2,6 SA
Neu5Aca2-6Galb1-4GlcNAcb1-3Galb1-4(Fuca1-3)GlcNAcb1-3Galb1-4(Fuca1-3)GlcNAcb-Sp0	44628	α2,6
Neu5Aca2-6GalNAcb1-4GlcNAcb-Sp0	41593	α2,6
Neu5Aca2-6Galb1-4(6S)GlcNAcb-Sp8	36903	α2,6
Neu5Aca2-6Galb1-4GlcNAcb1-3Galb1-4GlcNAcb1-3Galb1-4GlcNAcb1-2Mana1-6(Neu5Aca2-6Galb1-4GlcNAcb1-3Galb1-4GlcNAcb1-3Galb1-4GlcNAcb1-2Mana1-3)Manb1-4GlcNAcb1-4GlcNAcb-Sp12	35455	α2,6
Neu5Aca2-6Galb1-4GlcNAcb1-3Galb1-4GlcNAcb-Sp0	34159	α2,6
Neu5Aca2-6Galb1-4GlcNAcb1-3Galb1-4GlcNAcb1-3Galb1-4GlcNAcb-Sp0	32877	α2,6
Neu5Aca2-6Galb1-4GlcNAcb-Sp8	31044	α2,6
Neu5Aca2-6Galb1-4GlcNAcb-Sp0	30317	α2,6
Neu5Aca2-6Galb1-4GlcNAcb1-3Galb1-4GlcNAcb1-6(Galb1-3)GalNAca-Sp14	20914	α2,6
Neu5Aca2-6GalNAcb1-4(6S)GlcNAcb-Sp8	15903	α2,6
Neu5Aca2-3Galb1-4GlcNAcb1-3Galb1-4GlcNAcb-Sp0	9754	α2,3
Neu5Aca2-3Galb1-4GlcNAcb1-2Mana1-6(GlcNAcb1-4)(Neu5Aca2-3Galb1-4GlcNAcb1-2Mana1-3)Manb1-4GlcNAcb1-4GlcNAcb-Sp21	8028	α2,3
Neu5Aca2-3Galb1-4GlcNAcb1-3Galb1-4GlcNAcb1-3Galb1-4GlcNAcb-Sp0	7644	α2,3
Galb1-4GlcNAcb1-6(Neu5Aca2-6Galb1-3GlcNAcb1-3)Galb1-4Glc-Sp21	4353	α2,6
Neu5Aca2-3Galb1-4GlcNAcb1-3Galb-Sp8	4184	α2,3
Neu5Aca2-3Galb1-4GlcNAcb1-2Mana1-6(Neu5Aca2-3Galb1-4GlcNAcb1-2Mana1-3)Manb1-4GlcNAcb1-4GlcNAcb-Sp12	4119	α2,3
Neu5Aca2-3Galb1-4GlcNAcb-Sp0	3734	α2,3
Neu5Aca2-6(Neu5Aca2-3Galb1-3)GalNAca-Sp8	3214	α2,6
Neu5Aca2-3Galb1-4GlcNAcb1-3Galb1-3GlcNAcb-Sp0	3186	α2,3
Neu5Aca2-3Galb1-4GlcNAcb1-6(Galb1-3)GalNAca-Sp14	3153	α2,3

Table 2.1: WT HA A/Victoria/361/2011 CFG synthetic glycan array binding data
A/Victoria/361/2011 LAIV with WT HA used in CFG synthetic glycan array top 20 values. Sialic acid orientation indicated (α2,3 vs α2,6). RFU average was calculated by taking the 4 highest RFU values (out of 6 technical replicates). Out of the top 20, 12 glycans contain α2,6 SA linkages and 8 contains α2,3 SA.

Sample ID	Average RFU	2,3 or α2,6 SA
Neu5Aca2-6GalNAcb1-4GlcNAcb-Sp0	43634	α2,6
Neu5Aca2-3GalNAcb1-4GlcNAcb-Sp0	25436	α2,3
Neu5Aca2-6Galb1-4(6S)GlcNAcb-Sp8	19376	α2,6
Neu5Aca2-3Galb1-4(Fuca1-3)GlcNAcb-Sp8	17094	α2,3
Neu5Aca2-6Galb1-4GlcNAcb-Sp8	14351	α2,6
Neu5Aca2-6(Galb1-3)GlcNAcb1-4Galb1-4Glcb-Sp10	13421	α2,6
Neu5Aca2-6Galb1-4GlcNAcb-Sp0	12390	α2,6
Neu5Aca2-3Galb1-4(Fuca1-3)GlcNAcb-Sp0	12333	α2,3
Neu5Aca2-6GalNAca-Sp8	10025	α2,6
Neu5Aca2-6(Neu5Aca2-3Galb1-3)GalNAca-Sp8	10025	α2,6
Neu5Aca2-6Galb1-4GlcNAcb1-3Galb1-4GlcNAcb1-3Galb1-4GlcNAcb-Sp0	9878	α2,6
Neu5Aca2-3Galb1-4(Fuca1-3)GlcNAcb1-2Mana-Sp0	9869	α2,3
Neu5Aca2-6Galb1-4GlcNAcb1-3Galb1-4(Fuca1-3)GlcNAcb1-3Galb1-4(Fuca1-3)GlcNAcb-Sp0	9863	α2,6
Neu5Aca2-6GalNAcb1-4(6S)GlcNAcb-Sp8	9269	α2,3
Neu5Aca2-3Galb1-4(Neu5Aca2-3Galb1-3)GlcNAcb-Sp8	8602	α2,3
Neu5Aca2-3Galb1-4GlcNAcb-Sp8	6823	α2,3
Neu5Aca2-3Galb-Sp8	4391	α2,3
Neu5Aca2-3Galb1-4GlcNAcb1-6(Neu5Aca2-3Galb1-4GlcNAcb1-2)Mana1-6(GlcNAcb1-4)(Neu5Aca2-3Galb1-4GlcNAcb1-4(Neu5Aca2-3Galb1-4GlcNAcb1-2)Mana1-3)Manb1-4GlcNAcb1-4GlcNAcb-Sp21	4121	α2,3
Neu5Aca2-3Galb1-4(Fuca1-3)GlcNAcb1-3Galb-Sp8	4032	α2,3
Neu5Gca2-3Galb1-4(Fuca1-3)GlcNAcb-Sp0	3833	α2,3

Table 2.2: EA HA A/Victoria/361/2011 CFG synthetic glycan array binding data
A/Victoria/361/2011 LAIV with EA HA used in CFG synthetic glycan array top 20 values. Sialic acid orientation indicated (α2,3 vs α2,6). RFU average was calculated by taking the 4 highest RFU values (out of 6 technical replicates). Out of the top 20, 8 glycans contain α2,6 SA linkages and 12 contains α2,3 SA.

Structure ID	Average RFU	α2,3 or α2,6 SA linkage
Neu5Aca2-3Galb1-4(Fuca1-3)GlcNAcb-Sp0	21866	α2,3
Neu5Aca2-3Galb1-4(Fuca1-3)GlcNAcb-Sp8	19281	α2,3
Neu5Aca2-3Galb1-4(Fuca1-3)GlcNAcb1-3Galb-Sp8	15227	α2,3
Neu5Aca2-3Galb1-3(6S)GalNAca-Sp8	11236	α2,3
Neu5Aca2-6Galb1-4GlcNAcb1-3Galb1-4(Fuca1-3)GlcNAcb1-3Galb1-4(Fuca1-3)GlcNAcb-Sp0	10638	α2,6
Neu5Aca2-6GalNAcb1-4GlcNAcb-Sp0	10557	α2,6
Neu5Aca2-6Galb1-4(6S)GlcNAcb-Sp8	9451	α2,6
Neu5Aca2-6(Neu5Aca2-3Galb1-3)GalNAca-Sp8	8016	α2,6
Neu5Aca2-6Galb1-4GlcNAcb1-3Galb1-4GlcNAcb1-3Galb1-4GlcNAcb-Sp0	7312	α2,6
Neu5Aca2-3Galb1-4GlcNAcb1-6(Neu5Aca2-3Galb1-3)GalNAca-Sp14	7025	α2,3
Neu5Aca2-3Galb1-4(Fuca1-3)GlcNAcb1-3Galb1-4(Fuca1-3)GlcNAcb1-3Galb1-4(Fuca1-3)GlcNAcb-Sp0	6599	α2,3
Neu5Gca2-3Galb1-4(Fuca1-3)GlcNAcb-Sp0	6277	α2,3
Neu5Aca2-3Galb1-4(Fuca1-3)GlcNAcb1-2Mana-Sp0	6234	α2,6
Neu5Aca2-6(Neu5Aca2-3Galb1-3)GalNAca-Sp14	6220	α2,6
Neu5Aca2-3Galb1-3GlcNAcb1-3GalNAca-Sp14	5952	α2,3
Neu5Aca2-3Galb1-3GlcNAcb1-3Galb1-4GlcNAcb-Sp0	5725	α2,3
Neu5Aca2-3Galb1-3(6S)GlcNAc-Sp8	5359	α2,3
Neu5Aca2-3Galb1-3GalNAca-Sp8	5332	α2,3
Neu5Aca2-3Galb1-4(Fuca1-3)GlcNAcb1-3Galb1-4GlcNAcb-Sp8	4920	α2,3
Neu5Aca2-3Galb1-3(Fuca1-4)GlcNAcb1-3Galb1-4(Fuca1-3)GlcNAcb-Sp0	4836	α2,3

Table 2.3: 2,3 EA HA A/Victoria/361/2011 CFG synthetic glycan array binding data A/Victoria/361/2011 LAIV with 2,3 EA HA used in CFG synthetic glycan array top 20 values. Sialic acid orientation indicated (α2,3 vs α2,6). RFU average was calculated by taking the 4 highest RFU values (out of 6 technical replicates). Out of the top 20, 7 glycans contain α2,6 SA linkages and 13 contains α2,3 SA.

Chart ID	Sample ID
1	Fuca1-2Galb1-3GalNAcb1-4(Neu5Aca2-3)Galb1-4Glcb-Sp0
2	Fuca1-2Galb1-3GalNAcb1-4(Neu5Aca2-3)Galb1-4Glcb-Sp9
3	Galb1-3GalNAcb1-4(Neu5Aca2-3)Galb1-4Glcb-Sp0
4	GalNAcb1-4(Neu5Aca2-3)Galb1-4Glcb-Sp0
5	GalNAcb1-4(Neu5Aca2-3)Galb1-4GlcNAcb1-3GalNAca-Sp14
6	GalNAcb1-4(Neu5Aca2-3)Galb1-4GlcNAcb-Sp0
7	GalNAcb1-4(Neu5Aca2-3)Galb1-4GlcNAcb-Sp8
8	GlcNAcb1-6(Neu5Aca2-3Galb1-3)GalNAca-Sp14
9	Neu5Aca2-3(6S)Galb1-4GlcNAcb-Sp8
10	Neu5Aca2-3Galb1-3(6S)GalNAca-Sp8
11	Neu5Aca2-3Galb1-3(6S)GlcNAc-Sp8
12	Neu5Aca2-3Galb1-3(Fuca1-4)GlcNAcb1-3Galb1-3(Fuca1-4)GlcNAcb-Sp0
13	Neu5Aca2-3Galb1-3(Fuca1-4)GlcNAcb1-3Galb1-4(Fuca1-3)GlcNAcb-Sp0
14	Neu5Aca2-3Galb1-3(Fuca1-4)GlcNAcb-Sp8
15	Neu5Aca2-3Galb1-3GalNAca-Sp14
16	Neu5Aca2-3Galb1-3GalNAca-Sp8
17	Neu5Aca2-3Galb1-3GalNAcb1-3Gala1-4Galb1-4Glcb-Sp0
18	Neu5Aca2-3Galb1-3GalNAcb1-4(Neu5Aca2-3)Galb1-4Glcb-Sp0
19	Neu5Aca2-3Galb1-3GalNAcb1-4Galb1-4Glcb-Sp0
20	Neu5Aca2-3Galb1-3GlcNAcb1-2Mana1-6(GlcNAcb1-4)(Neu5Aca2-3Galb1-3GlcNAcb1-2Mana1-3)Manb1-4GlcNAcb1-4GlcNAc-Sp21
21	Neu5Aca2-3Galb1-3GlcNAcb1-2Mana-Sp0
22	Neu5Aca2-3Galb1-3GlcNAcb1-3Galb1-3GlcNAcb-Sp0
23	Neu5Aca2-3Galb1-3GlcNAcb1-3Galb1-4GlcNAcb-Sp0
24	Neu5Aca2-3Galb1-3GlcNAcb1-3GalNAca-Sp14

25	Neu5Aca2-3Galb1-3GlcNAcb1-6GalNAca-Sp14
26	Neu5Aca2-3Galb1-3GlcNAcb-Sp0
27	Neu5Aca2-3Galb1-4(6S)GlcNAcb-Sp8
28	Neu5Aca2-3Galb1-4(Fuca1-3)(6S)GlcNAcb-Sp8
29	Neu5Aca2-3Galb1-4(Fuca1-3)GlcNAcb1-2Mana-Sp0
30	Neu5Aca2-3Galb1-4(Fuca1-3)GlcNAcb1-3Galb1-4(Fuca1-3)GlcNAcb1-3Galb1-4(Fuca1-3)GlcNAcb-Sp0
31	Neu5Aca2-3Galb1-4(Fuca1-3)GlcNAcb1-3Galb1-4GlcNAcb-Sp8
32	Neu5Aca2-3Galb1-4(Fuca1-3)GlcNAcb1-3Galb-Sp8
33	Neu5Aca2-3Galb1-4(Fuca1-3)GlcNAcb1-3GalNAca-Sp14
34	Neu5Aca2-3Galb1-4(Fuca1-3)GlcNAcb1-6(Galb1-3)GalNAca-Sp14
35	Neu5Aca2-3Galb1-4(Fuca1-3)GlcNAcb1-6(Neu5Aca2-3Galb1-3)GalNAc-Sp14
36	Neu5Aca2-3Galb1-4(Fuca1-3)GlcNAcb-Sp0
37	Neu5Aca2-3Galb1-4(Fuca1-3)GlcNAcb-Sp8
38	Neu5Aca2-3Galb1-4(Neu5Aca2-3Galb1-3)GlcNAcb-Sp8
39	Neu5Aca2-3Galb1-4Glcb-Sp0
40	Neu5Aca2-3Galb1-4Glcb-Sp8
41	Neu5Aca2-3Galb1-4GlcNAcb1-2Mana1-6(GlcNAcb1-4)(Neu5Aca2-3Galb1-4GlcNAcb1-2Mana1-3)Manb1-4GlcNAcb1-4GlcNAcb-Sp21
42	Neu5Aca2-3Galb1-4GlcNAcb1-2Mana1-6(Neu5Aca2-3Galb1-4GlcNAcb1-2Mana1-3)Manb1-4GlcNAcb1-4(Fuca1-6)GlcNAcb-Sp24
43	Neu5Aca2-3Galb1-4GlcNAcb1-2Mana1-6(Neu5Aca2-3Galb1-4GlcNAcb1-2Mana1-3)Manb1-4GlcNAcb1-4GlcNAcb-Sp12
44	Neu5Aca2-3Galb1-4GlcNAcb1-2Mana1-6(Neu5Aca2-6Galb1-4GlcNAcb1-2Mana1-3)Manb1-4GlcNAcb1-4GlcNAcb-Sp12
45	Neu5Aca2-3Galb1-4GlcNAcb1-2Mana-Sp0

46	Neu5Aca2-3Galb1-4GlcNAcb1-3Galb1-3GlcNAcb-Sp0
47	Neu5Aca2-3Galb1-4GlcNAcb1-3Galb1-4(Fuca1-3)GlcNAcb-Sp0
48	Neu5Aca2-3Galb1-4GlcNAcb1-3Galb1-4GlcNAcb1-2Mana1-6(Neu5Aca2-3Galb1-4GlcNAcb1-3Galb1-4GlcNAcb1-2Mana1-3)Manb1-4GlcNAcb1-4GlcNAcb-Sp12
49	Neu5Aca2-3Galb1-4GlcNAcb1-3Galb1-4GlcNAcb1-3Galb1-4GlcNAcb1-2Mana1-6(Neu5Aca2-3Galb1-4GlcNAcb1-3Galb1-4GlcNAcb1-3Galb1-4GlcNAcb1-2Mana1-3)Manb1-4GlcNAcb1-4GlcNAcb-Sp12
50	Neu5Aca2-3Galb1-4GlcNAcb1-3Galb1-4GlcNAcb1-3Galb1-4GlcNAcb-Sp0
51	Neu5Aca2-3Galb1-4GlcNAcb1-3Galb1-4GlcNAcb1-3GalNAca-Sp14
52	Neu5Aca2-3Galb1-4GlcNAcb1-3Galb1-4GlcNAcb1-6(Galb1-3)GalNAca-Sp14
53	Neu5Aca2-3Galb1-4GlcNAcb1-3Galb1-4GlcNAcb1-6(Neu5Aca2-3Galb1-4GlcNAcb1-3Galb1-4GlcNAcb1-3)GalNAca-Sp14
54	Neu5Aca2-3Galb1-4GlcNAcb1-3Galb1-4GlcNAcb-Sp0
55	Neu5Aca2-3Galb1-4GlcNAcb1-3Galb-Sp8
56	Neu5Aca2-3Galb1-4GlcNAcb1-3GalNAc-Sp14
57	Neu5Aca2-3Galb1-4GlcNAcb1-4Mana1-6(GlcNAcb1-4)(Neu5Aca2-3Galb1-4GlcNAcb1-4(Neu5Aca2-3Galb1-4GlcNAcb1-2)Mana1-3)Manb1-4GlcNAcb1-4GlcNAcb-Sp21
58	Neu5Aca2-3Galb1-4GlcNAcb1-6(Galb1-3)GalNAca-Sp14
59	Neu5Aca2-3Galb1-4GlcNAcb1-6(Neu5Aca2-3Galb1-3)GalNAca-Sp14
60	Neu5Aca2-3Galb1-4GlcNAcb1-6(Neu5Aca2-3Galb1-4GlcNAcb1-2)Mana1-6(GlcNAcb1-4)(Neu5Aca2-3Galb1-4GlcNAcb1-2Mana1-3)Manb1-4GlcNAcb1-4GlcNAcb-Sp21
61	Neu5Aca2-3Galb1-4GlcNAcb1-6(Neu5Aca2-3Galb1-4GlcNAcb1-2)Mana1-6(GlcNAcb1-4)(Neu5Aca2-3Galb1-4GlcNAcb1-4(Neu5Aca2-3Galb1-4GlcNAcb1-2)Mana1-3)Manb1-4GlcNAcb1-4GlcNAcb-Sp21
62	Neu5Aca2-3Galb1-4GlcNAcb1-6(Neu5Aca2-3Galb1-4GlcNAcb1-3)GalNAca-Sp14
63	Neu5Aca2-3Galb1-4GlcNAcb1-6GalNAca-Sp14
64	Neu5Aca2-3Galb1-4GlcNAcb-Sp0

65	Neu5Aca2-3Galb1-4GlcNAcb-Sp8
66	Neu5Aca2-3Galb-Sp8
67	Neu5Aca2-3GalNAca-Sp8
68	Neu5Aca2-3GalNAcb1-4GlcNAcb-Sp0
69	Galb1-4(Fuca1-3)GlcNAcb1-6(Neu5Aca2-6(Neu5Aca2-3Galb1-3)GlcNAcb1-3)Galb1-4Glc-Sp21
70	Neu5Aca2-6(Neu5Aca2-3)GalNAca-Sp8
71	Neu5Aca2-6(Neu5Aca2-3Galb1-3)GalNAca-Sp14
72	Neu5Aca2-6(Neu5Aca2-3Galb1-3)GalNAca-Sp8
73	Neu5Aca2-6Galb1-4GlcNAcb1-2Mana1-6(Neu5Aca2-3Galb1-4GlcNAcb1-2Mana1-3)Manb1-4GlcNAcb1-4GlcNAcb-Sp12
74	Galb1-4GlcNAcb1-2Mana1-6(Neu5Aca2-6Galb1-4GlcNAcb1-2Mana1-3)Manb1-4GlcNAcb1-4GlcNAcb-Sp12
75	Galb1-4GlcNAcb1-6(Neu5Aca2-6Galb1-3GlcNAcb1-3)Galb1-4Glc-Sp21
76	Mana1-6(Neu5Aca2-6Galb1-4GlcNAcb1-2Mana1-3)Manb1-4GlcNAcb1-4GlcNAc-Sp12
77	Neu5Aca2-6(Galb1-3)GalNAca-Sp14
78	Neu5Aca2-6(Galb1-3)GalNAca-Sp8
79	Neu5Aca2-6(Galb1-3)GlcNAcb1-4Galb1-4Glcb-Sp10
80	Neu5Aca2-6Galb1-4 GlcNAcb1-6(Neu5Aca2-6Galb1-4GlcNAcb1-3)GalNAca-Sp14
81	Neu5Aca2-6Galb1-4(6S)GlcNAcb-Sp8
82	Neu5Aca2-6Galb1-4Glcb-Sp0
83	Neu5Aca2-6Galb1-4Glcb-Sp8
84	Neu5Aca2-6Galb1-4GlcNAcb1-2Mana1-3Manb1-4GlcNAcb1-4GlcNAc-Sp12
85	Neu5Aca2-6Galb1-4GlcNAcb1-2Mana1-6(Galb1-4GlcNAcb1-2Mana1-3)Manb1-4GlcNAcb1-4GlcNAcb-Sp12
86	Neu5Aca2-6Galb1-4GlcNAcb1-2Mana1-6(GlcNAcb1-2Mana1-3)Manb1-4GlcNAcb1-4GlcNAcb-Sp12

87	Neu5Aca2-6Galb1-4GlcNAcb1-2Mana1-6(GlcNAcb1-4)(Neu5Aca2-6Galb1-4GlcNAcb1-2Mana1-3)Manb1-4GlcNAcb1-4GlcNAcb-Sp21
88	Neu5Aca2-6Galb1-4GlcNAcb1-2Mana1-6(Mana1-3)Manb1-4GlcNAcb1-4GlcNAc-Sp12
89	Neu5Aca2-6Galb1-4GlcNAcb1-2Mana1-6(Neu5Aca2-6Galb1-4GlcNAcb1-2Mana1-3)Manb1-4GlcNAcb1-4(Fuca1-6)GlcNAcb-Sp24
90	Neu5Aca2-6Galb1-4GlcNAcb1-2Mana1-6(Neu5Aca2-6Galb1-4GlcNAcb1-2Mana1-3)Manb1-4GlcNAcb1-4GlcNAcb-Sp12
91	Neu5Aca2-6Galb1-4GlcNAcb1-2Mana1-6(Neu5Aca2-6Galb1-4GlcNAcb1-2Man-a1-3)Manb1-4GlcNAcb1-4GlcNAcb-Sp21
92	Neu5Aca2-6Galb1-4GlcNAcb1-2Mana1-6(Neu5Aca2-6Galb1-4GlcNAcb1-2Mana1-3)Manb1-4GlcNAcb1-4GlcNAcb-Sp24
93	Neu5Aca2-6Galb1-4GlcNAcb1-2Mana1-6Manb1-4GlcNAcb1-4GlcNAc-Sp12
94	Neu5Aca2-6Galb1-4GlcNAcb1-2Man-Sp0
95	Neu5Aca2-6Galb1-4GlcNAcb1-3Galb1-3GlcNAcb-Sp0
96	Neu5Aca2-6Galb1-4GlcNAcb1-3Galb1-4(Fuca1-3)GlcNAcb1-3Galb1-4(Fuca1-3)GlcNAcb-Sp0
97	Neu5Aca2-6Galb1-4GlcNAcb1-3Galb1-4GlcNAcb1-2Mana1-6(Neu5Aca2-6Galb1-4GlcNAcb1-3Galb1-4GlcNAcb1-2Mana1-3)Manb1-4GlcNAcb1-4GlcNAcb-Sp12
98	Neu5Aca2-6Galb1-4GlcNAcb1-3Galb1-4GlcNAcb1-3Galb1-4GlcNAcb1-2Mana1-6(Neu5Aca2-6Galb1-4GlcNAcb1-3Galb1-4GlcNAcb1-3Galb1-4GlcNAcb1-2Mana1-3)Manb1-4GlcNAcb1-4GlcNAcb-Sp12
99	Neu5Aca2-6Galb1-4GlcNAcb1-3Galb1-4GlcNAcb1-3Galb1-4GlcNAcb-Sp0
100	Neu5Aca2-6Galb1-4GlcNAcb1-3Galb1-4GlcNAcb1-3GalNAca-Sp14
101	Neu5Aca2-6Galb1-4GlcNAcb1-3Galb1-4GlcNAcb1-6(Galb1-3)GalNAca-Sp14
102	Neu5Aca2-6Galb1-4GlcNAcb1-3Galb1-4GlcNAcb1-6(Neu5Aca2-6Galb1-4GlcNAcb1-3Galb1-4GlcNAcb1-3)GalNAca-Sp14
103	Neu5Aca2-6Galb1-4GlcNAcb1-3Galb1-4GlcNAcb-Sp0
104	Neu5Aca2-6Galb1-4GlcNAcb1-3GalNAc-Sp14

105	Neu5Aca2-6Galb1-4GlcNAcb1-4Mana1-6(GlcNAcb1-4)(Neu5Aca2-6Galb1-4GlcNAcb1-4(Neu5Aca2-6Galb1-4GlcNAcb1-2)Mana1-3)Manb1-4GlcNAcb1-4GlcNAcb-Sp21
106	Neu5Aca2-6Galb1-4GlcNAcb1-6(Fuca1-2Galb1-3GlcNAcb1-3)Galb1-4Glc-Sp21
107	Neu5Aca2-6Galb1-4GlcNAcb1-6(Fuca1-2Galb1-4(Fuca1-3)GlcNAcb1-3)Galb1-4Glc-Sp21
108	Neu5Aca2-6Galb1-4GlcNAcb1-6(Galb1-3)GalNAca-Sp14
109	Neu5Aca2-6Galb1-4GlcNAcb1-6(Galb1-3GlcNAcb1-3)Galb1-4Glcb-Sp21
110	Neu5Aca2-6Galb1-4GlcNAcb1-6(Neu5Aca2-6Galb1-4GlcNAcb1-2)Mana1-6(GlcNAcb1-4)(Neu5Aca2-6Galb1-4GlcNAcb1-2Mana1-3)Manb1-4GlcNAcb1-4GlcNAcb-Sp21
111	Neu5Aca2-6Galb1-4GlcNAcb1-6(Neu5Aca2-6Galb1-4GlcNAcb1-2)Mana1-6(GlcNAcb1-4)(Neu5Aca2-6Galb1-4GlcNAcb1-4(Neu5Aca2-6Galb1-4GlcNAcb1-2)Mana1-3)Manb1-4GlcNAcb1-4GlcNAcb-Sp21
112	Neu5Aca2-6Galb1-4GlcNAcb1-6GalNAca-Sp14
113	Neu5Aca2-6Galb1-4GlcNAcb-Sp0
114	Neu5Aca2-6Galb1-4GlcNAcb-Sp8
115	Neu5Aca2-6Galb-Sp8
116	Neu5Aca2-6GalNAca-Sp8
117	Neu5Aca2-6GalNAcb1-4(6S)GlcNAcb-Sp8
118	Neu5Aca2-6GalNAcb1-4GlcNAcb-Sp0
119	Neu5Aca2-6GlcNAcb1-4GlcNAcb1-4GlcNAc-Sp21
120	Neu5Aca2-6GlcNAcb1-4GlcNAc-Sp21
121	GalNAcb1-4(Neu5Aca2-8Neu5Aca2-3)Galb1-4Glcb-Sp0
122	GalNAcb1-4(Neu5Aca2-8Neu5Aca2-8Neu5Aca2-3)Galb1-4Glcb-Sp0
123	GalNAcb1-4(Neu5Aca2-8Neu5Aca2-8Neu5Aca2-8Neu5Aca2-3)Galb1-4Glcb-Sp0
124	Neu5,9Ac2a2-3Galb1-3GlcNAcb-Sp0
125	Neu5,9Ac2a2-6Galb1-4GlcNAcb-Sp8
126	Neu5,9Ac$_2$a-Sp8

127	Neu5Aca2-3Galb1-3GalNAcb1-4(Neu5Aca2-8Neu5Aca2-3)Galb1-4Glcb-Sp0
128	Neu5Aca2-8Neu5Aca2-3Galb1-3GalNAcb1-4(Neu5Aca2-3)Galb1-4Glc-Sp21
129	Neu5Aca2-8Neu5Aca2-3Galb1-3GalNAcb1-4(Neu5Aca2-8Neu5Aca2-3)Galb1-4Glcb-Sp0
130	Neu5Aca2-8Neu5Aca2-3Galb1-4Glcb-Sp0
131	Neu5Aca2-8Neu5Aca2-3Galb1-4GlcNAc-Sp0
132	Neu5Aca2-8Neu5Aca2-8Neu5Aca2-3Galb1-4Glcb-Sp0
133	Neu5Aca2-8Neu5Aca2-8Neu5Aca-Sp8
134	Neu5Aca2-8Neu5Aca2-8Neu5Acb-Sp8
135	Neu5Aca2-8Neu5Aca-Sp8
136	Neu5Aca2-8Neu5Acb-Sp17
137	Neu5Aca2-8Neu5Gca2-3Galb1-4GlcNAc-Sp0
138	Neu5Aca-Sp11
139	Neu5Aca-Sp8
140	Neu5Acb2-6(Galb1-3)GalNAca-Sp8
141	Neu5Acb2-6Galb1-4GlcNAcb-Sp8
142	Neu5Acb2-6GalNAca-Sp8
143	Neu5Acb-Sp8
144	Neu5Gca2-3Galb1-3(Fuca1-4)GlcNAcb-Sp0
145	Neu5Gca2-3Galb1-3GlcNAcb-Sp0
146	Neu5Gca2-3Galb1-4(Fuca1-3)GlcNAcb-Sp0
147	Neu5Gca2-3Galb1-4Glcb-Sp0
148	Neu5Gca2-3Galb1-4GlcNAcb-Sp0
149	Neu5Gca2-6Galb1-4GlcNAcb-Sp0
150	Neu5Gca2-6GalNAca-Sp0
151	Neu5Gca2-8Neu5Aca2-3Galb1-4GlcNAc-Sp0

152	Neu5Gca2-8Neu5Gca2-3Galb1-4GlcNAcb1-3Galb1-4GlcNAc-Sp0
153	Neu5Gca2-8Neu5Gca2-3Galb1-4GlcNAc-Sp0
154	Neu5Gca2-8Neu5Gca2-6Galb1-4GlcNAc-Sp0
155	Neu5Gca-Sp8
156	Neu5Gcb2-6Galb1-4GlcNAc-Sp8

Table 2.4: Synthetic glycan array structure ID
Chart ID on Table 1-3 glycan array data. Numbers on chart correspond to structure ID. Full structure information found on the CFG website [155]. Sp8 or Sp0 refers to chemical linkage of synthetic glycan to array chip. More information can be found on CFG website.

CHAPTER 3: Novel Neuraminidase glycosylation genotype in clade 3c.2a H3N2 2014-2015 isolates impacts viral growth on human nasal epithelial cells and neuraminidase function

Harrison Powell, Deena Blumenkrantz and Andrew Pekosz

Abstract

In the 2014-15 influenza season, clinical isolates generated from the Johns Hopkins Center of Excellence in Influenza Research and Surveillance sampling network contained a novel neuraminidase (NA) genotype. These isolates, which quickly emerged as the dominant genotype in the 3c.2a clade of H3N2 viruses, had a novel glycosylation site at position 245-247 in the NA protein. Addition of glycosylation sites can impact virus replication and enzymatic function. To verify the utilization of the glycosylation site at position 245 in the NA protein, the NA gene segments for the glycosylation positive and glycosylation negative genes were cloned into human expression vectors. After transient expression in HEK293T cells, utilization of the putative glycosylation site in the 245 NA Gly+ gene was verified via mobility shift SDS PAGE and western blotting. To test the effect this glycosylation had on replication, viruses containing either the NA glycosylation at residue 245 (245 NA Gly+) or viruses lacking the NA glycosylation at residue 245 (245 NA Gly-) were grown on Madin-Darby Canine Kidney Cells (MDCK), MDCK-SIAT1 cells and human nasal epithelial cells (hNEC). Viruses with the 245 NA Gly+ genotype grew to a significantly lower titer compared to viruses with the 245 NA Gly- genotype only in hNEC cultures. Additionally, viruses with the 245 NA Gly+ genotype had significantly less NA activity compared to 245 NA Gly- viruses in two activity assays tested. Temperature had no significant effect on the difference in activity for the 245 NA Gly+ or 245 NA Gly- isolates. These results suggest that the addition of a new glycosylation site at position 245-247 in contemporary clade 3c.2a H3N2 NA proteins decreases viral replication in hNECs and decrease NA activity.

Introduction

Seasonal influenza virus infects millions of people and causes thousands of deaths worldwide each year [3, 136]. Influenza viruses that circulate in the human population routinely undergo genetic changes between influenza seasons as a result of host immune pressure [180-182]. This constant evolution, due to an error prone polymerase and immune pressure, results in the emergence of novel and unique variants that challenge our ability to protect individuals from infection [183, 184]. A small number of changes in the hemagglutinin (HA) protein can significantly alter immunogenicity of influenza A viruses and render the millions of influenza vaccine doses useless to a particular strain [183, 185-188]. In recent years, there has been an increased effort to study the genetic variation of influenza A viruses including all eight genomic segments and the 10-14 proteins these segments encode. Increased surveillance efforts can lead to identification and characterization of novel variants and how genetic variants lead to phenotypic differences between virus isolates. More importantly, routine surveillance and studying the fitness of variants is important for informing public health policy, influenza vaccine development and emerging threats [189-191].

One influenza A virus protein, the neuraminidase (NA) viral enzyme, has come into the spotlight in recent years as universal vaccine efforts increase. The NA protein is critical for both entry into cells and exit of progeny virus from cells. The well-studied HA protein, and variants that circulate in the human population, often dictate changes to the vaccine formulation by the World Health Organization (WHO). These minor variations in the HA protein sequence can lead to escape from neutralizing antibodies and changes

in HA receptor function [72, 108, 192, 193]. While variations in the NA protein are less frequently studied, understanding how these changes impact viral fitness and protein function are crucial to understanding influenza A virus evolution.

In the 2014-15 season a novel H3N2 NA genotype was sequenced through the Johns Hopkins Centers of Excellence for Influenza Research and Surveillance (JH CEIRS). This novel genotype, the addition of a new n-linked glycosylation site at position 245-247 in the NA protein, quickly became the dominant genotype the following year. After the introduction of this genotype in the human H3N2 population virtually all H3N2 isolates have gained this genotype. N-linked glycosylations are large post translationally added modifications that dramatically alter the antigenicity of viral proteins, and potentially the protein function. Based on the 3D protein structure this glycosylation is near the active site of the enzyme [109].

Using clinical isolates that represent the two neuraminidase genotypes (245 NA Gly- and 245 NA Gly+ where “Gly” means n-glycosylation), we demonstrate that this glycosylation site is utilized and added to the viral protein. Surprisingly, this glycosylation incurs a significant fitness cost to the virus. Viral replication on primary differentiated human nasal epithelial cells (hNEC) is significantly impacted and enzymatic activity of the protein is significantly decreased in two different activity assays.

Materials and Methods

Cell Lines and Primary Cells

Madin-Darby Canine Kidney Cells (MDCK), MDCK-SIAT1 and human embryonic kidney cells 293T (HEK293T) were maintained in complete medium (CM) consisting of Dulbecco's Modified Eagle Medium (DMEM) supplemented with 10% fetal bovine serum, 100U/ml penicillin/streptomycin (Life Technologies) and 2mM Glutamax (Gibco). Human nasal epithelial cells (hNEC) were isolated from non-diseased donor tissue following endoscopic sinus surgery. Cells were grown, differentiated and maintained at the air liquid interface as previously described [129, 138, 145]. hNEC differentiation medium and maintenance medium was prepared as previously described [129, 132, 138, 142]. hNEC cultures were used for low MOI growth curves only when fully differentiated. All cells were maintained at 37ºC in a humidified incubator supplemented with 5% CO_2.

Plasmids

The mammalian expression plasmid pCAGGS was used for transient expression of C-terminal flag-tagged neuraminidase proteins as previously described [129]. Briefly, vRNA was isolated from two representative clinical isolates A/Bethesda/55/2015 (245 NA Gly+) and A/Columbia/41/2014 (245 NA Gly-) using a Qiagen mini-vRNA isolation kit. Gene specific primers with restriction sites were used to create cDNA via a one-step RT-PCR (SuperScript III Platinum Taq mix, ThermoFisher Scientific). The cDNA was cut with the appropriate enzymes and ligated into the plasmid pCAGGS. C-terminal flag tag (DYKDDDDK) was added to pCAGGs-NA encoding plasmids via site directed mutagenesis (Agilent).

Transient Transfection for NA-Flag expressing cells

Transient transfection of HEK293T was performed with TransIT-LT1 per the manufacturers protocol. Briefly, cells were grown in complete medium until time of transfection to roughly 50% confluency. On the day of transfection, complete medium was removed and replaced with Opti-MEM serum free medium. Opti-MEM, TransIT-LT1 and 2.5ug of plasmids encoding gene of interest were mixed then added to HEK293T cells. At 16hr post transfection wells were lysed with 1% sodium dodecyl sulfate (SDS) in phosphate buffer saline (PBS) for western blot and PNGase analysis.

SDS-PAGE and Western Blotting

Cell lysates prepared from HEK293T cells transiently expressing NA proteins of interest were used for western blotting. Cells were lysed in 1% SDS Page on ice then treated with 4X-Laemli buffer (Bio-Rad) containing 250mM dithiothreitol (DTT, ThermoFisher Scientific) and boiled at 100ºC for 5 minutes. Samples were run on 4-20% Mini-PROTEAN TGX gels (Bio-Rad) with an All-Blue precision plus protein ladder (Bio-Rad) at 70v. Proteins were transferred onto an immobilon-FL membrane (Millipore) at 75v for 1hr. After transfer, membranes were blocked with blocking buffer (PBS containing .05% Tween-20 (Sigma) and 5% non-fat milk (Bio-Rad)) for 1 hour at room temp. Primary antibody (FLAG and Beta-Actin) was incubated overnight at 4ºC in blocking buffer. Membranes were washed in PBS with .05% Tween-20 (wash buffer). Secondary antibody was added for 1hr at room temperature (25ºC) in blocking buffer then washed again in wash buffer. Blots were imaged and analyzed with the FluorChem Q system (ProteinSimple).

Immunoprecipitation and PNGase F treatment

FLAG-Tagged neuraminidase protein was immunoprecipitated from cell lysates per the manufacturer's instruction (Abcam). Briefly, cell lysates were made using RIPA

buffer and allowed to lyse at 4ºC for 1 hour. After extended lysis step, lysates were clarified by centrifuging at 10,000g for 10 minutes to precipitate cellular debris. Clarified lysates were then incubated with mouse anti-FLAG antibody (Sigma, clone M2) over night at 4ºC. The next day, washed protein A/G coupled agarose beads were added to the cleared lysate and incubated with rocking for 2 hours at room temperature (25ºC). After, the beads and lysate mix was centrifuged at 3,000g for 3 minutes to pellet immunoprecipitation beads. The immunoprecipitation beads were washed three times with kit wash buffer. Next, 100ul of 1% SDS in PBS was added and mixture was boiled at 100ºC for 10 minutes. The mixture was centrifuged again at 3,000g for 3 minutes and the supernatant containing precipitated NA protein was used for PNGase treatment. PNGase F treatment was done according to the manufacturer's instructions with no modifications to the provided protocol (NEB). After PNGase F treatment, product was used for western blotting as described above.

Primary Antibodies

The primary antibody against the FLAG epitope (DYKDDDDK) was used at a concentration of 1ugl/ml for western blotting (Sigma clone M2). Beta-Actin (Abcam ab8227) was used at 1µg/ml for a loading control.

Secondary Antibodies

Secondary antibodies were used to detect binding of primary unconjugated monoclonal antibodies. Goat anti-Mouse IgG Alexa Fluor 488 and Goat anti-Rabbit IgG Alexa Fluor 488 were used at a concentration of 1µg/ml concentration in blocking buffer for Western blotting.

Influenza H3N2 Database Sequence Analysis

Human H3N2 isolates were downloaded from the EpiFlu database from September of 2014 through March of 2018 during August of 2019. Neuraminidase

sequences were trimmed to the start codon (ATG) then analyzed for presence of a glycosylation (NXS/T) at amino acid positions 245-247. Any isolate without an NXS/T genotype was considered “245 glycosylation negative” for analysis purposes. No isolates contained a proline at position 246, which is unable to be glycosylated.

Virus Isolation

hNEC cultures were washed twice with PBS- for 10 minutes and PBS aspirated after each wash. Then, 100ul of nasopharyngeal swab (NPS) from a PCR+ flu positive specimen was inoculated on the hNECs for 2 hours at 32ºC. After inoculation, NPS was aspirated and cells were washed three times in PBS. Cells were returned to 32ºC apical sample was taken every 24 hours, frozen at -70ºC, then used at a later timepoint to assess viral titer via $TCID_{50}$.

Virus Working Stock Generation

For generation of clinical isolate virus working stocks, a 95-100% confluent flask of MDCKs was infected at a multiplicity of infection (MOI) of 0.001 $TCID_{50}$ units. Cells were washed twice with PBS containing 2mm calcium and magnesium. The inoculum was diluted infection medium (IM), consisting of DMEM with 0.3% BSA (Sigma), 100U/ml pen/strep (Life Technologies), 2mM Glutamax (Gibco) and 5µg/ml N-acetyl trypsin((Sigma)). Inoculation was done at 32ºC for 1 hour with gentle rocking of the flask every 15 minutes. After infection, inoculum was removed and fresh IM was added. Cells were placed in a 32ºC incubator and monitored daily for CPE. Working stock was harvested between 3 and 5 days or when CPE reached approximately 75-80%. Viral working stocks were then Sanger sequenced with gene specific primers for all eight segments and infectious virus titer determined by $TCID_{50}$ as described below. Neither isolate showed any tissue culture adaptation comparing the working stock to the original

NPS sequence with the exception of the HA protein. Both isolates had the amino acid mutation K160T in the HA protein, resulting in the loss of a putative glycosylation site in the sequence.

Plaque Assay

MDCK cells were grown in CM to 95-100% confluency in 6-well plates. Complete medium was removed, cells were washed twice with PBS containing 2mm calcium and magnesium (PBS+). Virus stocks were serially 10-fold diluted and 250ul of the appropriate dilution was added. Cells and virus were incubated at 32ºC for 1hour with rocking every 15 minutes. After 1hr, the virus inoculum was removed and phenol-red free DMEM supplemented with 3% BSA (Sigma), 100U/ml pen/strep (Life Technologies), 2mM Glutamax (Gibco),5mM HEPES buffer (Gibco), 5µg/ml N-acetyl trypsin (Sigma) and 1% agarose was added. Cells were incubated at 32ºC for 3-5 days and then fixed with 4% formaldehyde. After removing the agarose, cells were stained with napthol-blue black. One image per well was collected using an Olympus OM-D E-M5 Mark II digital camera. Plaque size was calculated in Image J [151]. 40-60 plaques were analyzed for each virus.

Low-MOI Infections

Low-MOI growth curves were performed at a MOI of 0.001 in MDCK cells and 0.01 in hNEC cultures. For MDCK cells and MDCK-SIAT1 cells infection took place at 32ºC for 1 hour. After the infection, the inoculum was removed and the MDCK cells were washed three times with PBS+. After washing fresh IM was added and the cells were placed at 32ºC. At the indicated times post inoculation, IM was removed from the MDCK cells and frozen at -70ºC. Fresh IM was then added. In low-MOI hNEC growth curves, the apical surface was washed three times with PBS and the basolateral media

was changed at time of infection. hNEC cultures were inoculated at a MOI of 0.01. hNEC cultures were then placed in a 32ºC incubator for 2 hours. After inoculation, the hNECs were washed three times with PBS. At the indicated times, 100ul of IM without N-acetyl trypsin was added to the apical surface of the hNECs. The hNECs were then incubated for 5 minutes at 32ºC and the IM was harvested and frozen at -80ºC. Basolateral media was changed every 48hrs post infection for the duration of the experiment.

$TCID_{50}$

MDCK cells were seeded in a 96 well plate 2 days before assay and grown to 100% confluence. Cells were washed twice with PBS+ then 180uL of IM was added to each well. Ten-fold serial dilutions of virus was created and then 20uL of the virus dilution was added to the MDCK cells. Cells were incubated for 6 days at 32ºC then fixed with 2% formaldehyde. After fixing, cells were stained with napthol blue-black, washed and virus titer was calculated [145, 150].

NA-*Star* Assay

NA-Star Influenza Neuraminidase Inhibitor Resistance Detection Kit assay was performed according to manufactures specifications (ThermoFisher Scientific). Briefly, virus titer was equalized via plaque assay. Serial two-fold dilutions of virus stock was prepared using NA-STAR assay buffer. Virus dilutions were placed in a 96 well white opaque plate. 10ul of 1X NA-*Star* substrate was then added and the plates were incubated at room temp for 30 minutes while shaking. After adding substrate, accelerator was added, and plates were read immediately by measuring luminescence of the resulting enzymatic product on a FilterMax F5 multimode microplate reader.

Enzyme Linked Lectin Assay

Enzyme linked lectin assays (ELLA) were performed as previously. Flat-Bottom Nunc MaxiSorp plates (ThermoFisher Scientific) were coated with 100ul of fetuin (Sigma) at 25µg/ml. Plates were kept at 4ºC for at least 18 hours, up to 1 month before use. Virus stock was normalized via plaque assay. Virus stocks were serially two-fold diluted in Dulbecco's phosphate buffered saline with calcium and magnesium (ThermoFisher Scientific) containing 1% BSA (Sigma) and 0.2% Tween-20 (referred to as sample buffer). Dilutions were performed in 60ul in duplicate on a Nunclon Delta Surface Round bottom 96 well plate. Fetuin coated plates were washed immediately before addition of 100ul virus dilutions. Plates were covered with a plastic lid then placed in 37ºC, 32ºC or 25ºC incubator with 5% $C0_2$ for 16-18 hours overnight. The following day, plates were washed six times with PBS containing 0.05% Tween 20 (referred to as PBST). After the last wash, 100ul of biotinylated peanut agglutinin lectin at 1µg/ml was added to every well and incubated at room temperature for 2 hours. After peanut lectin addition, plates were washed three times with PBST. Next, 100ul of 1µg/ml streptavidin-horse radish peroxidase (Millipore Sigma) was added to every well and plates were incubated at room temperature for 1 hour. Plates were then washed 3 times with PBST before the addition of 100ul of 0.5mg/ml *o*-Phenylenediamine (Sigma) diluted in phosphate-citrate buffer with sodium perborate (Sigma). Plates were incubated for 10 minutes at room temperature and reactions were stopped and developed by addition of 100ul of 2N sulfuric acid diluted in water. Absorbance was read at 405nm on a FilterMax F5 multimode microplate reader (Molecular Devices). Background of the assay (mock wells with no virus added) were then subtracted from the values.

Statistical Analysis

Statistical analysis was performed using Graph Pad Prism Software (GraphPad v8.4.2). Viral growth was analyzed using two-way anova with a Bonferroni post test correction. Differences were considered significant if $p < .05$. Plaque size and enzyme activity was analyzed using an unpaired t-Test. Differences were considered significant if $p < .05$.

Results

In the 2014-15 influenza season a novel NA genotype emerged within the human H3N2 population of viruses. The EpiFlu database was analyzed for isolates that contained either the 245 NA Gly- amino acid sequence (SAS genotype) or the 245 NA Gly+ amino acid sequence (NAS/T genotype). The 245 NA Gly+ genotype emerged in the 2014-15 season, and through the following seasons (2015 through 2018) the majority of isolates contained the putative NA glycosylation sequence at position 245 (Fig 3.1A). The addition of N-linked glycosylation sites in influenza HA and NA can significantly impact the function of either protein as well as dramatically alter the antigenicity of the viral proteins. However, it's important to verify utilization of the n-linked glycosylation site before studying the phenotype of the added 245 NA glycosylation. N-linked glycans are added co-translationally as peptides are being translated in the endoplasmic reticulum. In order for the host cell oligosaccharyl transferase enzymes to add the core glycan to the asparagine residue, N-linked glycosylation sites must be exposed to these enzymes during protein translation [194]. To assess putative glycosylation site utilization, mammalian expression vectors for representative 245 NA Gly- and 245 NA Gly+ proteins were created and transfected into human embryonic kidney cells (HEK293T) then used for SDS-PAGE and western

blotting. N-linked glycans typically increase protein molecular weight by 2-4 kDa depending on the complexity of the added glycan [195]. When the NA proteins from A/Columbia/41/2014 (245 NA Gly-) and A/Bethesda/55/2015 (245 NA Gly+) were expressed in HEK293T cells and used for western blotting, A/Bethesda/55/2015 (245 NA Gly+) was about 6 kDa heavier than the NA from A/Columbia/41/2014 (245 NA Gly-) (Fig 3.1B). This result, a size increase of 6 kDa, is larger than expected but it's important to note that much is unknown about the size or complexity of this n-glycosylation and the effect this glycan has on other n-glycans on the protein. To further verify glycan utilization, both NA proteins were immunoprecipitated and used for PNGase treatment. Treatment with PNGase F, an asparagine amidase, leaves native proteins without added n-linked glycosylations [195-197]. When the NA proteins from A/Bethesda/55/2015 (245 NA Gly+) and A/Columbia/41/2014 (245 NA Gly-) were immunoprecipitated and not treated with PNGase F, there was the expected 6 kDA difference in molecular weight due to the added N-glycan in A/Bethesda/55/2015 at position 245. However, when both proteins were treated with PNGase F, both proteins ran at the predicted molecular weight of NA at 49 kDa (Fig 3.1C). These assays confirm that the putative 245 N linked glycosylation site in A/Bethesda/55/2015 is in fact utilized, and any phenotypic differences between the isolates in viral replication and NA activity are likely due to the presence of this N-linked glycosylation at position 245 in the NA protein.

The clinical isolates that represent each NA glycosylation genotype A/Bethesda/55/2015 (245 NA Gly+) and A/Columbia/41/2014 (245 NA Gly-) were used to assess viral growth. There are a number of amino acid differences in the polymerase

enzymes, however no amino acid differences in the HA and only the glycosylation site difference in the NA (Table 3.1). These viruses were first used for plaque size and morphology on MDCK cells (Figure 3.2A). Even though both isolates showed a decreased ability to produce clear and defined plaques, when quantifying plaque area both isolates produced similar sized plaques (Figure 3.2B). Next, the virus isolates were characterized with a low MOI growth curve on MDCK cells (Figure 3.2C). Both viruses had similar kinetics and showed no significant difference in peak virus titer. The isolates were then characterized on MDCK-SIAT1 cells, which overexpress the human enzyme CMP-*N*-acetylneuraminate:β-galactoside α-α2,6-sialyltransferase that results in these MDCK-SIAT1 cells producing more surface carbohydrates with terminal α-α2,6 sialic acid. Both isolates showed nearly identical kinetics of infectious virus production and peak infectious virus titer after a low MOI infection (Figure 3.2D). However, when using these isolates for a low MOI growth curve with hNEC cultures, the isolate with the 245 NA Gly- genotype grew to a significantly higher titer compared to the isolate with the 245 NA Gly+ genotype. Both viruses reached a similar peak titer of infectious virus production, but the 245 NA Gly+ isolate reached peak titer 24 hours after the 245 NA Gly- isolate. This data suggests that the 245 NA glycosylation does not impact replication on immortalized cells, but significantly decreases replication of 245 NA Gly+ isolates on primary differentiated hNEC cultures.

Because there was a replication difference on hNECs, but not immortalized cell cultures with clinical isolates that differed in 245 NA glycosylation status, we next assessed the enzymatic function of each isolate in two different enzymatic activity assays. Human nasal epithelial cells express membrane-bound mucins as well as

secrete mucins from the apical surface of the cells [198-200]. We hypothesized that a difference in NA activity could contribute to the difference in replication kinetics seen on hNEC cultures. Mucins are rich in o-linked glycosylations that contain a terminal sialic acid residue and serve as decoy receptors to protect the cells from influenza viruses and other viruses that use sialic acid as a receptor [198, 201, 202]. The NA protein from both clinical isolates used in this study have a nearly identical amino acid sequence, with the only difference being the 245-247 N-linked glycosylation sequence. Residues 245-247 are not known to be involved in enzymatic function or coordinating ligands for the NA protein. Therefore, we assessed the ability of this glycan to impact enzymatic activity with a relatively small luminescent substrate with the NA-STAR assay and a large, more physiologically relevant, glycan as substrate in the ELLA assay. With viral content normalized via plaque forming units, A/Columbia/41/2014 with the 245 NA Gly- genotype had a significantly higher amount of enzymatic activity in the NA-STAR assay, suggesting that this glycan blocks the ability of even this small substrate to access the active site (Figure 3.3A). When comparing the activity of each NA protein at the highest concentration of virus, A/Bethesda/55/2015 (245 NA Gly+) had on average 62% of the activity of A/Columbia/41/2014 (245 NA Gly-) (Figure 3.3B). Using the ELLA assay, we found that at a broad range of temperatures tested (37ºC, 32ºC and 25ºC) the same trend held true, where A/Bethesda/55/2015 (245 NA Gly+) genotype had 25-30% of the activity of A/Columbia/41/2014 (245 NA Gly-) (Figure 3.3C-3G). This suggests that regardless of temperature the 245 NA Glycosylation significantly decreases enzymatic activity of isolates that carry the 245 NA glycosylation genotype.

Discussion

In this study we show that H3N2 clinical isolates that contain a putative 245 N-linked glycosylation site quickly dominated the human H3N2 population. This putative glycosylation site is utilized when the NA proteins are expressed in human cells (Figure 3.1). Within a year of seasonal circulation, this H3N2 virus became the dominant genotype, with the glycosylation site utilized. We next studied how this glycosylation impacted viral fitness. We found that the glycosylation did not impact virus replication in plaque assays, nor multi-step viral growth using immortalized MDCK or MDCK-SIAT1 cells. However, this glycosylation had a significant impact on virus growth when primary differentiated hNEC cultures were used as a substrate for viral growth (Figure 3.2). We then studied the effect that this 245 NA glycosylation had on viral enzyme function in two different activity assays, the NA-STAR assay and the ELLA assay. In both assays, the isolate A/Columbia/41/2014 with the 245 NA Gly- genotype showed a significantly higher enzymatic activity compared to the isolate A/Bethesda/55/2015 with the 245 NA Gly+ genotype (Figure 3.3). The spectrum of temperatures used in the ELLA assays in Figure 3 was designed to assess enzymatic activity at temperatures present in areas of virus replication in the entire respiratory tract. The upper airway for humans averages 32ºC as ambient or room-temperature (25ºC) air is drawn in through the nasal passage, and warmer air (core body temperature of 37ºC) is exhaled [203, 204]. Regardless of temperature (37ºC, 32ºC or 25ºC), enzymatic activity was decreased in the ELLA assay if the neuraminidase protein contained the 245 n-glycosylation. As expected, the activity of each neuraminidase protein decreased as the assay temperature decreased but the difference between 245 NA Gly- and 245 NA Gly+ activity remained roughly the same at

each temperature (Figure 3.3D, E, G). This suggests that at any physiological relevant temperature, the 245 n-linked glycan decreases enzymatic activity.

Taken together, these results suggest that the addition of a large n-glycan near the active site of the enzyme incurs a significant fitness cost to the currently circulating H3N2 viruses. The 2014-15 season was a moderate to severe influenza season [205]. The vaccine efficacy during this season for H3N2 viruses was around 6% (95% CI -5% to 17%) in all age groups and thus offered no significant protection against H3N2 infection [205, 206]. Poor vaccine efficacy in the 2014-15 season has been attributed to the emergence of a new HA clade, the H3N2 3c.2a clade, but it's likely that the emergence of the 245 NA glycosylation genotype could further impact the ability of host antibodies to neutralize the virus [207]. Antibodies against NA are correlates of protection in many age groups and a drastic change in the antigenicity of the NA protein could impact the ability of individuals' pre-existing immunity [208, 209]. The 245 N-linked glycosylation has been shown to mask an important antigenic epitope near the active site of the enzyme and block inhibitory antibodies that target residues in and around the active site [109].

One important note of this study is using the representative clinical isolates and not isogenic recombinant viruses. The clinical isolates have an identical HA sequence to each other, but importantly both isolates lost a glycosylation on the HA protein during isolation. The effect of this HA glycosylation is unknown at this time, especially considering the balance of HA and NA function and how glycosylations on both proteins play into this balance [97-99]. While not the focus of this study, A/Bethesda/55/2015 (245 NA Gly+) had non-synonymous mutations in each polymerase segment compared

to A/Columbia/41/2014 (245 NA Gly-). Another mutation occurs in an alternate reading frame of PB1, the PB1-F2 protein [210]. The function of this PB1-F2 mutation, which has also fixed in the circulating human H3N2 population, is unknown at this time. It is also possible that one of the amino acid differences noted in Table 3.1 could compensate for the fitness cost of the 245 NA glycosylation in regard to transmission in the human population.

This study, and others like it, highlight the necessity to study how variants in circulating human influenza viruses become dominant in the span of a few influenza seasons. Since the introduction of the 245 NA glycosylation site, nearly all circulating human H3N2 influenza viruses contain this glycosylation. While this glycosylation seemingly decreases virus fitness, it potentially gives an important fitness benefit by blocking active site-specific antibodies from recognizing and inhibiting NA activity.

Figures and Tables

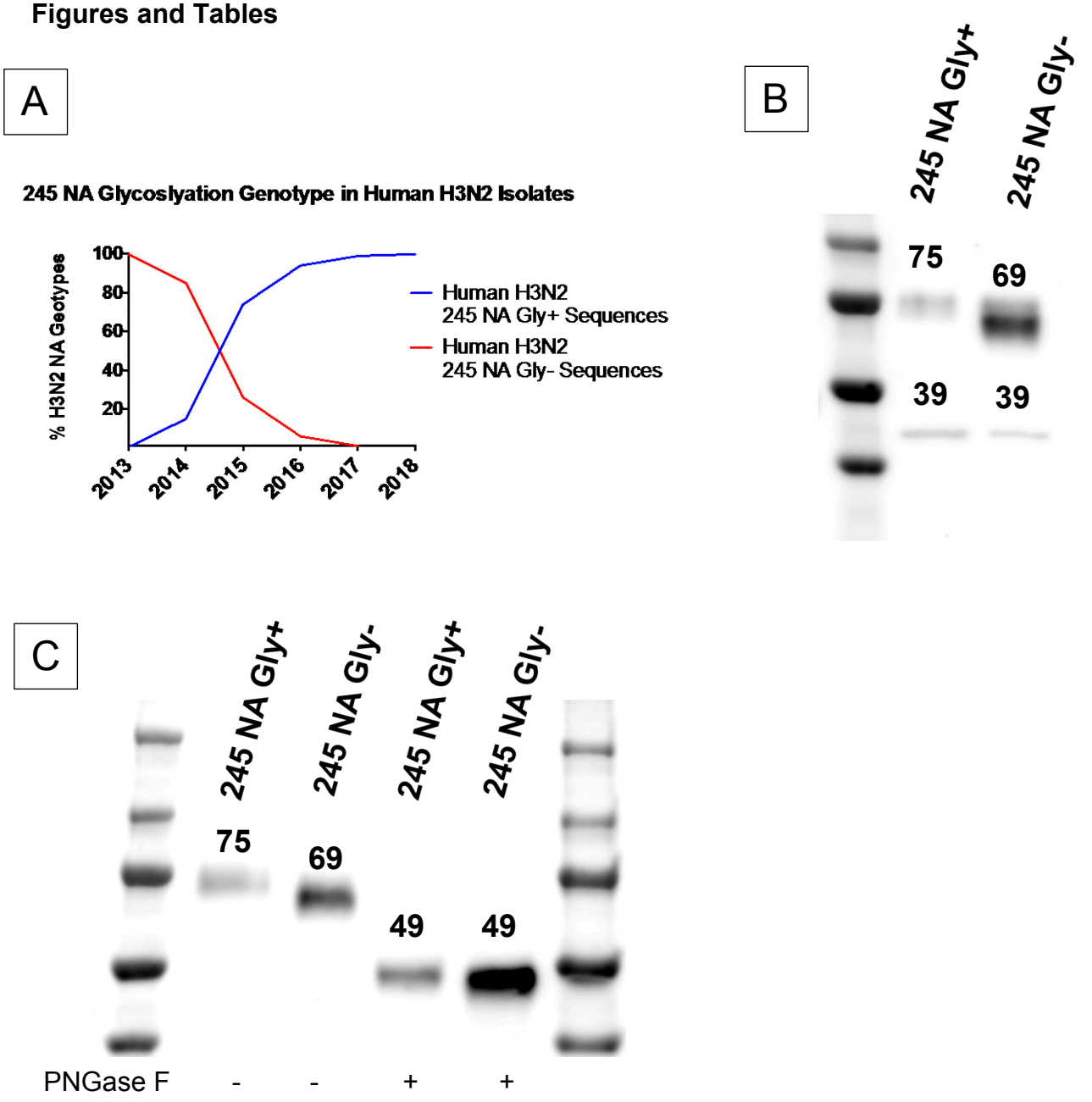

Figure 3.1: Emergence of 245 NA Gly+ genotype in human isolates and utilization of the putative 245 NA Glycosylation site.

(**A**) EpiFlu data base human H3N2 NA sequence analysis from 2013 through 2018 season. Sequences were pulled from EpiFlu database and analyzed for presence of either SAS amino acid sequence at positions 245-247 (NA Gly-) or NAS/T amino acid sequence at position 245-247 (245 NA Gly+). Data are representated as a percentage of all complete NA sequences that had either amino acid sequence present at 245-247 in the NA protein. (**B**)The FLAG tagged NA protein from A/Bethesda/55/2015 (245 NA Gly+) and A/Columbia/41/2014 (245 NA Gly-) protein was transiently expressed in

HEK293T cells and subjected to SDS-PAGE and western blotting. Numbers above protein bands indicate measured size in kilo Daltons (kDa). Beta-Actin was used as a loading control (39 kDa each lane). The NA from A/Bethesda/55/2015 was calculated to be 6 kDa heavier. (**C**) The FLAG tagged NA proteins treated with or without PNGase. Fully glycosylated proteins (lanes 1 and 2) have a 6 kDa difference in size whereas PNGase treated proteins (lanes 3 and 4) have the same size (49kDa). NA and Beta-Actin protein size in A and B were determined using Bio-Rad software and via true-blue protein ladder (Bio-Rad) as a size standard.

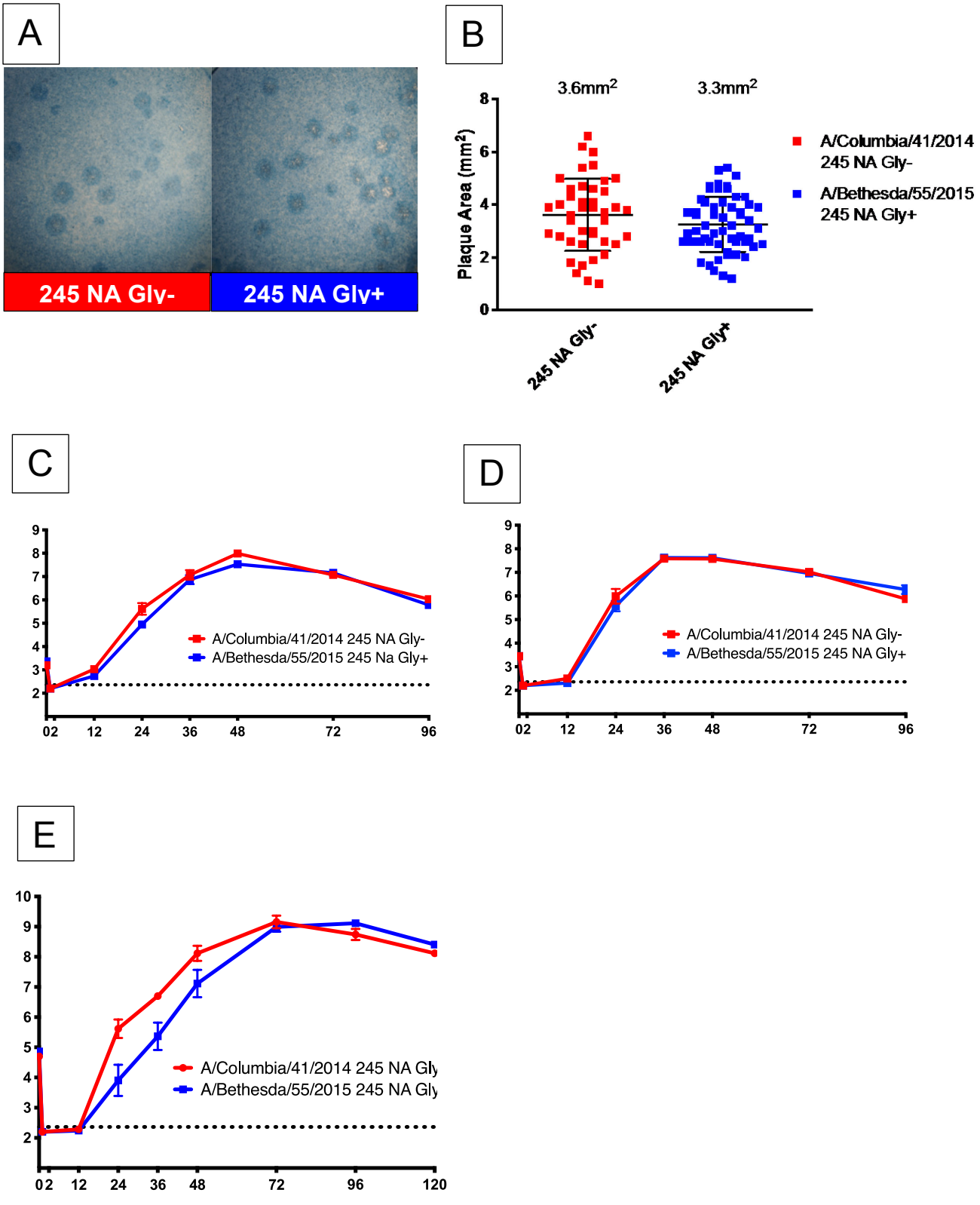
A
245 NA Gly-
245 NA Gly+
B
3.6mm2
3.3mm2
Plaque Area (mm2)
A/Columbia/41/2014
245 NA Gly-
A/Bethesda/55/2015
245 NA Gly+
245 NA Gly-
245 NA Gly+
C
A/Columbia/41/2014 245 NA Gly-
A/Bethesda/55/2015 245 Na Gly+
D
A/Columbia/41/2014 245 NA Gly-
A/Bethesda/55/2015 245 NA Gly+
E
A/Columbia/41/2014 245 NA Gly
A/Bethesda/55/2015 245 NA Gly

Figure 3.2: Replication of clinical isolate H3N2 viruses with or without 245 NA glycosylation in MDCK, MDCK-SIAT1, or hNEC cultures

(**A**) Plaque assay performed with clinical isolates with 245 NA Gly + or 245 NA Gly - genotype on MDCK cells. (**B**) Quantification of plaque area from 40-60 individual plaques per virus from 3 independent experiments. *p<.05 unpaired T test. Error bars are SEM. Multi-step low MOI growth curves with MDCK (**C**) MDCK-SIAT1 cultures (**D**) or hNEC (**E**) with the indicated clinical isolates at 32ºC. Hours post infection (HPI) on X axis, Log of TCID50/ml on Y axis. Data are pooled from 3 independent experiments with four replicates per virus per experiment (total n = 12 wells per virus timepoint). Data were analyzed with *p<.05 and two-way repeated measures ANOVA with Bonferroni multiple comparison posttest. The limit of detection (L.O.D.) is indicated with a dotted line at log 2.37 TCID50/ml. Error bars in A and B are SEM. Stats calculated in GraphPad Prism 8.

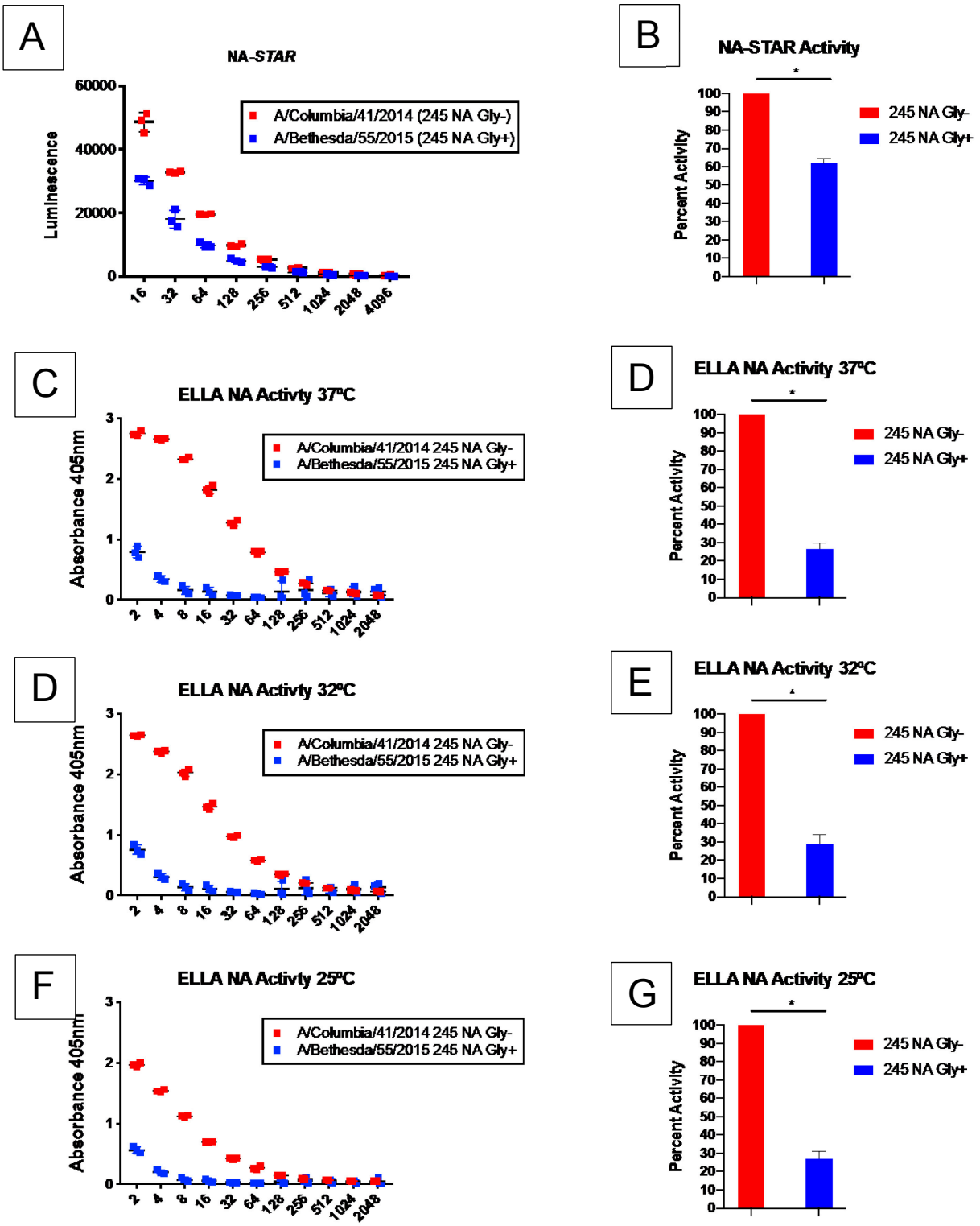

Figure 3.3: Neuraminidase activity of H3N2 clinical isolates that differ in 245 NA glycosylation status

With viral content normalized via plaque assay, clinical isolates NA activity was tested via the NA-STAR (**A-B**) and ELLA (**C-G**) assay. ELLA assay was conducted at three

separate temperatures in humidified incubators (C-G) to asses temperature effect on NA activity for each clinical isolate. In B, D, E, G A/Columbia41/2014 245 NA Gly- average activity for the highest virus concentration was set to 100%. The average activity for the highest virus concentration of A/Bethesda/55/2015 245 NA Gly+ is shown as a percentage of that activity. In Figures A, C, D, F numbers on x-axis are the dilution of virus, where for example “2” indicates a 1:2 dilution of the viral stock. * $p < .05$ unpaired T test.

Segment/Protein	A/Columbia/41/2014 number and residue	A/Bethesda/55/2015 number and residue
HA	-	-
NA	245S 247S	245N 247T
PB1	525T	525M
PB1-F2	75H	75P
PB2	739N	739D
PA	313M	313I
NP	-	-
NS1	-	-
NEP	-	-
M1	-	-
M2	-	-

Table 3.1: Amino acid differences between A/Bethesda/55/2015 (245 NA Gly+) and A/Columbia/41/2014 (245 NA Gly-) used for isolate characterization
Differences are shown with standard single letter abbreviations for amino acid names. No difference or presence of synonymous mutation is shown with a dash.

CHAPTER 4: A neuraminidase glycosylation in H3N2 clade 3c.2a impacts virus growth on human nasal epithelial cells, neuraminidase activity, and inhibitory antibody binding

Harrison Powell and Andrew Pekosz

Manuscript Submitted to PLOS Pathogens and Biorxiv [211]

Doi: 10.1101/2020.02.20.957399

Abstract

In the 2014-2015 influenza season a novel neuraminidase (NA) genotype emerged in the Johns Hopkins Center of Excellence for Influenza Research and Surveillance (JH CEIRS) surveillance network as well as globally. This novel genotype encoded a glycosylation site at position 245-247 in the NA protein from clade 3c.2a H3N2 viruses. In the years following the 2014-2015 season, this novel NA glycosylation genotype quickly dominated the human H3N2 population of viruses. To assess the effect this novel glycosylation has on virus fitness and antibody binding, recombinant viruses with (NA Gly+) or without (NA Gly-) the novel NA glycosylation were created. Viruses with the 245 NA Gly+ genotype grew to a significantly lower infectious virus titer on primary, differentiated human nasal epithelial cells (hNEC) compared to viruses with the 245 NA Gly- genotype, but growth was similar on immortalized cells. The 245 NA Gly+ blocked human and rabbit monoclonal antibodies that target the enzymatic site from binding to their epitope. Additionally, viruses with the 245 NA Gly+ genotype had significantly lower enzymatic activity compared to viruses with the 245 NA Gly- genotype. Human monoclonal antibodies that target residues near the 245 NA glycosylation were less effective at inhibiting NA enzymatic activity and virus replication of viruses encoding an NA Gly+ protein compared to ones encoding NA Gly- protein. Additionally, a recombinant H6N2 virus with the 245 NA Gly+ protein was more resistant to enzymatic inhibition from convalescent serum from H3N2-infected humans compared to viruses with the 245 NA Gly- genotype. Finally, the 245 NA Gly+ protected from NA antibody mediated virus neutralization. These results suggest that while the 245 NA Gly+ decreases virus replication in hNECs and decreases enzymatic activity, the

glycosylation blocks the binding of monoclonal and human serum NA specific antibodies that would otherwise inhibit enzymatic activity and virus replication.

Introduction

Each year seasonal influenza accounts for 3 to 5 million incidences of severe disease and up to 650,000 deaths [212]. Most influenza vaccines rely on the generation of antibodies against the hemagglutinin (HA) protein, one of the two major glycoproteins on the virion surface. The anti-HA protein antibodies inhibit virus entry into cells but also provide an immune pressure which leads to the emergence of virus strains with mutations in HA antigenic sites [213, 214]. This antigenic drift leads to escape from vaccine- and infection-induced immunity and results in the need to change influenza vaccine strains on a fairly frequent basis.

There is renewed interest in generating influenza vaccines that provide broader and stronger protection against several virus strains [215-217] and the other major influenza surface glycoprotein, the NA protein, has emerged as a potential candidate for such a universal influenza vaccine [217]. The NA protein has a neuraminidase activity that is critical in two stages of the virus life cycle[60, 61, 218]. The NA protein cleaves sialic acid from mucins that coat airway epithelial cells which reduces HA protein binding to mucins and facilitates entry into respiratory epithelial cells[102]. The neuraminidase activity also removes sialic acid from host cell membrane bound proteins and viral HA and NA proteins at late times post infection, allowing viral particles to efficiently bud and spread to other respiratory epithelial cells[61, 219].

Anti-NA antibodies can prevent or decrease the severity of influenza infection[94-96, 220]. High titer anti-NA antibodies have been correlated with decreased disease severity and protection in adults[209, 221]. Seasonal influenza A and B viruses have a

conserved epitope in the NA protein which is necessary for enzymatic function[88, 89]. Antibodies that target this epitope inhibit neuraminidase function and virus replication. Neuraminidase antibodies can be potent and broadly reactive [95, 222]. Anti-NA antibodies increase in titer with age and are capable of recognizing influenza strains isolated in many different influenza seasons [89, 95, 222]. Additionally, a subset of anti-NA antibodies raised in a human infection are broadly cross reactive and protective against influenza A and B virus strains [88, 89].

Neuraminidase antibodies can directly inhibit NA function as well as virus replication. Antibodies that bind neuraminidase can inhibit enzymatic activity, presumable through steric inhibition of substrate accessing the active site [94, 95]. Blocking NA activity prevents the virus from properly budding, leading to virions which aggregate at the cell surface [60, 95, 223]. Furthermore, escape mutants that decrease binding of certain active site targeting anti-NA antibodies incur a significant fitness disadvantage in virus replication and enzymatic activity [89]. This is due to mutating residues critical for the enzymatic function which these broadly reactive antibodies target. These studies indicate the NA protein has a highly conserved and critical epitope which can be targeted by neutralizing antibodies. Targeting the NA protein has recently become one strategy for generating a universal influenza vaccine [94, 208, 209, 222]. As such, a polyclonal antibody response to the NA protein assures inhibition of NA function as well as steric hindrance of the HA protein - effectively neutralizing virus entry and release.

While the HA protein is the immunodominant antigen on the influenza virion, previous studies have shown the function and significance of anti-NA antibodies in

vaccination and natural infection [94, 95, 222, 224, 225]. However, this immune pressure can also lead to the selection of viruses that have accumulated mutations in NA protein antigenic sites. NA antigenic drift has been suggested to occur at lower frequency than HA antigenic drift but can have an impact on influenza spread and antibody recognition of NA [226-228].

In 2014-2015 a novel genotype emerged in the human H3N2 influenza viruses. This new genotype encoded an N-linked glycosylation at position 245-247 in the N2 NA protein. This glycosylation is located in close proximity to the NA active site and near a known antigenic site [229]. In chapter 3, we found that this glycosylation could impact virus replication, but that work was done using clinical isolates. Therefore, in this chapter we used recombinant isogenic viruses to study only the effect that the 245 NA glycosylation has on virus replication. Using infectious clone technology to assess viral fitness and enzymatic activity, we demonstrate that this NA glycosylation prevents binding of inhibitory antibodies but also reduces NA enzymatic activity and virus fitness in human nasal epithelial cell cultures. The fitness cost of this mutation is therefore balanced by the advantage provided through the escape of preexisting immunity, contributing to viruses with this NA genotype becoming the dominant global H3N2 human virus strain.

Materials and Methods

Cell Lines and Primary Cells

Madin-Darby Canine Kidney Cells (MDCK) and human embryonic kidney cells 293T (HEK293T) were maintained in complete medium (CM) consisting of Dulbecco's Modified Eagle Medium (DMEM) supplemented with 10% fetal bovine serum, 100U/ml penicillin/streptomycin (Life Technologies) and 2mM Glutamax (Gibco). Human nasal

epithelial cells (hNEC) were isolated from non-diseased donor tissue following endoscopic sinus surgery. Cells were grown, differentiated and maintained at the air liquid interface as previously described [129, 138, 145]. hNEC differentiation medium and maintenance medium was prepared as previously described [138, 142, 146]. hNEC cultures were used for low MOI growth curves only when fully differentiated. All cells were maintained at 37ºC in a humidified incubator supplemented with 5% CO2.

Plasmids

The plasmid pHH21 was used to generate full length influenza hemagglutinin (HA) or neuraminidase (NA) plasmids for recombinant virus production. Briefly, viral RNA was isolated from the clade 3c.2a H3N2 viruses A/Bethesda/P0055/2015 (NA Gly+ ID 253812) and A/Columbia/P0041/2014 (NA Gly- ID 253817) with a Qiagen mini-vRNA isolation kit. Gene specific primers with cloning sites for H3N2 neuraminidase or hemagglutinin were used to create cDNA via a one-step RT-PCR reaction (SuperScript III-Platinum Taq mix, ThermoFisher Scientific). The cDNA products were cut with appropriate restriction enzymes, column purified (QIAquick PCR Purification kit) and ligated with restriction enzyme cut-pHH21 using T4-ligase (New England Biolabs, NEB). Ligation products were transformed into DH5a (NEB) cells and colonies were mini-prepped (QIAprep spin mini-prep) and Sanger sequence verified. Sequence verified colonies were maxi-prepped (ZymoPURE) and used for recombinant virus preparation. Since the HA amino acid sequence between A/Bethesda/55/2015 is identical to A/Columbia/41/2014, A/Bethesda/55/2015 HA-pHH21 plasmid was used for both H3N2 viruses. The codon at amino acid position 160 in HA (H3 numbering, Threonine) was modified via site-directed mutagenesis (Agilent) from the wild type (ACA, Thr) to a new

codon (ACT, Thr) less likely to revert to a lysine codon- which occurred frequently during previous attempts to virus rescue.

H6 hemagglutinin-pHH21 was synthesized by Genscript (www.genscript.com) in the pHH21 vector. The H6 HA coding sequence from A/Environment/Hubei-Jinzhou/02/2010 [230] was inserted into pHH21 flanked by human H3 5' (*GCAAAAGCAGGGGATAATTCTATTAACC*) and 3' (*TAAGAGTGCATTAATTAAAAACACCCTTGTTTCTACTAA*) UTR sequences. After gene synthesis, two mutations (Q223L and G225S) were added in the HA coding sequence to increase HA protein binding to α2,6 sialic acid [150]. The gene product was transformed into DH5a (NEB) and maxi-prepped for recombinant virus production. pHH21 plasmids encoding the internal segments for A/Victoria/361/2011 (H3N2, rVic recombinant viruses) or A/WSN/33 (H6N2, rWSN recombinant viruses) were generated as previous described [148].

The plasmid pCAGGS was used for transient expression of C-terminal flag-tagged NA Gly+ or NA Gly- neuraminidase proteins. C-terminal flag tag (DYKDDDDK) was added to pHH21-NA encoding plasmids via site directed mutagenesis (Agilent). cDNA was generated from the pHH21-NA flag plasmids with Q5 Hot-Start PCR (NEB). This cDNA product was then cloned into the mammalian expression vector pCAGGS for transient transfection experiments as previously described [145].

Recombinant Virus Production

Recombinant H3N2 or H6N2 viruses were generated using the 12-plasmids reverse genetics system as previously described [148]. Briefly HEK293T cells were plated at 50% confluency 1 day before transfection in complete media. On the day of transfection, media was replaced with serum free Opti-MEM. HEK293Ts were then

transfected with eight plasmids encoding full length influenza segments in the pHH21 vector (PB2, PB1, PA, HA, NP, NA, M, NS) and four plasmids encoding the influenza replication proteins in the pcDNA3.1 vector (PB2, PB1, PA and NP). At one day post transfection 5μg/ml N-acetyl trypsin was added to the transfection reaction. MDCK cells were over-laid four hours post trypsin treatment. Every 24 hours post MDCK-overlay virus containing supernatant was sampled for virus production. Fresh Opti-MEM with 5μg/ml N-acetyl trypsin was added when a sample was taken. Virus from the transfected cell supernatants was plaque purified as described below, sequenced, and used to generate seed stocks by infecting MDCK cells at a MOI of 0.001. Working stocks were generated from sequence confirmed seed stocks by infecting MDCK cells at a MOI of .001 as described below.

Plaque Assay

MDCK cells were grown in complete medium to 100% confluency in 6-well plates. Complete medium was removed, cells were washed twice with PBS containing 2mm calcium magnesium (PBS+) and 400μL of inoculum was added. Cells were incubated at 32ºC for 1hr with rocking every 15 minutes. After 1hr, the virus inoculum was removed and phenol-red free DMEM supplemented with .3% BSA (Sigma), 100U/ml pen/strep (Life Technologies), 2mM Glutamax (Gibco), 5mM HEPES buffer (Gibco) 5μg/ml N-acetyl trypsin (Sigma) and 1% agarose was added. Cells were incubated at 32ºC for 3-5 days and then fixed with 4% formaldehyde. After removing the agarose, cells were stained with napthol-blue black. Plaque size was analyzed in ImageJ [151]. For recombinant virus production, virus plaques were picked with a pipette instead of fixing with formaldehyde and placed in IM and stored at -80ºC for later seed stock generation.

Virus Seed and Working Stocks

For generation of recombinant virus seed stocks, 400µl of plaque picked virus was added to confluent MDCK cells plated in 6 well plates and infected for 1hr as previously described [145, 150]. The plaque pick inoculum was removed and infection media (IM) was added. Infection medium (IM), consisted of DMEM with .3% BSA (Sigma), 100U/ml pen/strep (Life Technologies), 2mM Glutamax (Gibco) and 5µg/ml N-acetyl trypsin((Sigma)). Cells were placed in a 32ºC incubator and monitored daily for CPE. Seed stock was harvested between 3 and 5 days or when CPE reached approximately 75-80%. Seed stocks were then sequenced, and infectious virus titer determined by TCID50. A working stock for each virus was generated by infecting confluent MDCK cells in a T75 flask at a MOI of .001 for 1 hour at 32ºC. The inoculum was removed, and IM was added. Cells were monitored daily for CPE and working stock harvested when CPE reached approximately 75-80%. Working stocks were sequenced verified and infectious virus determined via TCID50 as described below.

Low-MOI Infections

Low-MOI growth curves were performed at a MOI of 0.001 in MDCK cells and 0.01 in hNEC cultures. MDCK cell infections were performed as described above. After the infection, the inoculum was removed and the MDCK cells were washed three times with PBS+. After washing, IM was added and the cells were placed at 32ºC. At the indicated times post inoculation, IM was removed from the MDCK cells and frozen at -80ºC. Fresh IM was then added. For low-MOI growth curves in the presence of monoclonal antibodies, the indicated antibodies were added to the IM after the virus was allowed to attach to cells. In low-MOI hNEC growth curves, the apical surface was washed three times with PBS and the basolateral media was changed at time of

infection. hNEC cultures were inoculated at a MOI of 0.01. hNEC cultures were then placed in a 32ºC incubator for 2 hours. After inoculation, the hNECs were washed three times with PBS. At the indicated times, 100µl of IM without N-acetyl trypsin was added to the apical surface of the hNECs. The hNECs were then incubated for 5 minutes at 32ºC and the IM was harvested and frozen at -80ºC. Basolateral media was changed every 48hrs post infection for the duration of the experiment.

$TCID_{50}$

MDCK cells were seeded in a 96 well plate 2 days before assay and grown to 100% confluence. Cells were washed twice with PBS+ then 180µL of IM was added to each well. Ten-fold serial dilutions of virus was created and then 20µL of the virus dilution was added to the MDCK cells. Cells were incubated for 6 days at 32ºC then fixed with 2% formaldehyde. After fixing, cells were stained with napthol blue-black, washed and virus titer was calculated [145, 150].

Transient Transfection for NA-Flag expressing cells

Transient transfection of HEK293T was performed with TransIT-LT1 per the manufacturers protocol. Briefly, cells were grown in complete medium until time of transfection to roughly 50% confluency. On the day of transfection, complete medium was removed and replaced with Opti-MEM serum free medium. Opti-MEM, TransIT-LT1 and 2.5ug of plasmids encoding gene of interest were mixed then added to HEK293T cells. At 16hr post transfection wells were used for flow cytometric analysis.

NA Antibodies

NA specific monoclonal antibodies 229-1G03, 235-1C02 and HCA2 were used to assess binding to NA proteins. 229-1G03 and 235-1C02 were provided by Patrick Wilson [222]. 235-1C02 binds to residues 249 and 428 on the NA protein as described and the 229-1G03 binds to an as yet uncharacterized epitope on the N2 NA protein.

HCA-2 monoclonal antibody was provided by Sean Li [88]. HCA-2 binds to a known, highly conserved epitope in the active site of the NA protein, residues 222-230 ILRTQESEC. To assess antibody binding to expressed NA proteins, all monoclonal antibodies were diluted to 1µg/ml 1X PBS (Quality Biologics) containing .1% BSA, (Sigma) was used throughout antibody staining protocol (FACS buffer). The antibodies were then serially diluted 1:2 in FACS buffer. Mouse anti-FLAG (clone M2, Sigma) was diluted in FACS buffer to 1µg/ml. For western blotting mouse anti-FLAG and anti-influenza M1 antibody were diluted to 2µg/ml in blocking buffer. Antibodies were diluted in IM for virus neutralization assays. For low MOI growth curve viral inhibition, NA inhibitory antibodies were diluted in IM + 5ug N-Acetyl Trypsin. 229-1G03 was diluted to 1.5nm, 235-1C02 1.3nm, and human IgG isotype clone IGHG1 diluted to 5nM.

Secondary Antibodies

Secondary antibodies were used to detect binding of primary unconjugated monoclonal antibodies. Goat anti-Mouse IgG Alexa Fluor 488, Goat anti-Rabbit IgG Alexa Fluor 647 and Goat anti-Human IgG Alexa Fluor 647 were used at 1µg/ml concentration in FACS buffer (ThermoFisher Scientific). For western blotting, all secondary antibodies were diluted in blocking buffer at a concentration of 1µg/ml.

Human Serum

Convalescent human serum obtained through the JH-CEIRS study (HHSN272201400007C) were used in this study. Serum samples were treated with receptor destroying enzyme (Cosmos Biological) and heat treated according to the manufacturers protocol for use in ELLA studies.

Flow Cytometry

HEK293T cells were detached with 0.05% Trypsin-EDTA (Life Technologies) and fixed with 2% paraformaldehyde (Affymetrix) at room temperature for 15 minutes. Cells

were washed with FACS buffer after fixation and stained with the indicated amounts of human or rabbit monoclonal antibody and anti-FLAG mouse monoclonal antibody. Cells were washed twice in FACS butter between each antibody incubation step. Cells were analyzed on a BD-FACS Calibur and data analyzed with FlowJo V10.5.3 software. Geometric mean was used to identify mean fluorescence intensity (MFI).

Partially Purifying Virus Particles

Virus partially purified by ultracentrifugation over a sucrose cushion for SDS-PAGE and western blotting. Clarified virus working stock supernatant was overlaid onto a 25% sucrose-NTE (100nM NaCl (ThermoFisher Scientific), 10mM Tris-HCl (Promega) and 1mM EDTA (Sigma)) buffer pH of 7.5. Virus was centrifuged at 27,000 RPM in a SW-28 rotor in a Beckman Coulter Optima L90-K UltraCentrifuge for 2 hours. After the first ultracentrifugation, the supernatant was removed. The virus pellet was re-suspended in PBS. Pellet was further concentrated by ultracentrifugation in an SW-28ti rotor at 23,000 RPM for 1hr. The pellet was resuspended in PBS for use in NA activity, western blotting and PNGase assays.

PNGase, SDS-PAGE and Western Blotting

Partially purified virus particles were used for SDS-PAGE. For PNGase treatment, the PNGase kit from (NEB) was used per manufacturer's instructions. After PNGase treatment, all samples were treated with 4X-Laemli buffer (Bio-Rad) containing 250mM dithiothreitol (DTT, ThermoFisher Scientific) and boiled at 100ºC for 5 minutes. Samples were run on 4-20% Mini-PROTEAN TGX gels (Bio-Rad) with an All-Blue precision plus protein ladder (Bio-Rad) at 70v. Proteins were transferred onto an immobilon-FL membrane (Millipore) at 75v for 1hr. After transfer, membranes were blocked with blocking buffer (PBS containing 0.05% Tween-20 (Sigma) and 5% non-fat

milk (Bio-Rad)) for 1 hour at room temp. Primary antibody (HCA2 and anti-M1) was incubated overnight at 4ºC in blocking buffer. Membranes were washed in PBS with .05% Tween-20 (wash buffer). Secondary antibody was added for 1hr at room temperature (25ºC) in blocking buffer then washed again in wash buffer. Blots were imaged and analyzed with the FluorChem Q system (ProteinSimple).

NA-*Star* Assay

NA-Star Influenza Neuraminidase Inhibitor Resistance Detection Kit assay was performed according to manufactures specifications (ThermoFisher Scientific). Briefly, serial two-fold dilutions of human serum or monoclonal antibodies were mixed in NA-STAR assay buffer. An equal volume of partially purified virus diluted in NA-Star assay buffer was added to the antibody dilutions. This mixture of virus and antibody was placed in a 96 well white opaque plate and incubated at room temp for 30 minutes with gently horizontal shaking. After incubation, 10ul of 1X NA-*Star* substrate was added and the plates were incubated at room temp for an additional 30 minutes while shaking. After adding substrate, accelerator was added and plates were read immediately by measuring luminescence on a FilterMax F5 multimode microplate reader. To assess overall NA activity, no monoclonal antibody was added. Data was analyzed in Prism (GraphPad) and 50% inhibition was defined as antibody or serum concentration that resulted in at least 50% inhibition of NA activity compared to virus without antibody.

Enzyme Linked Lectin Assay

Enzyme linked lectin assays (ELLA) were performed as previously [231, 232]. Flat-Bottom Nunc MaxiSorp plates (ThermoFisher Scientific) were coated with 100µl of fetuin (Sigma) at 25µg/ml. Plates were kept at 4ºC for at least 18 hours, up to 1 month

before use. Monoclonal antibodies, human serum or oseltamivir were serially two-fold diluted in Dulbecco's phosphate buffered saline with calcium and magnesium (ThermoFisher Scientific) containing 1% BSA (Sigma) and .2% Tween-20 (referred to as sample buffer). Dilutions were performed in 60µl in duplicate on a Nunclon Delta Surface Round bottom 96 well plate. Virus was added to sample buffer, and 60µl of virus was added to the dilution plate. For monoclonal antibody and inhibitor experiments recombinant H3N2 virus was used. For human serum, recombinant H6N2 virus was used. NA content was equalized via western blotting for H3N2 or virus content equalized via plaque assay for H6N2. Fetuin coated plates were washed immediately before addition of 100µl virus premixed with antibody, serum or oseltamivir. Plates were covered with a plastic lid then placed in 37ºC incubator with 5% $C0_2$ for 16-18 hours overnight. The following day, plates were washed six times with PBS containing .05% Tween 20 (referred to as PBST). After the last wash, 100µl of biotinylated peanut agglutinin lectin at 1µg/ml was added to every well and incubated at room temperature for 2 hours. After peanut lectin addition, plates were washed three times with PBST. Next, 100µl of 1µg/ml streptavidin-horse radish peroxidase (Millipore Sigma) was added to every well and plates were incubated at room temperature for 1 hour. Plates were then washed 3 times with PBST before the addition of 100µl of .5mg/ml *o*-Phenylenediamine (Sigma) diluted in phosphate-citrate buffer with sodium perborate (Sigma). Plates were incubated for 10 minutes at room temperature and reactions were stopped and developed by addition of 100µl of 2N sulfuric acid diluted in water. Absorbance was read at 405nm on a FilterMax F5 multimode microplate reader (Molecular Devices). To assess NA activity, no monoclonal antibody was added. Data

was analyzed in Prism (GraphPad8) and 50% inhibition was defined as antibody or serum concentration that resulted in at least 50% inhibition of NA activity compared to virus without antibody.

NA-Fluor Assay

NA-Fluor Influenza Neuraminidase Assay was performed according to manufacturer's specifications and enzyme kinetics experiments performed as previously reported [233]. For enzyme kinetics, MUNANA substrate was serially two-fold diluted in assay buffer on an opaque black 96 well plate. Virus was prepared in assay buffer then added to the plate containing MUNANA substrate dilutions. Fluorescence was measured every 60s for 1 hour after addition of virus on a FilterMax F5 multimode microplate reader (Molecular Devices). Enzyme Vmax and Km was calculated using Prism software (GraphPad).

NA Neutralizing Antibody Assay

To assess the ability of monoclonal antibodies ability to inhibit virus replication, a neutralizing assay was performed. MDCK cells were plated to 100% confluency on 96 well plates and washed twice with PBS+. A two-fold serial dilution of monoclonal antibody was made in IM + 5µg/ml N-acetyl trypsin at a starting concentration of 100nm in a volume of 60µl in duplicate on round bottom Nunclon plates. Next, 60µl (total of 2,000 PFU) of either 245 NA Gly+ or 245 NA Gly- H3N2 recombinant virus diluted in IM with 5µg/ml N-Acetyl Trypsin was added to the dilution plate and 100µl of the mixture of virus and antibody was then added to MDCK plates. After 6 days plates were fixed with 4% formaldehyde and stained with napthol blue-black as described above. Wells were considered negative for virus replication if the entire monolayer was intact.

NA Neutralizing Antibody Virus Replication Assay

To study monoclonal antibody inhibition of multistep viral growth, viral replication assays were conducted in the presence of NA monoclonal antibodies or human IgG isotype. Confluent MDCKs were infected with a MOI of 0.001 as described above. After infection, viral inoculum was removed, the cells washed twice with PBS+ and monoclonal antibodies (235-1C02, 229-1G03 or human IgG isotype clone IGHG1) were added at the indicated concentration in IM containing 5µg/ml n-Acetyl trypsin. Infected cells were incubated at 32ºC. At each timepoint post infection, supernatant was removed and stored at -80C. Fresh IM with 5µg/ml N-acetyl trypsin and the indicated antibody was added. Viral titer was determined via $TCID_{50}$.

Statistical Analysis

Statistical analysis was performed using Graph Pad Prism Software (GraphPad v8.4.2). Viral growth with or without NA neutralizing antibodies was analyzed using two-way anova with a Bonferroni post test correction. Differences were considered significant if $p < .05$. Plaque size, enzyme activity, virus inhibition and infectivity was analyzed using an unpaired t-Test. Differences were considered significant if $p < .05$.

Results

We previously showed that human H3N2 clinical isolates with an NA protein containing a glycosylation at position 245 had decreased replication on primary human nasal epithelial cell (hNEC) cultures, but not immortalized Madin-Darby Canine Kidney (MDCK) cells [234]. To further study the effect that 245 NA glycosylation has on virus replication and enzymatic activity, recombinant viruses were generated which encoded either the 2014/15 N2 NA proteins with (245 NA Gly+) or without (245 NA Gly-) the NA 245 glycosylation and an 2014/2015 HA protein. The remaining six influenza virus segments from A/Victoria/361/2011 (H3N2) were used as the virus genetic backbone.

These viruses were first characterized on MDCK-SIAT1 cells, which overexpress the human enzyme CMP-*N*-acetylneuraminate:β-galactoside α-α2,6-sialyltransferase producing more cell surface carbohydrates with terminal α-α2,6 sialic acid [235]. Both viruses showed similar kinetics of infectious virus production and peak infectious virus amounts after a low MOI infection (Figure 4.1A). In contrast, infection of hNEC cultures at a low MOI with the 245 NA Gly- virus yielded significantly higher amounts of infectious virus for a prolonged period of time when compared to the 245 NA Gly+ virus (Figure 4.1B). Plaque appearance, morphology and size was then assessed using MDCK cells. Both viruses produced clear, distinct plaques (Figure 4.1C) of similar size (Figure 4.1D). This data indicates that while the 245 NA glycosylation does not impact virus replication on immortalized MDCK-SIAT1 or MDCK cells, it has an adverse effect on virus replication in hNEC cultures.

To understand how the additional of a N-linked glycosylation could impact virus replication, a model of the N2 neuraminidase monomer was generated with UCSF Chimera 3D modeling software. A similar N2 NA strain (A/Tanzania/2010) was used to highlight key residues and add a complex N-linked glycan at position 245 (Figure 4.2A) via the online program Glyprot. From the model, it is clear that the 245 N-linked Glycan is uniquely situated near the active site of the protein. To assess whether this N-linked glycan could interfere with the binding of antibodies that target epitopes close to the NA enzymatic active site, the coding sequences for both the 245 NA Gly+ and 245 NA Gly- gene were inserted into a mammalian cDNA expression vector (pCAGGS), with an C-terminal FLAG epitope tag before the stop codon (C-terminus). The NA-FLAG plasmids were transfected into HEK293T cells and the reactivity of the proteins assessed using

monoclonal antibodies specific for the NA protein or the FLAG epitope. Three different anti-NA monoclonal antibodies were used. HCA-2 is a rabbit IgG that recognizes a highly conserved 9 amino acid sequence (ILRTQESEC) in the active site of most influenza A and B virus NA proteins. [88, 89]. This antibody was unable to bind to the 245 NA Gly+ protein but showed robust binding of the 245 NA Gly- protein (Figure 4.2B). The human monoclonal antibodies (235-1C02 and 229-1G02) were also used to study epitope masking. The binding of these antibodies to N2 NA proteins have been described previously [222]. NA proteins encoding amino acid changes at 248 and 429 [222] allow for escape from binding with 235-1C02, suggesting that glycosylation at 245 could inhibit antibody binding to its epitope. Binding of the 235-1C02 to the 245 NA Gly+ protein was not detected but the antibody recognized the 245 NA Gly- protein (Figure 4.2C). The monoclonal antibody 229-1G03 was previously shown to robustly bind to 245 NA Gly- proteins, but its binding epitope has not been mapped. This antibody can inhibit NA enzymatic activity, suggesting it binds near the NA active site [222]. We found that this antibody recognizes both 245 NA Gly- and 245 NA Gly+ proteins but shows decreased binding to the 245 NA Gly+ protein, suggesting that the 245 NA glycan partially disrupts 229-1G03 antibody epitope recognition (Figure 4.2D). Taken together these results indicate that the 245 NA glycan masks epitopes in and around the active site of the protein as well as multiple epitopes recognized by human monoclonal antibodies, some of which are potent, broadly reactive inhibitory antibodies. Similar results have recently been reported using the NA protein of the A/Hong Kong/4801/2014 vaccine strain [229].

To understand how 245 NA glycosylation impacted NA function a variety of enzymatic and kinetic activity assays were performed. To standardize NA content, we chose to partially purify virus particles using ultracentrifugation over a sucrose cushion then normalize for NA content using Western blotting with the HCA-2 monoclonal antibody. While the HCA-2 antibody binding to conformationally intact 245 NA Gly+ protein is inhibited, when the protein is denatured, the HCA-2 linear epitope [88, 89] is recognized in both the 245 NA Gly- and Gly+ proteins (Figure 4.3A). The NA enzymatic activity was measured using three different NA assays. The Enzyme Linked Lectin Assay (ELLA) uses fetuin (Figure 4.3B) as a complex carbohydrate substrate which mimics the natural ligands seen by the NA protein during natural infection [231, 232]. The NA-*STAR* (Figure 3C) and NA-Fluor assays (Figure 4.3D) utilize smaller sialic acid mimics that release luminescent or fluorescent molecules after cleavage. Using all three substrates, the enzymatic activity of 245 NA Gly- was significantly higher than that of the 245 NA Gly+, suggesting that the 245 glycosylation was adversely affecting NA enzymatic activity. This NA activity difference was highest in the ELLA assay, suggesting that the 245 N-linked glycan sterically blocks the full carbohydrate substrate in this assay from the active site. However, the relatively smaller NA-STAR and NA Fluor substrates were still utilized less efficiently by the 245 NA Gly+ protein, suggesting this glycosylation may have more extensive structural effects on the NA active site.

In addition to bulk activity assays, we performed an enzyme kinetic assay to determine enzyme velocity and affinity for substrate (Figure 4.3E). As expected, the 245 NA Gly+ protein has lower enzyme velocity and a lower affinity for substrate (Figure 4.3E, Table 4.1). All of these findings indicate that the 245 NA glycan significantly

decreases NA enzymatic activity by decreasing substrate access to the active site of the protein.

Since the 245 NA glycosylation blocked or decreased binding of the two human monoclonal antibodies 235-1C02 and 229-1G03 and we tested the ability of these antibodies to inhibit viral enzymatic activity. First, viral stocks of 245 NA Gly+ and 245 NA Gly- were equalized via NA content and virus was incubated with a dilution series of the human monoclonal antibodies or oseltamivir. Vehicle (assay buffer) was used for a control and used to subtract background. As expected from the antibody binding studies, the monoclonal antibody 235-1C02 was unable to inhibit the NA enzymatic activity of the 245 NA Gly+ in the NA star assay even at the highest concentration tested (100nM) but inhibited the 245 NA Gly- virus at a concentration of 0.8nm (Figure 4A). The 229-1G03 inhibited both the 245 NA Gly+ and 245 NA Gly- at a concentration of 4.7nm and 1.1nm respectively, suggesting a partial inhibition of inhibitory activity (Figure 4.4A) via the 245 NA glycan. The same trend is seen in the ELLA assay (4.4B) with 235-1C02 unable to inhibit the neuraminidase activity of the 245 NA Gly+ virus and 229-G03 showing reduced inhibitory activity. Importantly, in both assays oseltamivir inhibition was clearly observed and not different between viruses, suggesting that the drug was fully capable of inhibiting NA enzymatic activity irrespective of 245 NA glycosylation status. These results confirm that 245 NA glycosylation can result in reduced inhibitory activity of antibodies that bind near the NA active site. In addition to monoclonal antibody studies we investigated how human convalescent serum from the 2014 through 2016 influenza seasons could inhibit enzymatic activity of the 245 NA Gly+ and 245 NA Gly- protein. We generated H6N2 viruses to avoid the confounding

effect that anti-HA antibodies in human serum can have on NA enzymatic activity [231, 236]. Twenty serum samples taken from individuals approximately 28 days after confirmed H3N2 infection were used. Ten serum samples were from patients infected with a 245 NA Gly- virus and 10 from patients infected with a 245 NA Gly+ virus (Table 4.2). Regardless of the source of serum, the 245 NA Gly+ protein was more resistant to serum based enzymatic inhibition, indicated by a higher concentration of serum needed to inhibit 50% of the enzymatic activity (Figure 4.4C-E, Table 2) when compared to the 245 NA Gly- virus. In 18 of the 20 serum samples tested, two to three-fold more serum was necessary to inhibit the 245 NA Gly+ protein compared to the 245 NA Gly- protein (Figure 4F). Together these results demonstrate that the 245 NA glycosylation sequence reduces the recognition of serum NA antibodies consistent with antigenic drift of the NA protein.

Neuraminidase inhibitory antibodies have previously been shown to inhibit virus replication by inhibiting enzymatic activity of the protein or by inducing a cellular immune response through antibody dependent cellular cytotoxicity (ADCC) [95, 222, 231, 237] or a combination of both. With two recombinant viruses only differing in the 245 NA glycosylation sequence, we sought to understand how this glycan would impact the ability of 229-1G03 and 235-1C02 to neutralize virus infectivity. Using the two recombinant viruses we found that the antibody 235-1C02 was unable to neutralize the 245 NA Gly+ virus, but effectively neutralized the 245 NA Gly- virus at an average concentration of 1.3nm (Figure 4.5A). Using 229-1G03, we found this antibody was able to neutralize both 245 NA Gly+ and 245 NA Gly- viruses, with an average concentration of 6.4nm and 1.5nm respectively, indicating somewhat reduced neutralizing activity

against the 245 NA Gly+ virus (Figure 4.5B). Using the experimentally determined 50% neutralizing antibody concentration with the 245 NA Gly- virus in Figure 4.5 and 5.5B, a multistep growth curve in the presence or absence of these antibodies was performed. Figure 54.5C demonstrates that the 245 NA Gly+ virus was not impacted with the 235-1C02 antibody, as no significant difference was found in infectious virus production comparing human IgG isotype (clone IGHG1) and 235-1C02. However, antibody 229-1G03 did significantly decrease infectious virus production of the 245 NA Gly+ virus, showing a partial ability to neutralize infectious virus, consistent with the binding (Figure 4.2) and enzymatic inhibition results (Figure 4.3). This suggests that the epitope this antibody binds is partially accessible on the 245 NA Gly+ protein. In Figure 4.5D, both human monoclonal antibodies significantly decreased infectious virus production of the 245 NA Gly- virus to near undetectable levels, suggesting potent neutralizing activity. These results confirm our previous findings with protein binding (Figure 4.2) and enzymatic inhibition (Figure 4.3). The 245 NA glycan prevents NA active site-specific antibodies from binding and inhibiting the NA protein, and significantly decreases antibody mediated neutralization of other NA-specific neutralizing antibodies.

Discussion

In this study, we demonstrated that the recently acquired 245 N-linked glycosylation site in the NA protein of currently circulating human H3N2 viruses significantly alters the function and antigenicity of the NA protein. The 245 NA glycan decreased in vitro replication on primary hNECs but did not decrease replication on immortalized MDCK cells nor decrease plaque area of isogenic viruses (Figure 4.1). These data suggest that some aspect of primary hNECs, likely the presence of respiratory mucins, decreases virus replication. Neuraminidase is necessary for virus

motility through mucins [100, 102] and decreasing NA enzymatic activity likely decreases the ability of the virus to move through mucus. The decrease in NA activity found in three separate activity assays (Figure 4.3) but was most pronounced when fetuin was used as a substrate, indicating recognition of sialic acid on longer carbohydrate chains is especially affected by 245 NA glycosylation. We conclude that the 245 NA glycan likely blocks substrate access to the active site and decreases enzymatic activity. Decreasing enzymatic activity is likely tied to a decrease in replication seen in mucin secreting hNECs but not seen in immortalized MDCK cells, which to this point have not been shown to secrete mucins.

The presence of a glycosylation site at NA 245 did not affect NA sensitivity to the antiviral drug oseltamivir. While oseltamivir access to the NA active site may be reduced due to the 245 NA glycosylation in a manner similar to that seen with the other enzyme substrates used, subsequent release of oseltamivir is most likely not effected, resulting in efficient inhibition of NA enzymatic activity. Further studies of the kinetics of oseltamivir inhibition of 245 NA Gly+ and 245 NA Gly- viruses could provide additional insights into this observation.

Recently there have been attempts to map the antigenic regions of the NA protein. The 245 NA glycan is located near the enzymatic active site ([229], Figure 4.2) and is poised to mask this region of the NA protein. We sought to understand how this glycosylation, which incurs a significant fitness disadvantage as judged by virus replication in hNEC cultures, could still fix in the human H3N2 virus population in such a short timeframe. Through multiple assays we found this glycan has an important role in masking NA antigenic sites. This glycan blocks NA active site-specific antibodies from

binding (Figure 4.2), prevents NA active site-specific antibodies from inhibiting enzyme function (Figure 4.4), and blocks the ability of active site antibodies to neutralizing virus replication (Figure 4.5). Additionally, another NA specific monoclonal (229-1G03) antibody with an as yet undefined binding epitope is partially blocked from binding to their epitope by this glycan (Figure 4.2, 4.4, 4.5), suggesting that the 245 NA glycan masks multiple epitopes on the NA protein. This inhibition of NA inhibitory antibody activity was shown with specific monoclonal antibodies and with polyclonal serum from H3N2 infected individuals. The ability to escape from preexisting NA immunity therefore provides a significant fitness advantage for the virus. While we used serum antibody levels to show reduced activity towards 245 NA Gly+ viruses, assessing escape from NA antibody in respiratory tract secretions would be more relevant. This antibody evasion presumably counters the reduced replication of 245 NA Gly+ viruses in hNEC cultures, resulting in a virus whose overall fitness for infecting humans is increased compared to 245 NA Gly- viruses. Since the virus replication fitness deficits were only observed in hNEC cultures while the antibody inhibition of virus replication was evident in immortalized cell lines, our use of hNEC cultures has allowed for a more complete understanding of the effects of 245 NA glycosylation on virus fitness.

Neuraminidase works in conjunction with the HA receptor of influenza A viruses to infect and spread virus effectively [98, 99]. As such, studying the NA and HA proteins together is crucial to understanding viral evolution. Both the HA and the NA protein interact with the same ligand, sialic acid, and thus balancing each proteins' affinity for this ligand is critical to the influenza cycle [97-99, 104]. Both proteins are necessary for in vivo replication, but the nuance of their interaction is important as well. Too strong of

an HA-sialic acid interaction compared to NA activity results in the HA protein being trapped in respiratory mucins or not being able to release progeny virions from the infected cell [238, 239]. On the other side of the spectrum, too weak of an HA-sialic acid interaction compared to NA activity results in removal of sialic acid receptors before the HA protein can engage its ligand and initiate infection. This fine balance between affinity for sialic acid impacts virus fitness [99, 104]. Whether the adverse effects of 245 NA Gly+ are observed with more contemporary H3 HA proteins should be investigated to determine whether HA mutations that compensate for the reduced 245 NA Gly+ enzymatic activity have fixed in human H3N2 viruses.

In recent years, the NA protein has had renewed interest as a relatively conserved protein that's an attractive vaccine target [95, 208, 240]. In some respects, the NA protein is an excellent candidate for a universal vaccine. A single monoclonal antibody can neutralize decades of influenza virus isolates regardless of strain at nanomolar amounts. Neuraminidase inhibitory antibodies can inhibit viral spread, and replication at multiple stages of the virus life cycle [241]. Finally, many different studies show that NA inhibitory antibodies can decrease disease severity and virus transmission as well as provide sterilizing immunity [88, 89, 96, 216, 222, 225].

Antibody responses to NA are not induced effectively in all age groups by current influenza vaccines because the amount of NA is not standardized in vaccine preparations and the NA protein conformation is more sensitive to the current vaccine production methods than the HA protein [95, 222, 242, 243]. While other methods for inducing NA immunity are being developed, our data show that two amino acid changes in N2 NA can lead to escape from antibodies that bind to one of the most universal

antigenic sites of the protein. It is important that future studies of universal influenza vaccines utilize a multi-epitope vaccine that would require multiple mutations from the virus to escape the vaccine-induced immunity.

This study highlights the necessity to consider multiple aspects of the NA protein in regard to vaccine production and virus evolution. Decades of influenza research have focused on the HA protein for vaccine development, viral evolution and pandemic potential. As the interest in NA protein as a vaccine increases, many of the lessons learned studying influenza HA may also be applied to NA. The NA protein is immunogenic and can provide protection against many strains of influenza viruses[240]. However, like the HA protein, the NA protein can undergo antigenic drift and evade the humoral immune response. As immune pressure mounts due to a renewed vaccination effort at targeting NA protein, the NA protein will likely also become a “moving target” for vaccine development, in a manner similar to what has already been documented for the HA proteins.

Figures and Tables

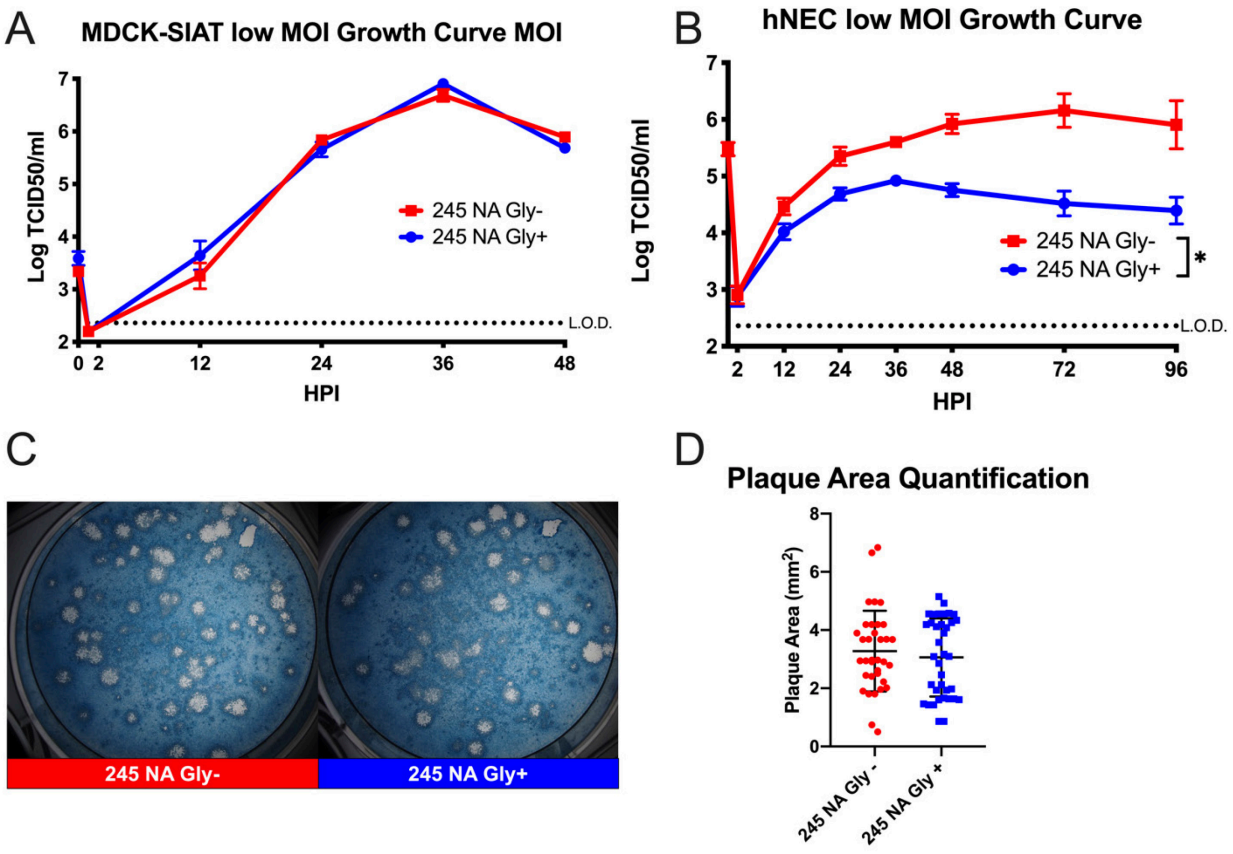

Figure 4.1: Replication of recombinant H3N2 viruses in MDCK-SIAT1, MDCK or hNEC cultures with or without 245 NA glycosylation

Low MOI growth curves with MDCK-SIAT1 (**A**) or hNEC cultures (**B**) with the indicated recombinant viruses at 32ºC. Hours post infection (HPI) on X axis, Log of TCID50/ml on Y axis. Data are pooled from 3 independent experiments with four replicates per virus per experiment (total n = 12 wells per virus timepoint). Data were analyzed with *p<.05 and two-way repeated measures ANOVA with Bonferroni multiple comparison posttest. The limit of detection (L.O.D.) is indicated with a dotted line at log 2.37 TCID50/ml. Error bars in A and B are SEM. (**C**) Plaque assay performed with recombinant 245 NA Gly + and 245 NA Gly - viruses on MDCK cells. (**D**) Quantification of plaque area from 30-50 individual plaques per virus from 3 independent experiments. *p<.05 unpaired T test.

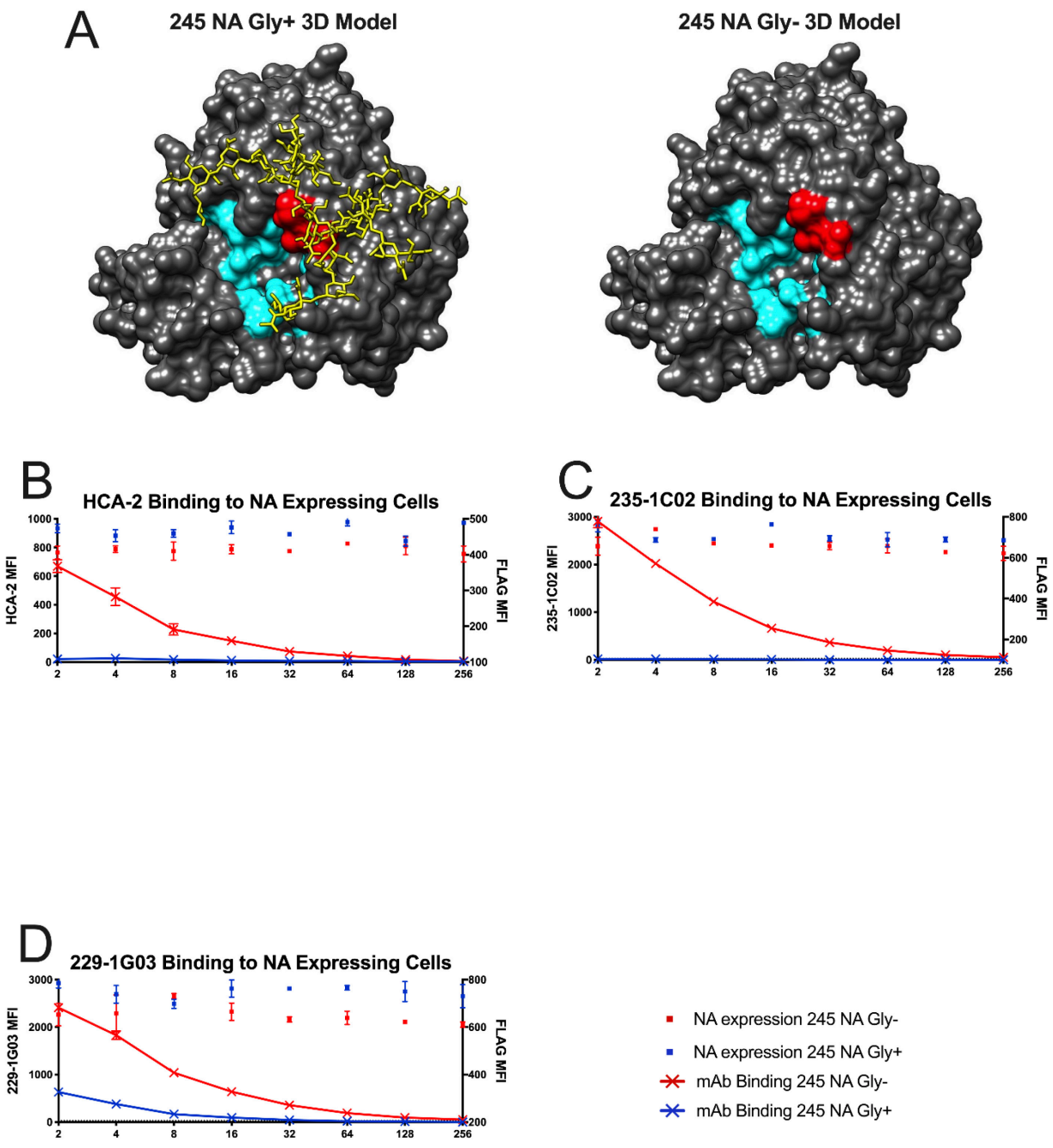
A
245 NA Gly+ 3D Model
245 NA Gly- 3D Model
B
HCA-2 Binding to NA Expressing Cells
HCA-2 MFI
FLAG MFI
C
235-1C02 Binding to NA Expressing Cells
235-1C02 MFI
FLAG MFI
D
229-1G03 Binding to NA Expressing Cells
229-1G03 MFI
FLAG MFI
NA expression 245 NA Gly-
NA expression 245 NA Gly+
mAb Binding 245 NA Gly-
mAb Binding 245 NA Gly+

Figure 4.2: Binding of neuraminidase inhibitory antibodies to cells expressing NA Gly+/- proteins

(**A**) 3D model of N2 NA with (Left, 245 NA Gly+) or without (Right, 245 NA Gly-) the predicted 245 N-glycan. Catalytic and framework residues are highlighted in cyan. Residues 245-247 are highlighted in red. Protein structure modeled and modified via UCSF Chimera, Protein Data Bank ID code 4GZP (Tanzania/2010 N2 NA). A typical complex style N-glycan was added via the Glyprot program. (**B**-**D)** 245 NA Gly+ (blue dots) or 245 NA Gly- (red dots) FLAG-tagged proteins expressed in HEK293T cells. NA expressing cells were incubated with dilutions of monoclonal antibodies HCA2 (**B**), 235-1C02 (**C**) or 229-1G03 (**D**) in addition to a mouse monoclonal antibody recognizing the FLAG epitope (to measure overall NA expression). Red lines indicate mAb binding to cells expressing 245 NA Gly- protein. Blue lines indicate mAb binding to cells expressing 245 NA Gly+ protein. Representative data from 3 experiments. * $p < .05$ two-way repeated measures ANOVA with Bonferroni multiple comparison posttest.

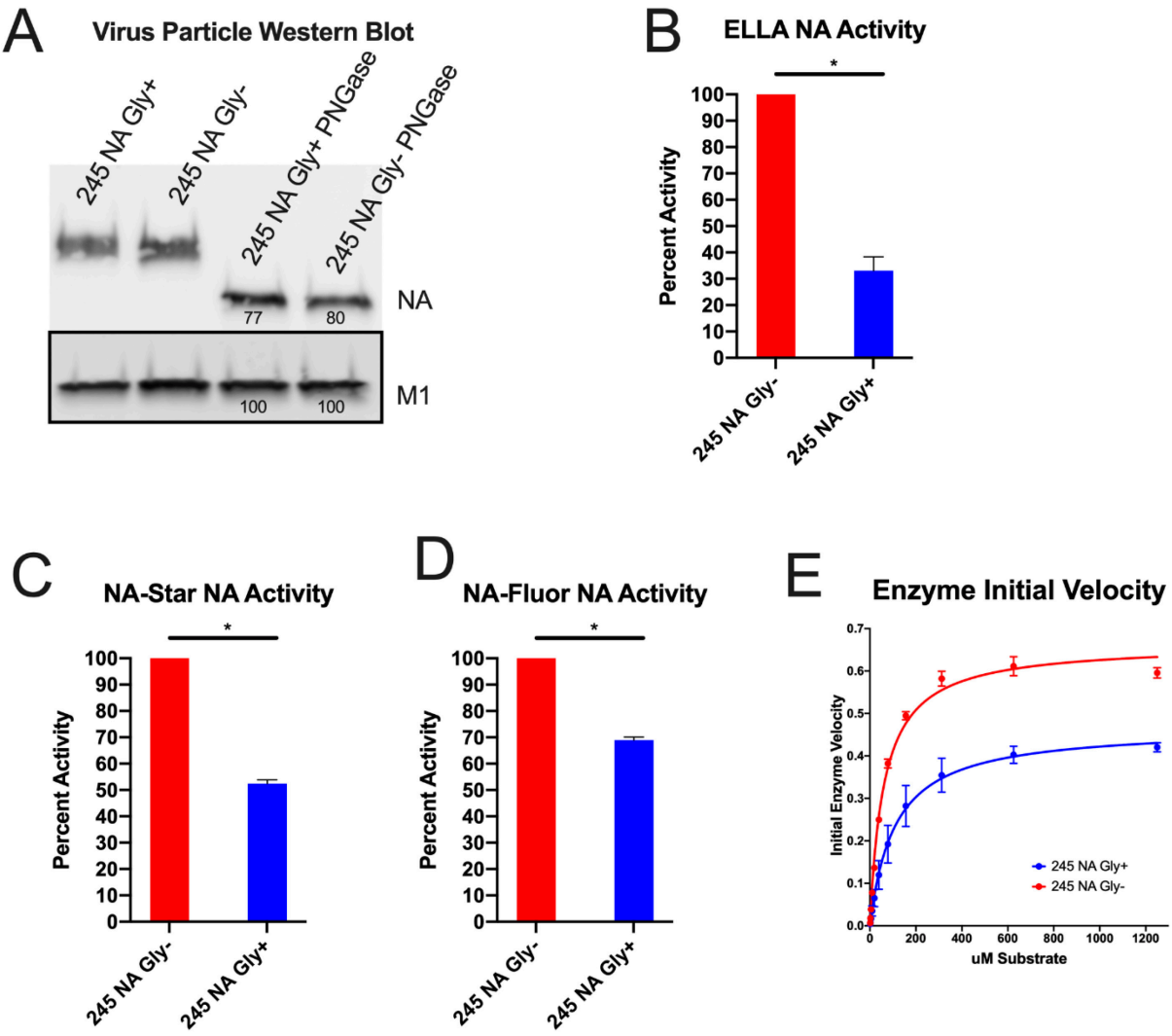

Figure 4.3: Effect of 245 NA glycosylation on neuraminidase activity

The NA content in partially purified influenza virus particles was measured via SDS-PAGE and western blot (**A**) using HCA-2 mAb to detect NA and M1 antibody GTX125928 to detect M1. Numbers below protein bands indicate measured intensity. NA content was normalized to the M1 content of the same virus sample. With NA content normalized, the NA activity in the partially purified virus preparations was measured in the enzyme linked lectin assay (ELLA) (**B**), NA-STAR assay (**C**) and NA-Fluor MUNANA based assay (**D**). In B, C, and D, 245 NA Gly- enzymatic activity was set to 100. X axis label is viral NA genotype 245 NA Gly+ activity is graphed as a percentage of that activity. (**E**) To assess enzyme kinetics, 245 NA Gly- and 245 NA Gly+ viruses were incubated with a dilution of MUNANA substrate and fluorescence was measured every 60s for 1 hour. Initial velocity plotted as uM product generated per minute. Non-linear regression plotted (line) with individual values (points). * $p < .05$ unpaired T test. NA and M1 protein content in A were determined using ImageJ

software. Enzyme kinetics was determined using a non-linear curve fit Michaelis-Menten equation in GraphPad prism 8.

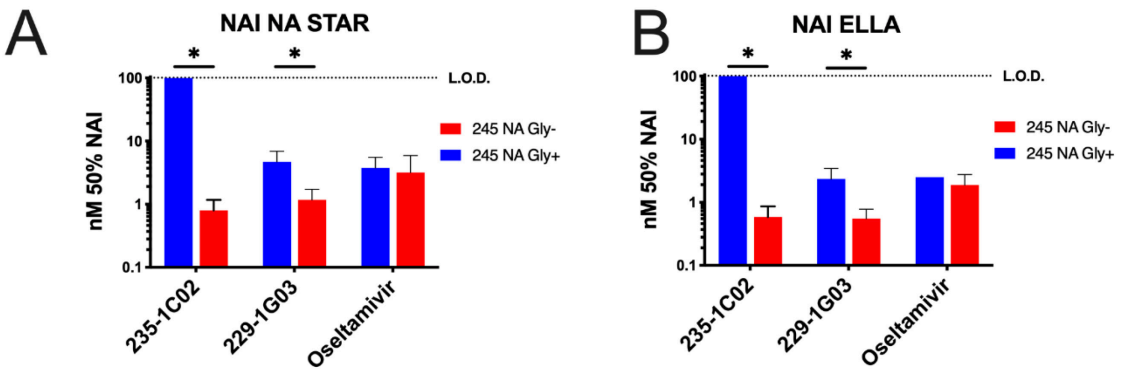
A
NAI NA STAR
nM 50% NAI
100
10
1
0.1
L.O.D.
245 NA Gly-
245 NA Gly+
235-1C02
229-1G03
Oseltamivir
B
NAI ELLA
nM 50% NAI
100
10
1
0.1
L.O.D.
245 NA Gly-
245 NA Gly+
235-1C02
229-1G03
Oseltamivir

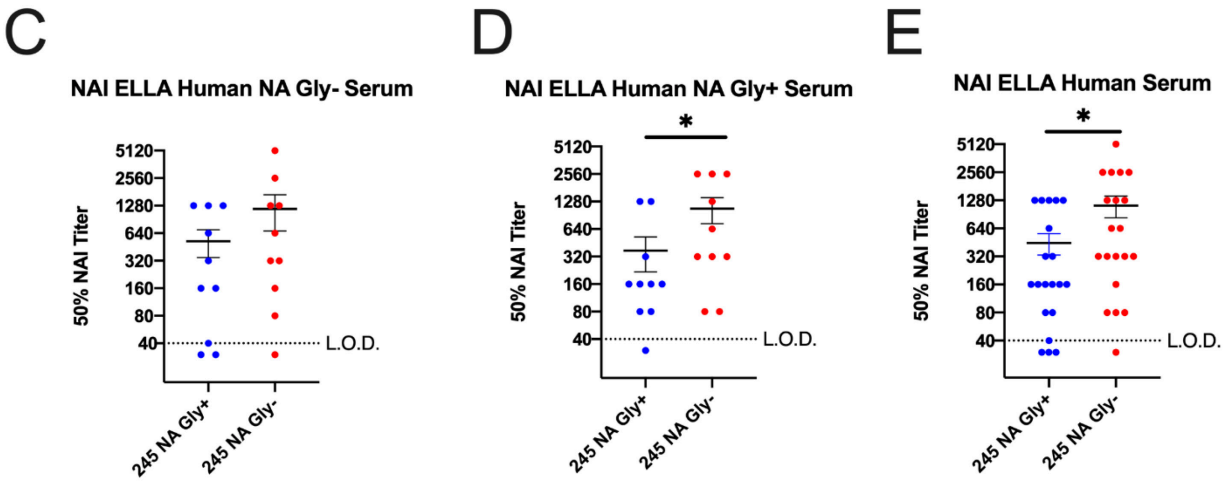
C
NAI ELLA Human NA Gly- Serum
50% NAI Titer
5120
2560
1280
640
320
160
80
40
L.O.D.
245 NA Gly+
245 NA Gly-
D
NAI ELLA Human NA Gly+ Serum
50% NAI Titer
5120
2560
1280
640
320
160
80
40
L.O.D.
245 NA Gly+
245 NA Gly-
E
NAI ELLA Human Serum
50% NAI Titer
5120
2560
1280
640
320
160
80
40
L.O.D.
245 NA Gly+
245 NA Gly-

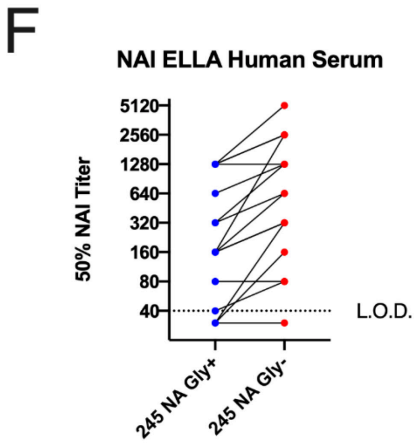
F
NAI ELLA Human Serum
50% NAI Titer
5120
2560
1280
640
320
160
80
40
L.O.D.
245 NA Gly+
245 NA Gly-

Figure 4.4: Effect of inhibitory antibodies and human serum on NA enzymatic function ELLA and NA Star.

Concentration of N2 monoclonal antibody needed to inhibit 50% of NA activity of 245 NA Gly+ and 245 NA Gly- viruses in NA-STAR (**A**) or ELLA (B) NA activity assays using partially purified H3N2 viruses. Upper limit of detection shown with a dotted line in A and B, indicating the highest concentration of inhibitory antibody used (100nM). (**C-E**) NA inhibition (NAI) ELLA assay performed with human convalescent serum from patients with confirmed H3N2 infection using H6N2 recombinant viruses. Virus content equalized via plaque assay. Convalescent serum NAI assay from all patients with confirmed H3N2 infection with NA Gly- virus (**C**), and NA Gly+ virus (**D**) and all serum samples regardless of NA genotype (**E**). X axis label indicates virus NA genotype. All patient serum samples with connecting lines between matched serum samples (**F**). Serum samples from the same individual are connected to indicate relative activity to the 245 NA Gly+ and 245 NA Gly- viruses. Dotted line shown is lower limit of detection in C-F, highest concentration of convalescent serum used (1:40 dilution). * $p<.05$ paired T-Test

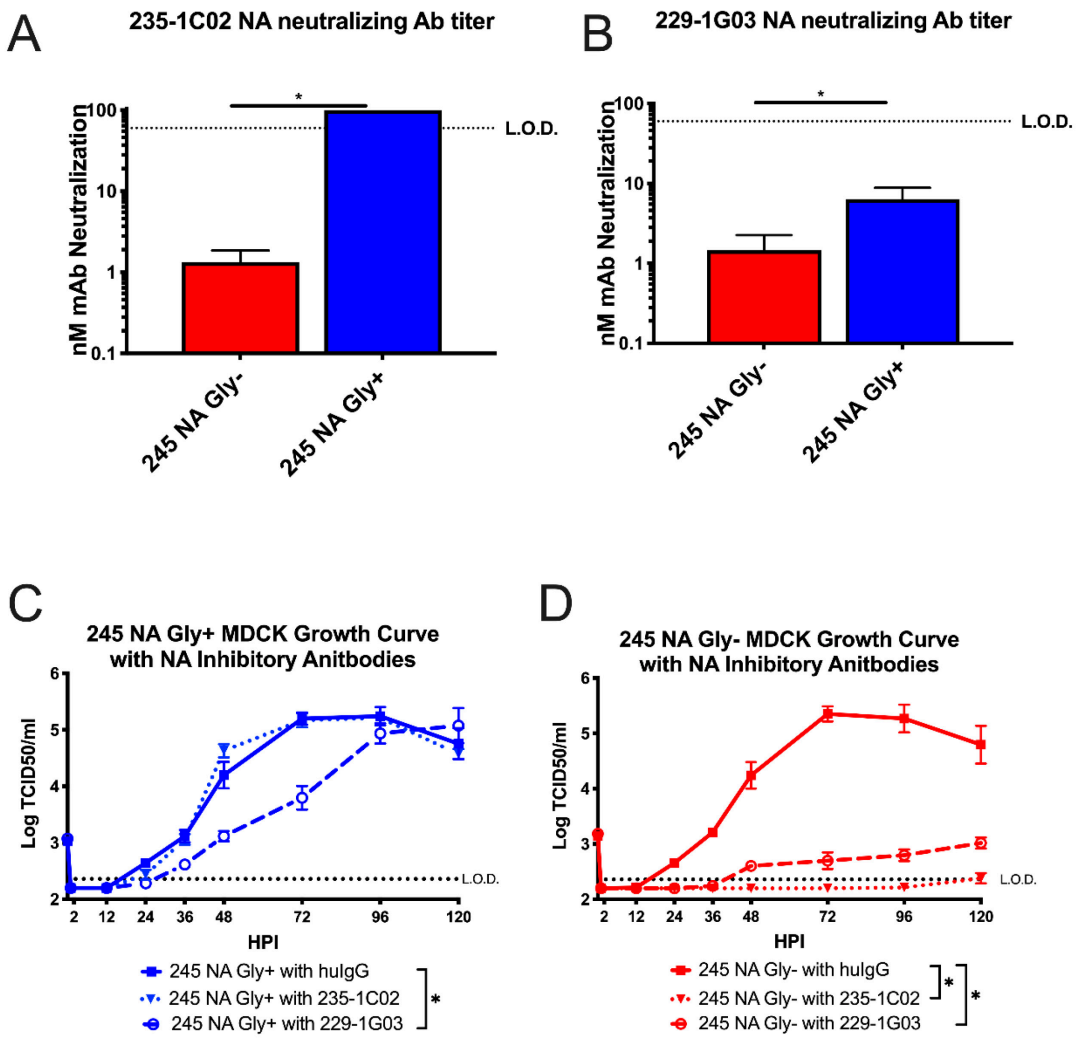

Figure 4.5: Effect of neuraminidase activity inhibiting antibodies on virus growth

The concentration of anti-neuraminidase monoclonal antibody 235-1C02 (**A**) and 229-1G03 (**B**) needed to neutralize 50% of the infectivity of 245 NA Gly – or 245 NA Gly+ viruses was determined on MDCK cells. Low MOI growth curve with recombinant viruses on MDCK cells (**C-D**). Hours post infection (HPI) on X axis, Log of TCID50/ml on Y axis. MDCK cells were infected with an MOI of .001 with either 245 NA Gly+ virus (**C**) or 245 NA Gly- virus (**D**). After 1hr of inculation, viruses were treated with either human IgG isotype control (clone IGHG1), mAb 235-1C02 or mAb 229-1G03. Dotted line in A and B indicated upper limit of detection, highest concentration of mAb used (100nM). .* p< .05 unpaired T test A and B. Dotted line in C and D indicated lower limit of detection, 2.37 TCID50/ml. Data are pooled from 3 independent experiments with four replicates per virus per experiment (total n = 12 wells per virus timepoint) in C and D Error bars in C and D is SEM. * p<.05 two way repeated measures ANOVA with Bonferroni multiple comparison posttest in C and D.

Test Virus	vMAX (95% CI)	Km (95% CI)	R squared of line
245 NA Gly-	.6645 (0.6305 to 0.7001)	61.55 (50.59 to 74.76)	.9942
245 NA Gly+	.4680 (0.4551 to 0.4813)	108.9 (99.12 to 119.6)	.9988

Table 4.1: Enzyme kinetics of 245 NA Gly- and 245 NA Gly+ viruses
NA-Flour assay conducted in triplicate, representative of two biological replicates. Values calculated with Graph Pad prism 8 with Michaelis-Menten non-linear regression. 95% confidence interval (CI) shown.

Convalescent Serum ID	Serum NA Genotype	245 NA Gly+ NAI_{50} Titer	245 NA Gly- NAI_{50} Titer	Fold NA Gly+ / NA Gly-
01-23-A-0081	NA Gly Positive	80	80	1
01-23-A-0023	NA Gly Positive	160	640	4
01-23-A-0051	NA Gly Positive	160	320	2
01-11-A-0262	NA Gly Positive	1280	2560	2
01-21-A-0268	NA Gly Positive	1280	2560	2
02-11-Pro-0003	NA Gly Positive	80	80	1
02-11-Pro-0005	NA Gly Positive	160	320	2
02-11-Pro-0023	NA Gly Positive	320	1280	4
02-11-Pro-0029	NA Gly Positive	<40	320	8
02-11-Pro-0101	NA Gly Positive	160	2560	8
01-11-A-0148	NA Gly Negative	40	80	2
01-11-A-0256	NA Gly Negative	1280	5120	4
01-11-A-0307	NA Gly Negative	640	1280	2
02-11-Pro-0006	NA Gly Negative	1280	1280	1
01-21-A-0192	NA Gly Negative	320	640	2
02-11-Pro-0030	NA Gly Negative	<40	<40	1
02-11-Pro-0036	NA Gly Negative	<40	160	4
02-11-Pro-0056	NA Gly Negative	160	320	2
02-11-Pro-0057	NA Gly Negative	160	320	2
01-21-A-0185	NA Gly Negative	160	320	2

Table 4.2: Serum samples and 50% NAI values in ELLA Assay
Serum samples taken from CEIRS study. Serum genotype, 50% NAI (NAI_{50}) titer and fold difference shown. Twenty convalescent serum samples taken approximately 28 days after confirmed H3N2 infection used. Ten from 245 NA Gly+ infected patients, 10 from individuals infected with a 245 NA Gly- virus. NAI_{50} values are the highest titer that resulted in at least 50% inhibition of enzyme activity in ELLA assay using H6N2 viruses expressing either 245 NA Gly+ or 245 NA Gly- protein. Data shown from one biological replicate. Each NAI assay was conducted in duplicate and averaged to determine titer.

CHAPTER 5: Novel HA and NA Glycosylations of H3N2 viruses Impacts Fitness but not HA/NA Balance

Harrison Powell and Andrew Pekosz

Abstract

In the 2013-15 North Hemisphere influenza seasons, the H3N2 virus underwent significant changes to both the hemagglutinin (HA) and neuraminidase (NA) proteins. These changes included the addition of an n-linked glycosylation site to position 158-160 on the HA protein and an n-linked glycosylation site to the NA protein. Since the emergence of this variant, nearly all H3N2 viruses in the 3c.2a clade and subclades contain this double glycosylation genotype. To assess the effect that these glycosylation events had on HA receptor binding and viral fitness, recombinant viruses with or without the HA 158 glycosylation and with or without the NA glycosylation were created. Using this panel of four recombinant viruses, we found that the 158 HA glycosylation dramatically increased the receptor binding specificity for the HA protein. In *in vitro* replication studies, the 158 HA glycosylation decreased viral replication on both immortalized and primary hNEC cultures. There was no significant effect that either protein glycosylation had on HA and NA balance. Taken together, these data suggest that while both of the recent HA and NA glycosylation events decrease viral replication and there is no obvious change in the HA and NA balance, the ability to evade preexisting immunity likely provide a strong fitness advantage to allow emergence, or dominance of viruses carrying the HA 158 and NA 245 n-linked glycosylations.

Introduction

The 2013-14 season marked the beginning of significant changes to both the HA and NA proteins of H3N2 viruses. The HA protein is under constant immune pressure and as a result there are numerous amino acid changes in the HA head yearly [108, 179, 193]. Many of these changes occur in antigenic sites and some of which are near the receptor binding site (RBS) of the protein. During in the 2013-14 season, H3N2 clade 3c.2a viruses emerged and quickly dominated the circulating H3N2 virus population. This novel HA clade, highlighted by a novel n-linked glycosylation at position 158-160 in the HA protein (H3 numbering), decreased the effectiveness of the northern hemisphere seasonal influenza vaccine that season [205, 206, 244-246]. The position of this HA glycan at residue 158 is directly near the RBS of the HA protein based on 3D in silico modeling, and could impact receptor binding and recognition as seen in previous isolates [81, 244, 247]. This glycan also effectively blocks antibodies targeted to antigenic site B on the H3 HA near the receptor binding site [27, 64, 72, 248].

The following 2014-15 influenza season a small percentage circulating H3N2 isolates encoded a novel n-linked glycosylation at position 245-247 on the NA protein in addition to the recently added HA 158 glycosylation. This novel NA glycosylation masks an important antigenic epitope near the active site of the protein and significantly reduces enzymatic activity [109]. In the influenza seasons since, the majority of circulating H3N2 isolates encode the HA 158 Gly+ and 245 NA Gly+ protein. Based on the relatively quick and significant evolutionary changes to the HA and NA proteins of circulating H3N2 influenza viruses, we believe that the addition of an NA n-linked glycan next to the active site of the protein could play an important role in re-balancing the HA and NA balance of circulating H3N2 viruses. Pairing an HA protein with a decreased

affinity for certain sialic acid ligands with an NA protein with a proven decreased enzymatic rate would effectively rebalance the HA and NA interaction in the human H3N2 population [93, 104, 249-251]. Rebalancing HA and NA activity, in combination with an increased ability to evade humoral immunity targeting antigenic site B in the HA protein and the active site of the NA protein, could explain the dominance of the HA 158 Gly+ 245 NA Gly+ genotype of circulating H3N2 influenza viruses.

Using a panel of four recombinant viruses expressing a 158 HA Gly +/- protein and a 245 NA Gly +/- protein we found that HA and NA balance is not perceptibly altered in any of the four recombinant viruses. While the 158 HA Gly+ protein binds a broader amount of synthetic sialic acid containing ligands, viruses expressing the HA 158 Gly+ protein replicate significantly worse than the HA 158 Gly- viruses. The fitness cost of the HA 158 Gly+ protein is likely offset by the ability to evade pre-existing immunity which likely leads to the dominance of this HA genotype in the circulating H3N2 population of viruses.

Materials and Methods

Structural Analysis

To analyze the 3D structures of 158 Gly+/- HAs, the Protein Data Bank (PDB) structure ID 4WE9 from A/Victoria/361/2011 was used. The amino acid sequence was modified using UCSF Chimera to create the 158 HA Gly+ or 158 HA Gly- structure. Glycosylation was added via the online program Glyprot (Glycosciences.de).

Cell Lines and Primary Cells

Madin-Darby Canine Kidney Cells (MDCK) and human embryonic kidney cells 293T (HEK293T) were maintained in complete medium (CM) consisting of Dulbecco's Modified Eagle Medium (DMEM) supplemented with 10% fetal bovine serum, 100U/ml penicillin/streptomycin (Life Technologies) and 2mM Glutamax (Gibco). Human nasal

epithelial cells (hNEC) were isolated from non-diseased donor tissue following endoscopic sinus surgery. Cells were grown, differentiated and maintained at the air liquid interface as previously described [129, 138, 145]. hNEC differentiation medium and maintenance medium was prepared as previously described [138, 142, 146]. hNEC cultures were used for low MOI growth curves only when fully differentiated. All cells were maintained at 37ºC in a humidified incubator supplemented with 5% CO2.

Plasmids

The plasmid pHH21 was used to generate full length influenza hemagglutinin (HA) or neuraminidase (NA) plasmids for recombinant virus production. Briefly, viral RNA was isolated from the clade 3c.2a H3N2 viruses A/Bethesda/P0055/2015 (NA Gly+ EpiFlu DB ID 253812) and A/Columbia/P0041/2014 (NA Gly- EpiFlu DB ID 253817) with a Qiagen mini-vRNA isolation kit. Gene specific primers with cloning sites for H3N2 neuraminidase or hemagglutinin were used to create cDNA via a one-step RT-PCR reaction (SuperScript III-Platinum Taq mix, ThermoFisher Scientific). The cDNA products were cut with appropriate restriction enzymes, column purified (QIAquick PCR Purification kit) and ligated with restriction enzyme cut-pHH21 using T4-ligase (New England Biolabs, NEB). Ligation products were transformed into DH5a (NEB) cells and colonies were mini-prepped (QIAprep spin mini-prep) and Sanger sequence verified. Sequence verified colonies were maxi-prepped (ZymoPURE) and used for recombinant virus preparation. Since the HA amino acid sequence between A/Bethesda/55/2015 is identical to A/Columbia/41/2014, A/Bethesda/55/2015 HA-pHH21 plasmid was used for all of the H3N2 viruses in this study. The codon at amino acid position 160 in HA (H3 numbering, Threonine) was modified via site-directed mutagenesis (Agilent) from the wild type (ACA, Thr) to a new codon (ACT, Thr) less likely to revert to a lysine codon-

which occurred frequently during previous attempts to virus rescue. To create the HA 158 Gly- pHH21 plasmid, site directed mutagenesis was performed to alter the HA 160 codon from a Thr (WT) to a Lysine (Lys, K). Lysine was chosen as this residue appears in many clinical isolates at this position before the introduction of the 3c.2a clade.

Recombinant Virus Production

Recombinant H3N2 viruses were generated using the 12-plasmids reverse genetics system as previously described [148]. Briefly, HEK293T cells were plated at 50% confluency 1 day before transfection in complete media. On the day of transfection, media was replaced with serum free Opti-MEM. HEK293Ts were then transfected with eight plasmids encoding full length influenza segments in the pHH21 vector (PB2, PB1, PA, HA, NP, NA, M, NS) and four plasmids encoding the influenza replication proteins in the pcDNA3.1 vector (PB2, PB1, PA and NP). At one day post transfection 5μg/ml N-acetyl trypsin was added to the transfection reaction. MDCK cells were over-laid four hours post trypsin treatment. Every 24 hours post MDCK-overlay virus containing supernatant was sampled for virus production. Fresh Opti-MEM with 5μg/ml N-acetyl trypsin was added when a sample was taken. Virus from the transfected cell supernatants was plaque purified as described below, sequenced, and used to generate seed stocks by infecting MDCK cells at a MOI of 0.001. Working stocks were generated from sequence confirmed seed stocks by infecting MDCK cells at a MOI of .001 as described below.

Virus Working Stock Generation

For generation of recombinant virus working stocks, a 95-100% confluent flask of MDCKs was infected at a multiplicity of infection (MOI) of .001 $TCID_{50}$ units. Cells were washed twice with PBS containing 2mm calcium and magnesium (PBS+). The inoculum

was diluted infection medium (IM), consisting of DMEM with .3% BSA (Sigma), 100U/ml pen/strep (Life Technologies), 2mM Glutamax (Gibco) and 5µg/ml N-acetyl trypsin((Sigma)). Inoculation was done at 32ºC for 1 hour with gentle rocking of the flask every 15 minutes. After infection, inoculum was removed and fresh IM was added. Cells were placed in a 32ºC incubator and monitored daily for CPE. Working stock was harvested between 3 and 5 days or when CPE reached approximately 75-80%. Viral working stocks were then sanger sequenced with gene specific primers for all eight segments and infectious virus titer determined by $TCID_{50}$ as described below.

Partially Purifying Virus Particles

Virus partially purified by ultracentrifugation over a sucrose cushion for SDS-PAGE and western blotting. Clarified virus working stock supernatant was overlaid onto a 25% sucrose-NTE (100nM NaCl (ThermoFisher Scientific), 10mM Tris (Promega) and 1mM EDTA (Sigma)) buffer. Virus was centrifuged at 27,000 RPM in a SW-28 rotor in a Beckman Coulter Optima L90-K UltraCentrifuge for 2 hours. After the first ultracentrifugation, the supernatant was removed. The virus pellet was re-suspended in PBS. Pellet was further concentrated by ultracentrifugation in an SW-28ti rotor at 23,000 RPM for 1hr. The pellet was resuspended in PBS for use in glycan array.

Labeling Partially Purified Virus Particles

Partially purified virus particles were labeled with Alexa Fluor 488 Succinimidyl Ester per the manufacturer's instructions (Thermofisher Scientific).

Consortium for Functional Glycomics Glycan Array

To assess HA receptor specificity partially purified, whole virus particle labeled with fluorescent dye was allowed to bind to Consortium for Functional Glycomics Array version 5.3 synthetic glycan chip as previously described [79-82]. Labeled virus was allowed to bind to array chip for 1 hr. at room temperature, then excess was aspirated.

Slides were washed three times before fluorescence analysis. Array chip was scanned with GenePix 4300A Microarray scanner then data was analyzed with GenePix Pro Microarray Analysis Software and processed via Excel spreadsheets as previously described [79-82]. Only sialic acid containing ligands were considered for analysis.

Low-MOI Infections

Low-MOI growth curves were performed at a MOI of 0.001 in MDCK cells and 0.01 in hNEC cultures. Infection of MDCK cells took place at 32ºC for 1 hour. After the infection, the inoculum was removed and the MDCK cells were washed three times with PBS+. After washing, fresh IM was added and the cells were placed at 32ºC. At the indicated times post inoculation, IM was removed from the MDCK cells and frozen at -70ºC. Fresh IM was then added. In low-MOI hNEC growth curves, the apical surface was washed three times with PBS and the basolateral media was changed at time of infection. hNEC cultures were inoculated at a MOI of 0.01. hNEC cultures were then placed in a 32ºC incubator for 2 hours. After inoculation, the hNECs were washed three times with PBS. At the indicated times, 100ul of IM without N-acetyl trypsin was added to the apical surface of the hNECs. The hNECs were then incubated for 5 minutes at 32ºC and the IM was harvested and frozen at -80ºC. Basolateral media was changed every 48hrs post infection for the duration of the experiment. All samples from growth curves were used for infectious virus quantification via $TCID_{50}$.

$TCID_{50}$

MDCK cells were seeded in a 96 well plate 2 days before assay and grown to 100% confluence. Cells were washed twice with PBS+ then 180uL of IM was added to each well. Ten-fold serial dilutions of virus was created and then 20uL of the virus dilution was added to the MDCK cells. Cells were incubated for 6 days at 32ºC then

fixed with 2% formaldehyde. After fixing, cells were stained with napthol blue-black, washed and virus titer was calculated.

Plaque Assay

MDCK cells were grown in CM to 95-100% confluency in 6-well plates. Complete medium was removed, cells were washed twice with PBS+. Virus stocks were serially 10-fold diluted and 250ul of the appropriate dilution was added. Cells and virus were incubated at 32ºC for 1hour with rocking every 15 minutes. After 1hr, the virus inoculum was removed and phenol-red free DMEM supplemented with 3% BSA (Sigma), 100U/ml pen/strep (Life Technologies), 2mM Glutamax (Gibco),5mM HEPES buffer (Gibco), 5µg/ml N-acetyl trypsin (Sigma) and 1% agarose was added. Cells were incubated at 32ºC for 3-5 days and then fixed with 4% formaldehyde. After removing the agarose, cells were stained with napthol-blue black. One image per well was collected using an Olympus OM-D E-M5 Mark II digital camera. Plaque size was calculated in Image J [151]. 40-60 plaques were analyzed for each virus.

Statistical Analysis

Statistical analysis was performed using Graph Pad Prism Software (GraphPad v8.4.2). Viral growth was analyzed using two-way anova with a Bonferroni post test correction. Differences were considered significant if $p < .05$. Plaque was analyzed using an unpaired t-Test. Differences were considered significant if $p < .05$.

Results

To study the effect that HA and NA glycosylation has on virus fitness, a panel of viruses based off of the prototypic 3c.2a viruses A/Bethesda/0055/2015 and A/Columbia/0041/2014 were created. While both of these isolates have the same HA glycosylation genotype (158 HA Gly+), they differ in their NA glycosylation status at position 245-247. Recombinant viruses were generated with the four possible HA and

NA glycosylation genotypes to study this hypothesis. Two viruses with the HA glycosylation and only differing in NA glycosylation were rescued. These viruses are designated as 245 NA Gly+ 158 HA Gly+ and 245 NA Gly- 158 HA Gly+. Two additional recombinant viruses were produced with an HA missing the n-linked glycosylation site. These viruses, 245 NA Gly+ 158 HA Gly- and 245 NA Gly- 158 HA Gly-, differ in NA glycosylation but lack the HA glycosylation at position 158-160. All four recombinant viruses were created using the contemporary H3N2 A/Victoria/361/2011 internal segments and only differ in the amino acids involved in HA n-linked glycosylation (position 158-160) or NA glycosylation (position 245-247) The HA glycosylation is predicted to cover antigenic site B of the protein. A 3D model of both the HA 158 Gly+ (Figure 5.1A) and HA 158 Gly- (Figure 5.1B) reveals that this glycosylation site is near the sialic binding pocket of the HA protein.

N-linked glycans can dramatically alter the function of a protein, especially viral HA and NA proteins [252, 253]. Previous work has shown that the HA 158 glycosylation now present in many circulating H3N2 viruses masks an important antigenic epitope on the HA protein and protects the HA protein from antibody mediated neutralization [81, 254, 255]. We hypothesized that the addition of an n-linked glycan would have an additional effect of altering the glycan specificity of the HA protein, due to its proximity to the receptor binding pocket. We used two recombinant viruses (HA 158 Gly+ 245 NA Gly+ and HA 158 Gly- 245 NA Gly+) in a glycan array to assess sialic acid binding preference. The HA 158 Gly- virus bound to a few synthetic glycans and strongly preferred glycans with a α2,6 sialic acid linkage (Figure 5.2A, Table 5.1). Furthermore, a number of the highest binding ligands for the HA 158 Gly- virus were single chain and

short glycans (Table 5.1). The majority (18/20) of the synthetic ligands contained galactose as the penultimate sugar. Conversely, the HA 158 Gly+ virus displayed strong binding to α2,3 sialic acid and had much broader preference for on the glycan array (Figure 5.2B, Table 5.2). Many of the highest binding glycans for this virus were complex, multi-antennary glycans (Table 5.1) and all of them contained galactose as the penultimate sugar. Additionally, while not canonically considered influenza receptors, the HA 158 Gly+ protein bound to a number of non-traditional sialic acid linkage (2,8 linkage). Influenza A viruses have been shown bind 2,8 sialic acid in other glycan array studies, but their biological relevance to virus replication remains to be elucidated [75, 256, 257]. The difference in glycan array binding between these two viruses is striking. The addition of the 158 glycosylation on the HA protein appears to broaden the receptor preference, which is somewhat of a surprise as we hypothesized that a large bulky glycan would limit the ability of ligands to enter the receptor binding pocket of the HA protein. However, we did not see a dramatic change in preference for the penultimate sugar in the chain, suggesting that the 158 glycan does not play a role in recognition of other molecules in the sialic acid containing ligands. While microarray analysis cannot give a quantitative analysis of binding preferences between viruses, there is clearly a qualitative difference in receptor binding specificity.

Because there was a striking difference in receptor binding between viruses differing in HA 158 glycosylation, and we have previously shown that NA 245 glycosylation status dramatically impacts virus fitness, we decided to assess the viral fitness of the four recombinant viruses with different HA and NA proteins. We first characterized the four recombinant viruses (158 HA Gly +/- and 245 NA Gly +/-) with a

low MOI growth curve on immortalized Madin-Darby Canine Kidney epithelial cells. The viruses with the 158 HA Gly- protein replicated better than viruses with the 158 HA Gly+ protein, regardless of NA genotype (Figure 5.3A). Suggesting that the HA protein dictated replication fitness, and no combination of HA or NA was significantly better than the rest on MDCK cells. We next characterized the panel of viruses on primary hNEC cultures. Previously, we showed that the 245 NA glycosylation significantly impacts virus replication on hNECs when paired with a HA 158 Gly+ protein [211]. Within the pair of 158 HA Gly+ viruses, the virus with the 245 NA Gly- genotype replicated significantly better than the virus with the 245 NA Gly+ genotype, replicating previous results (Figure 5.3B). With the other pair of viruses (HA 158- 245 NA +/-) the same trend holds true, where 245 NA Gly+ decreases viral replication. Overall, in hNEC cultures the combination of HA 158 Gly- 245 NA Gly- replicated to the highest titer out of all four viruses. Plaque size and morphology was assessed via plaque assay on MDCK cells. All four viruses produced distinct plaques (Figure 5.3C) with no significant difference in plaque area (Figure 5.3D). However, viruses with the 158 HA Gly+ genotype had a visibly different plaque morphology and did not produce plaques as clear as the 158 HA Gly- viruses.

Discussion

In this study we demonstrated that the H3N2 158 HA glycosylation present in all circulating 3c.2a clade and all subclades does change receptor binding of the H3N2 3c.2a HA 158 Gly+ virus (Figure 5.1, 5.2) and virus replication (Figure 5.3). We aimed to study how this HA 158 glycosylation and associated HA receptor binding changes would impact virus replication in both immortalized MDCKs and human primary nasal epithelial cells. In immortalized MDCK cells, regardless of NA genotype, recombinant

viruses expressing the HA 158 Gly+ protein replicated worse than the HA 158 Gly- recombinant viruses (Figure 5.3A). NA genotype had no perceptible fitness effect in immortalized MDCK cells. This suggests that the HA 158 glycosylation is impacting viral fitness in this cell culture system. When using a physiologically relevant cell culture system of hNECs the same trend holds true. All four recombinant viruses used in these assays have different growth kinetics. First, the pair of the recombinant HA 158 Gly- viruses, the virus with the HA 158 Gly- 245 NA Gly- genotype replicated to a higher titer than the HA 158 Gly- 245 NA Gly+ virus (Figure 5.3B). In the pair of HA 158 Gly+ viruses, a similar trend holds where the HA 158 Gly+ 245 NA Gly+ protein replicates to a significantly lower titer compared to the HA 158 Gly- 245 NA Gly- recombinant virus. Taken together, these results suggest that suggesting that the NA protein genotype drives the replication phenotype in hNEC cells, regardless of HA protein.

In our hNEC studies, the HA 158 Gly- 245 NA Gly- virus replicated the best on hNECs, suggesting this virus would be the most fit in the human population. However, currently circulating strains all contain the 245 NA Gly+ gene and many have the HA 158 Gly+ protein. This indicates that regardless of increased replication fitness in *in vitro* models, evading host immune pressure via n-linked glycosylation is the major determinant of virus fitness and the ability of a virus to persist. Highlighting this is the fact that the HA 158 Gly+ 245 NA Gly+ virus was the dominant circulating strain at the end of the 2015 influenza season but showed the lowest growth on hNEC cultures in this study. While there is a significant replication fitness disadvantage, it's likely the ability to evade pre-existing HA and NA antibodies in the population far outweighed the loss of viral replication fitness in hNEC cultures and human hosts.

While we showed that the HA 158 Gly+ protein bound to a broader array of synthetic ligands it's worth noting a few caveats to this finding. At this point there have been no studies demonstrating presence of the synthetic ligands in the CFG synthetic glycan array version 5.3 in MDCKs and other tissue culture systems. Therefore, it's possible that the HA 158 Gly+ receptor has an enhanced binding to ligands that aren't physiologically relevant in either cell culture system tested. Influenza HA and NA proteins have a balanced interaction to the viral receptor, sialic acid. Both proteins are necessary for in vivo replication, but the nuance of their interaction is important as well. Too strong of an HA-sialic acid interaction compared to NA activity results in the HA protein being trapped in respiratory mucins or not being able to release progeny virions from the infected cell [98, 99, 258]. On the other side of the spectrum, too weak of an HA-sialic acid interaction compared to NA activity results in removal of sialic acid receptors before the HA protein can engage its ligand and initiate infection. This fine balance between affinity for sialic acid impacts virus fitness. It's possible that binding to a broader array of ligands disrupts the HA NA balance in viruses with the HA 158 Gly+ genotype, regardless of NA function, as shown by our results. However, more studies are necessary to prove this hypothesis.

This study highlights the necessity to study multiple aspects of viral fitness when considering influenza virus evolution. While both the 158 HA and 245 NA n-linked glycosylations impacted protein function, there is no obvious replication fitness advantage to encoding both of these n-linked glycosylations on their respective proteins. In the years since the introduction of the H3N2 3c.2a clade, numerous subclades such as the 3c.2a1 and 3c.2a2 have evolved and replaced the parental 3c.2a

clade. Future studies into how these subclades and the associated amino acid changes impact HA receptor binding and replication fitness are necessary to further understand HA and NA balance of the currently circulating H3N2 viruses.

Figures and Tables

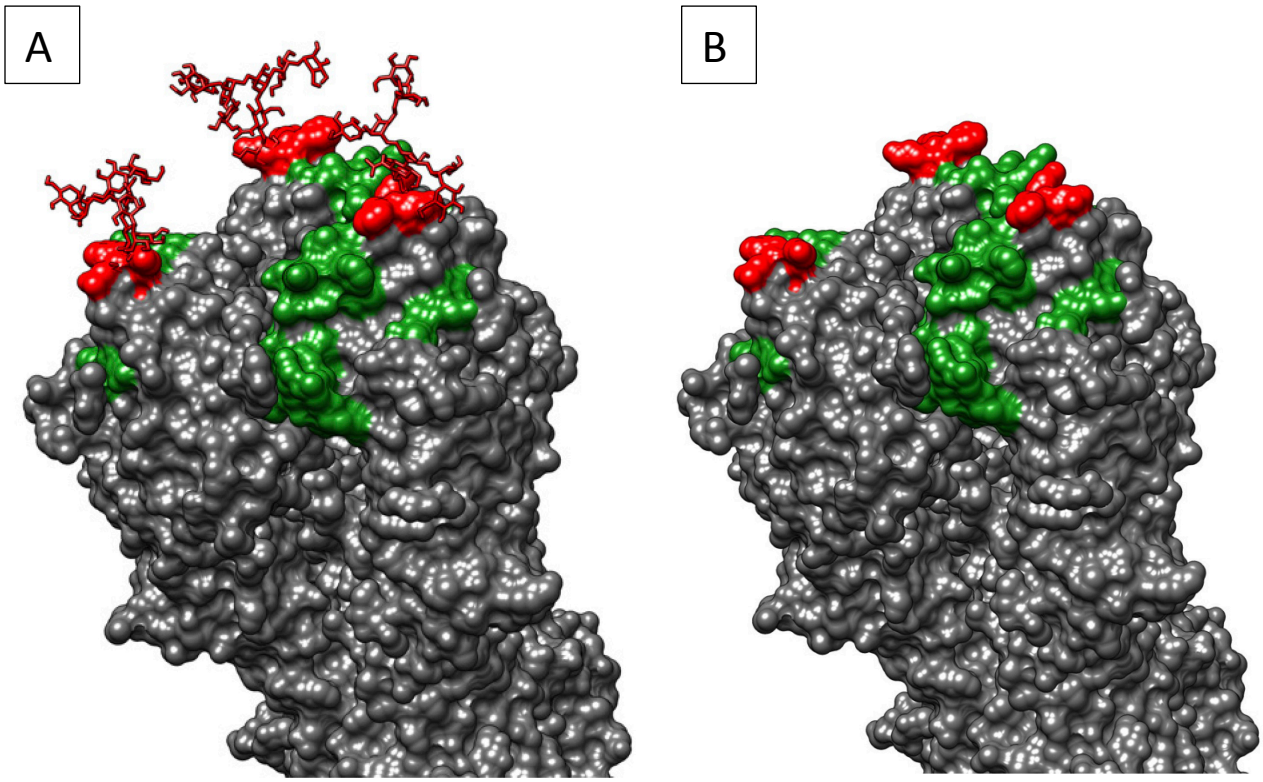

Figure 5.1: Structure of A/Bethesda/55/2015 HA trimer with or without 158-160 glycosylation used in recombinant virus preparation

(A) A/Bethesda/55/2015 HA (158 HA Gly+) with added simple glycosylation added at amino acid 158. (B) A/Bethesda/55/2015 HA (158 HA Gly-) without glycosylation due to removal of putative glycosylation sequence via site directed mutation of HA segment (T160K, H3 numbering). Figures prepared using HA trimer structure from A/Victoria/361/2011 (PDB 4WE8) via UCSF Chimera software. Glycosylation added via Glyprot (Glycosciences.de).

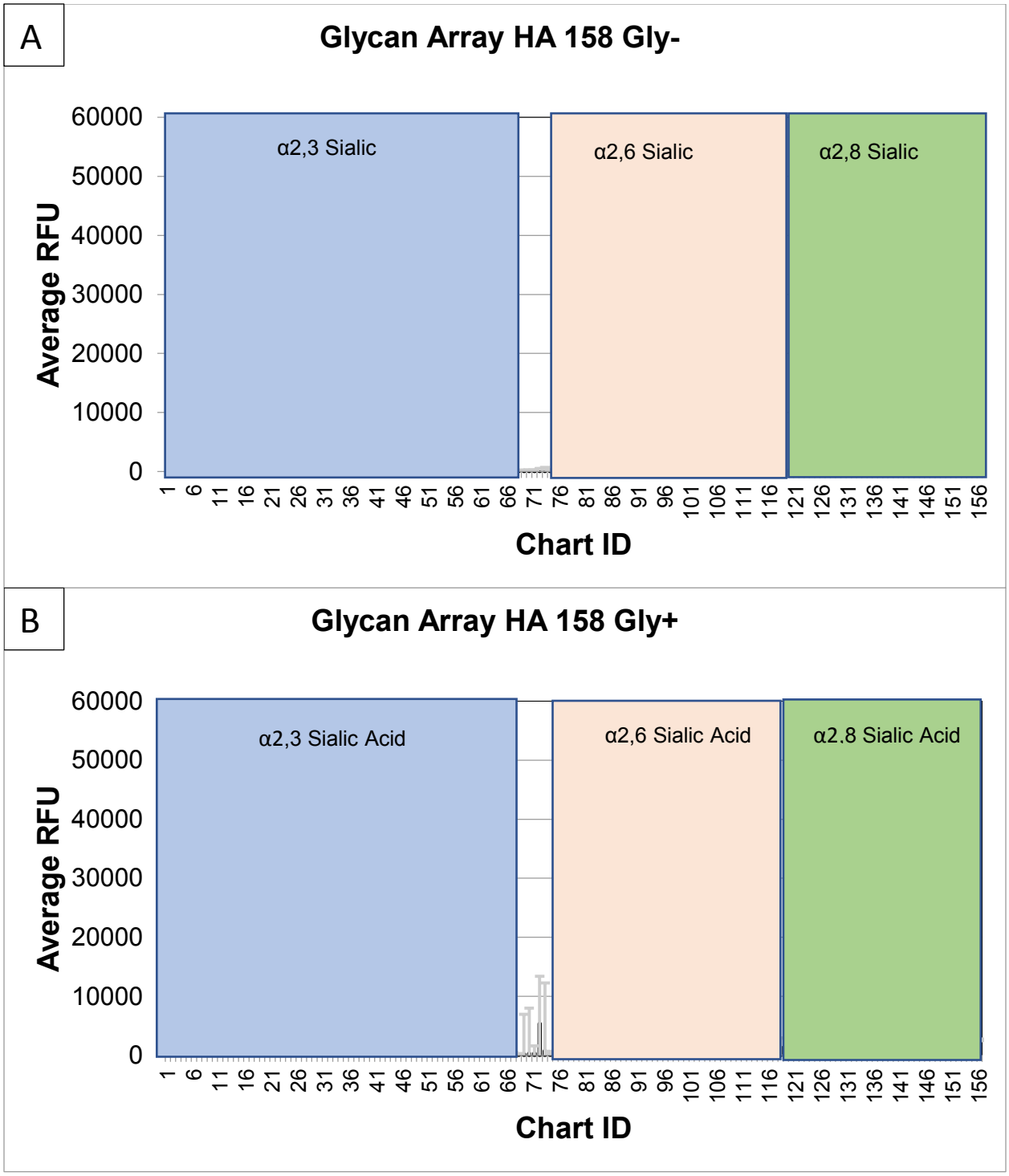

Figure 5.2: Glycan array analysis of two recombinant H3N2 viruses with different HA proteins

158 HA Gly- (**A**) 158 HA Gly+ (**B**) were subjected to glycan array analysis. Y axis indicates raw RFU, X axis indicates specific glycan ID. α2,3 Sialic acid containing ligands in blue box (glycans 2-68), α2,6 sialic acid containing glycans in off white box (glycans 75-118) and α2,8 sialic acid ligands in green box (Glycans 119-156). See

Table 2.4 in Chapter 2 for glycan ID and chemical structure. See Table 5.1 and 5.2 for highest binders for each structure.

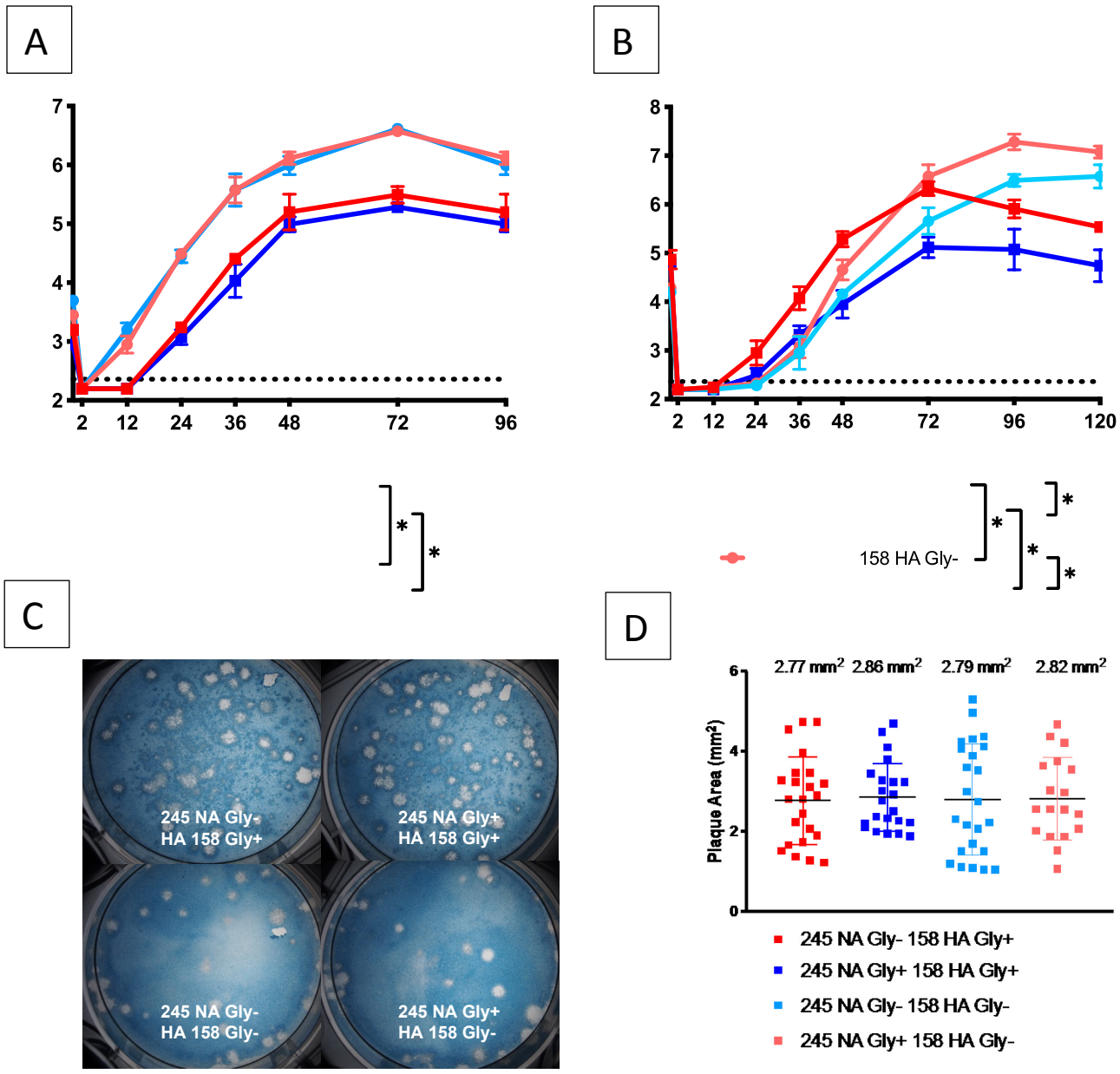

Figure 5.3: Replication of recombinant H3N2 viruses in MDCK cell cultures

Low MOI growth curves using MDCK at (**A**) or hNEC (**B**) with the indicated recombinant viruses. Hours post infection (HPI) on X axis, Log of TCID50/ml on Y axis. Data were analyzed with *p<.05 and two-way repeated measures ANOVA with Bonferroni multiple comparison posttest. The limit of detection (L.O.D.) is indicated with a dotted line at log 2.37 TCID50/ml. Error bars in A and B are SEM, error bars in D are SD. (**C**) Plaque assay performed with indicated recombinant viruses. (**D**) Quantification of plaque area from 20-30 individual plaques per virus from 2 independent experiments. *p<.05 unpaired T test.

Structure ID	Average RFU	α2,3 or α2,6 SA linkage
Neu5Aca2-6Galb1-4GlcNAcb1-3Galb1-4GlcNAcb1-3Galb1-4GlcNAcb-Sp0	38440	α2,6
Neu5Aca2-6Galb1-4GlcNAcb1-3Galb1-4(Fuca1-3)GlcNAcb1-3Galb1-4(Fuca1-3)GlcNAcb-Sp0	36956	α2,6
Neu5Aca2-6Galb1-4GlcNAcb1-3Galb1-4GlcNAcb-Sp0	24290	α2,6
Neu5Aca2-6Galb1-4GlcNAcb1-3Galb1-4GlcNAcb1-3Galb1-4GlcNAcb1-2Mana1-6(Neu5Aca2-6Galb1-4GlcNAcb1-3Galb1-4GlcNAcb1-3Galb1-4GlcNAcb1-2Mana1-3)Manb1-4GlcNAcb1-4GlcNAcb-Sp12	23608	α2,6
Neu5Aca2-6Galb1-4GlcNAcb-Sp8	21033	α2,6
Neu5Aca2-6GalNAcb1-4GlcNAcb-Sp0	19416	α2,6
Neu5Aca2-6Galb1-4(6S)GlcNAcb-Sp8	17384	α2,6
Neu5Aca2-6Galb1-4GlcNAcb1-3Galb1-4GlcNAcb1-6(Galb1-3)GalNAca-Sp14	12822	α2,6
Neu5Aca2-6Galb1-4GlcNAcb-Sp0	12036	α2,6
Neu5Aca2-6GalNAcb1-4(6S)GlcNAcb-Sp8	10215	α2,6
Galb1-4GlcNAcb1-6(Neu5Aca2-6Galb1-3GlcNAcb1-3)Galb1-4Glc-Sp21	2923	α2,6
Neu5Aca2-3Galb1-4GlcNAcb1-3Galb1-4GlcNAcb1-3Galb1-4GlcNAcb-Sp0	1531	α2,3
Neu5Aca2-3Galb1-4(6S)GlcNAcb-Sp8	1339	α2,3
Neu5Aca2-3Galb1-3GlcNAcb1-3Galb1-4GlcNAcb-Sp0	1330	α2,3
Neu5Aca2-3Galb1-4(Fuca1-3)GlcNAcb1-3Galb-Sp8	1122	α2,3
Neu5Aca2-3Galb1-4GlcNAcb1-3Galb1-3GlcNAcb-Sp0	1043	α2,3
Neu5Aca2-3Galb1-4GlcNAcb1-2Mana1-6(GlcNAcb1-4)(Neu5Aca2-3Galb1-4GlcNAcb1-2Mana1-3)Manb1-4GlcNAcb1-4GlcNAcb-Sp21	1033	α2,3
Neu5Aca2-3Galb1-4GlcNAcb1-6(Neu5Aca2-3Galb1-4GlcNAcb1-2)Mana1-6(GlcNAcb1-4)(Neu5Aca2-3Galb1-4GlcNAcb1-2Mana1-3)Manb1-4GlcNAcb1-4GlcNAcb-Sp21	907	α2,3
Neu5Aca2-3Galb1-4GlcNAcb1-3Galb-Sp8	622	α2,3

Table 5.1: HA 158 Gly- CFG synthetic glycan array binding data
A/Bethesda/55/2015 HA158 Gly- used in CFG synthetic glycan array top 20 values. Sialic acid orientation indicated (α2,3 vs α2,6). RFU average was calculated by taking the 4 highest RFU values (out of 6 technical replicates). Out of the top 20, 11 glycans contain α2,6 sialic acid (SA) linkages and 9 contains α2,3 SA.

Structure ID	Average RFU	α2,3 or α2,6 SA linkage
Neu5Aca2-6Galb1-4GlcNAcb1-3Galb1-4(Fuca1-3)GlcNAcb1-3Galb1-4(Fuca1-3)GlcNAcb-Sp0	54486	α2,6
Neu5Aca2-3Galb1-4GlcNAcb1-2Mana1-6(GlcNAcb1-4)(Neu5Aca2-3Galb1-4GlcNAcb1-2Mana1-3)Manb1-4GlcNAcb1-4GlcNAcb-Sp21	41319	α2,3
Neu5Aca2-3Galb1-4(6S)GlcNAcb-Sp8	39017	α2,3
Neu5Aca2-3Galb1-4GlcNAcb1-3Galb1-3GlcNAcb-Sp0	38168	α2,3
Neu5Aca2-6(Neu5Aca2-3Galb1-3)GalNAca-Sp8	37576	α2,6
Neu5Aca2-6Galb1-4GlcNAcb1-3Galb1-4GlcNAcb1-3Galb1-4GlcNAcb1-2Mana1-6(Neu5Aca2-6Galb1-4GlcNAcb1-3Galb1-4GlcNAcb1-3Galb1-4GlcNAcb1-2Mana1-3)Manb1-4GlcNAcb1-4GlcNAcb-Sp12	36718	α2,6
Neu5Aca2-3Galb1-3(6S)GalNAca-Sp8	36362	α2,3
Neu5Aca2-3Galb1-4GlcNAcb1-6(Neu5Aca2-3Galb1-4GlcNAcb1-2)Mana1-6(GlcNAcb1-4)(Neu5Aca2-3Galb1-4GlcNAcb1-4(Neu5Aca2-3Galb1-4GlcNAcb1-2)Mana1-3)Manb1-4GlcNAcb1-4GlcNAcb-Sp21	35713	α2,3
Neu5Aca2-3Galb1-3GlcNAcb1-3Galb1-3GlcNAcb-Sp0	35059	α2,3
Neu5Aca2-3Galb1-4GlcNAcb1-6(Neu5Aca2-3Galb1-4GlcNAcb1-2)Mana1-6(GlcNAcb1-4)(Neu5Aca2-3Galb1-4GlcNAcb1-2Mana1-3)Manb1-4GlcNAcb1-4GlcNAcb-Sp21	34130	α2,3
Neu5Aca2-3Galb1-3GalNAca-Sp8	33454	α2,3
Neu5Aca2-3Galb1-4(Fuca1-3)GlcNAcb1-3Galb1-4(Fuca1-3)GlcNAcb1-3Galb1-4(Fuca1-3)GlcNAcb-Sp0	31563	α2,3
Neu5Aca2-3Galb1-4GlcNAcb1-6(Neu5Aca2-3Galb1-3)GalNAca-Sp14	30540	α2,3
Neu5Aca2-6Galb1-4GlcNAcb1-3Galb1-4GlcNAcb1-3Galb1-4GlcNAcb-Sp0	29887	α2,6
Neu5Aca2-3Galb1-3GlcNAcb1-3Galb1-4GlcNAcb-Sp0	29466	α2,3
Neu5Aca2-6Galb1-4GlcNAcb1-3Galb1-4GlcNAcb-Sp0	29191	α2,6
Neu5Aca2-6Galb-Sp8	28754	α2,6
Neu5Aca2-3Galb1-4GlcNAcb1-3Galb-Sp8	28666	α2,6
Neu5Aca2-6Galb1-4Glcb-Sp0	28119	α2,6

Table 5.2: 158 Gly+ HA CFG synthetic glycan array binding data
A/Bethesda/55/2015 HA158 Gly+ used in CFG synthetic glycan array top 20 values. Sialic acid orientation indicated (α2,3 vs α2,6). RFU average was calculated by taking the 4 highest RFU values (out of 6 technical replicates). Out of the top 20, 8 glycans contain α2,6 SA linkages and 12 contains α2,3 SA.

CHAPTER 6: General Discussion

This dissertation improves the understanding of how the HA protein impacts LAIV vaccine effectiveness and how the NA protein impacts virus replication. By studying how egg adaptation of the LAIV vaccine strains increases viral attenuation, I showed that the current method of manufacturing the LAIV vaccine dramatically impacts HA receptor function and LAIV fitness. In my studies with the NA protein of recent H3N2 viruses, I was able to show how an n-linked glycosylation sequence on the H3N2 NA significantly decreased enzymatic function of the protein, virus replication, but ultimately provided a significant benefit in blocking the ability of neutralizing antibodies to bind and inhibit the protein. While recent N-linked glycosylation sites added to the H3N2 HA protein impact receptor function and decrease viral replication, there is no significant change in the balanced activity of the H3N2 HA and NA proteins. Taken together, this work has progressed our understanding of the LAIV attenuation phenotype, how evolution of the NA impacts virus fitness and antigenicity, and how glycosylations to the HA protein dramatically impact HA protein function and virus fitness. The research within this dissertation highlights the need to continuously assess the effects that evolution of viral proteins other than HA has on virus fitness and antigenicity.

Advisory Committee on Immunization Practices Has Recently Reversed Ruling in 2016-17 Which Advised Against LAIV Vaccination

During the 2014-2016 influenza seasons, the LAIV had little or no protection against circulating H1N1 strains in vaccinated children [163, 170, 171]. LAIV has historically been shown to offer greater protection for children between 2 and 17 years of age, compared to the IIV “flu shot” vaccine formulation [170, 171]. LAIV induces a systemic IgG response and a mucosal IgA and IgG response. Furthermore, LAIV induces a cytotoxic and helper T cell response, with reports of influenza-specific

follicular helper T cells being induced in the tonsils shortly after vaccination [259, 260]. For these reasons, a multi-armed and robust immune response, LAIV is theoretically an excellent vaccine. Multiple studies indicate that LAIV induces a broad, cross reactive T cell response to conserved epitopes between the LAIV strain and circulating isolates, even if the vaccine is considered a mismatch [261-264]. These cross reactive T cells theoretically make LAIV a better vaccine platform than the IIV, which does not consistently induce a cellular immune response [265, 266]. However, during the 2014 through 2016 seasons the effectiveness of the H1N1 component was significantly lower than the IIV, suggesting that the lack of effectiveness was due to LAIV viral replication and not an antigenic mismatch. There have been a number of hypothesis as to why this happened, but most have been disproved. Some hypothesized that because this H1N1 LAIV deficiency occurred in a similar timeframe as the CDC recommending that both the IIV and LAIV become four strain vaccines, adding an additional influenza B strain, that the added vaccine strain could be interfering with H1N1 LAIV in some manner [267-269]. However, data suggests that both the LAIV 3 (H1N1, H3N2 and one influenza B strain) has similar H1N1 issues as the LAIV 4 (LAIV 3 with an additional influenza B strain) [267]. Another hypothesis was that previous vaccination history could interfere with LAIV effectiveness. This hypothesis suggests that pre-existing antibodies are neutralizing the H1N1 component of the LAIV before the virus can infect respiratory epithelial cells, mainly because the H1N1 component had not been dramatically changed since the emergence of the 2009 pandemic H1N1. The results are not clear cut as some studies suggest that naïve children have a higher rate of LAIV vaccine response and other studies suggest that vaccination and infection history do not

significantly impact vaccine efficacy. [270, 271]. Thermo stability of the H1N1 vaccine component was one potential issue with the LAIV effectiveness but this has also been ruled out. The updated H1N1 LAIV strain used between 2014 and 2016 (A/Bolivia/559/2013) was proven to be thermostable [272, 273]. The most compelling reason of H1N1 LAIV ineffectiveness came from the manufacturer, MedImmune.

Since the introduction of 2009 pandemic swine-H1N1 into the human population, a number of viral replication deficiencies have been noted [274-277]. In general, when novel viruses emerge in the human population mutations in the HA, NA and/or multiple polymerase genes need to occur for a replication competent virus in human patients. This is due to HA receptor preferences, HA/NA balance, and the ability of the polymerase and non-structural genes to interact with host cell components and efficiently replicate in different species cell types [275]. These “species jump” issues are likely the root of the pandemic H1N1 LAIV replication issues. Historically, MedImmune has routinely screened LAIV vaccine strains for the ability to infect MDCK cells, with the fluorescent focus assay. While this assay tests the ability for LAIV to infect immortalized cells, it does not assess the ability of the vaccine virus to carry out multiple rounds of replication, nor the ability to infect more physiologically relevant hNECs [176]. During the two year period in which the Advisory Committee on Immunization Practices (ACIP) did not recommend LAIV in the United States, MedImmune revamped the protocol for testing LAIV vaccine strains [176]. They found that while the H1N1 component of LAIV from 2014-2016 (A/Bolivia/559/2013) was able to infect MDCKs, the virus showed a decreased ability to carry out multiple rounds of replication and had a significantly decreased ability to infect hNECs [176]. These new tests that MedImmune and other

members of the Pekosz Lab conducted suggest that the HA of the H1N1 LAIV component was significantly impairing viral replication competence. The new strain of H1N1 LAIV, A/Slovenia/2903/2015, has shown enhanced replication competency in both immortalized and primary hNECs, and the new strain showed similar vaccine effectiveness to the IIV formulation in studies in the UK [274, 278, 279]. Even though the H1N1 LAIV appears to once again be a functional component, the underlying issues of LAIV and viral replication competency still exist.

LAIV Replication Deficiencies Impact Vaccine Effectiveness

Historically, LAIV and to a greater extent other live attenuated vaccine are the gold standard of vaccines. These replication competent viruses antigenically mimic virulent circulating strains, but do not cause the level of disease associated with a natural infection. As discussed in Chapter 2, the dogma of LAIV has always been to use any H1N1 or H3N2 HA and NA proteins and create a temperature sensitive attenuated vaccine with the LAIV backbone [280-285]. The resulting virus will induce antibodies which should neutralize wild type viruses but not be able to cause significant disease. The recent issues with the H1N1 LAIV component should be cause for concern. The problem is twofold.

For one, it appears that certain strains of H1N1 IAV have an HA that, when combined with the LAIV backbone, will produce a replication deficient virus. This suggests that not all HA proteins from any circulating IAVs will be suitable for LAIV production. There are five amino acid differences in the HA protein between the poor H1N1 LAIV component from 2014-2016 (A/Bolivia/559/2013) and the updated H1N1 LAIV component for 2018-2020 (A/Slovenia/2903/2015). These amino acid changes (A39T, S101N, S179N, I233T, P288Q) are not in any canonical functional sites of the

HA protein, but it's important to note that S179N results in a putative n-linked glycosylation site [286-289]. How these amino acids change HA function remains to be studied, but the important point is that these amino acid changes completely change the effectiveness of the LAIV vaccine without significantly altering antigenicity of the protein. Moving forward, this problem of amino acid differences dramatically and unexpectedly impacting function could continue to cause issues with LAIV effectiveness. If we extrapolate this issue to a worst-case scenario, a potential animal reservoir pandemic influenza virus could also be incompatible with our current LAIV platform. Some studies with an avian influenza H7N9 LAIV virus show the H7N9 based LAIV is safe and effective in humans and ferrets, but it's impossible to know for every potential pandemic virus and the potential HA proteins [290-292].

The second issue with LAIV, as discussed in Chapter 2, relates to egg adaptation of all LAIV and IIV vaccine strains. The issue of egg adaptation is an unfortunate side effect of mass-producing vaccine antigen [76, 117, 121, 124]. Circulating viruses isolated form humans are passaged in eggs multiple times create a high growth reassortment that's used for vaccine testing and manufacturing [293-295]. Many amino acid changes occur in or around the receptor binding site, dramatically altering the receptor function of the HA protein. As studied in Chapter 2, I found that three amino acid changes that occurred in the H3N2 component of the LAIV in 2012/13 reduced replication of the LAIV strain in both immortalized and primary hNECs. Furthermore, these egg associated HA mutations led to a decreased innate immune response at both 32ºC and 37ºC.

There are both studies and currently licensed technologies for overcoming the egg associated mutations. Balancing high growth in eggs and maintaining genetic integrity of the HA protein is likely a non-possible outcome due to the differences between avian eggs and human nasal epithelium. However, one study looked at the incompatibility of two common egg associated mutations in the H3N2 LAIV strains, L294P and G186V, based on database sequence analysis. Their research showed that L294P significantly alters antigenicity of the protein, but it is incompatible with G186V. The G186V mutation does not dramatically alter the antigenicity of the protein and prevents the antigenic change of L294P [296-298]. Inducing the G186V mutation could create a vaccine virus capable of growing in eggs, but not dramatically changing the antigenicity of the protein. Taking these results, the next step would be to create a panel of H3N2 vaccine viruses and creating the G186V mutation before egg adaptation. This specific mutation, or others like it, could stabilize the rest of the HA protein and allow human isolates to grow to high titers in eggs. Using G186V egg adapted viruses, a rational next step would be to test their antigenicity, their ability to replicate on hNECs, and the ability to induce an innate immune response. While my work in Chapter 2 used a virus with the G186V egg associated mutation, it's unknown how this mutation impacts viral fitness of both historic and contemporary vaccine strains. This method could be an attractive solution balancing the need of an antigenically stable LAIV capable of replicating in both eggs and hNECs. While this would be a "stop-gap" measure of using an egg adapted LAIV vaccine, it could increase the replication deficiencies seen with some H3N2 LAIV vaccines.

Utilizing a Dual HA LAIV to Balance Egg Growth and Antigenic Stability

Influenza viruses acquire egg associated mutations in a somewhat random fashion, and it's impossible to predict how these mutations impact vaccine efficacy in humans. One group has published studies using a recombinant virus that expresses two HA proteins. This "dual HA" virus expresses the wild type HA protein and an egg adapted HA protein on the same virus particle [299]. This system removes the adaptation pressure for the wild type HA, allows the egg adapted HA protein to drive virus infection in eggs, which prevents wild type HA protein mutations. The virus replicates sufficiently in both eggs and cell culture, and still maintains the genetic integrity of the wild type HA protein after many passages. This approach is important because single amino acid changes in HA proteins can dramatically reduce vaccine efficacy, and this approach theoretically addresses that issue [113, 153, 300, 301]. One approach to take with this recombinant virus platform is to assess the ability of this dual HA system with the LAIV vaccine. Applying this idea with the LAIV platform and assessing the ability of this virus to replicate efficiently on hNECs would be the first step in validating this dual HA LAIV. Additionally, assessing the dominant immune response to the vaccine virus would be necessary. It's possible that, due to the phenomenon of antigenic sin, that the host immune response will focus on the egg adapted protein and not develop new antibodies to the wild type HA protein [302-314]. Technological breakthroughs like this study are primarily focused on bettering the IIV vaccine platform, but they should be assessed in the context of the LAIV vaccine.

Utilizing a Cell Based Approach to Manufacturing LAIV

In addition to changing the input virus to prevent egg associated mutations, another approach to avoiding egg associated HA mutations is to change the substrate on which the virus is grown. Novartis is currently licensed to produce Flucelvax, an

inactivated influenza vaccine using cell culture [315]. Flucelvax is unlike traditional inactivated influenza vaccines because it is entirely cell grown, completely avoiding using eggs as a substrate. Many studies have shown that Flucelvax is at least as good or better than the standard egg grown influenza vaccine [316-319], showing that no significant antigenic differences occur when growing vaccine virus on cells. Considering that MedImmune is now licensed to produce LAIV via a reverse genetics approach that utilizes mammalian cells, growing the LAIV in cells could be straightforward and prevent these common egg associated mutations. There are some caveats to this approach that need to be considered. As reported by others, some N-linked glycosylations on the HA protein (specifically site 158-160 on the H3 HA) will be lost during cell or egg culture [247, 320-323]. The presence of n-linked glycosylations on the HA protein dramatically alter the antigenicity of the protein and developing antibodies against a vaccine without specific HA glycosylations will not efficiently neutralize viruses with specific HA glycosylations [324-330]. There are also other cell culture associated mutations that occurring during cell passage [108, 193, 330, 331]. Furthermore, the cells used to manufacture Flucelvax are MDCK cells. MDCK cells express the avian like α2,3 linked sialic acid so the issue of receptor switching could still occur when passaging human isolates into either cells or eggs [156]. A potential solution to the MDCK cell receptor issue would be to use MDCK-SIAT 1 cells, which over express the human receptor α2,6 sialic acid [235]. Following my work in Chapter 2, it is also necessary to test how both a WT HA and EA HA can protect against influenza infection in either humans or ferrets. The WT HA protein replicated better on hNECs and induced a stronger IFN-λ immune response, but these two factors don't guarantee there will be an appreciable difference

in efficacy between WT and EA HA LAIV vaccine strains. Following my work in chapter 2 and utilizing a cell-based vaccine manufacturing process, I would test whether or not the WT HA (which maintains genetic integrity on cells) is a more effective vaccine than an EA HA LAIV. I would set up a study to test serum neutralizing antibody in humans before and after vaccination (with the appropriate placebo group). Furthermore, testing the ability of WT and EA HA LAIV's to induce protection with ferrets would be another appropriate test. Assuming that the WT HA is a better and safe vaccine platform than the EA HA in these suggested experiments it would be beneficial to adjust how we manufacture LAIV. Combining LAIV with a cell-based approach could alleviate the issues of receptor switching that results in deficiencies of virus growth, innate immune induction, cell tropism and ultimately vaccine effectiveness.

Temperature Sensitivity of Egg Adapted HA protein

In Chapter 2 I demonstrated that regardless of cell type the EA HA LAIV showed significant attenuation at 37ºC compared to the WT HA LAIV at 37ºC. The mutations between this EA HA and this WT HA, H156Q, G186V and S219Y, are in known receptor binding or antigenic sites of the HA protein. However, the mechanism of which they reduce viral fitness at higher temperature (37ºC) is unclear. Many studies in the thermostability of the HA protein are focused on H1N1 viruses, but none of the amino acids pertaining to H1 HA thermostability align with either of the three egg adapted mutations in this H3 HA [332-334]. Furthermore, studies into protein dynamics in the ER suggest that there are many ER components (chaperones, calnexin and calreticulin) that bind to the HA protein and assist in folding and stability [333, 335, 336]. All of these studies are done using an H1 HA and none of the amino acid residues noted as being important in stability and folding align with the A/Victoria/361/2011 EA HA used in this

study. Therefore, the next step would be to create a panel of viruses and assess how the individual egg associated amino acid changes impact viral growth. This panel of six recombinant viruses with either single or double mutations for the EA HA amino acid changes would indicate which pair or single mutations causes the phenotype of temperature attenuation. It's also possible that only the three amino changes together (H156Q, G186V, S219Y) create this phenotype however that still allow me to conduct experiments to determine how these amino acids impact temperature attenuation. Based on the amino acid(s) discovered in the viral screen the next step would be to identify which step in the viral life cycle is being impacted by the HA mutations. It could be attachment, and I would look at the infectivity of the virus at high temperatures. It could be protein stability or trafficking in the cell, and I would fractionate infected cells and see where the HA protein is localizing or if it's being degraded. It could also be interaction with specific ER components, and I would test this with immunoprecipitation assays and determine the extent of chaperones or other ER proteins interacting with the HA protein. With this line of questions, I propose that discovering the mechanism behind this temperature-based attenuation is an important step for vaccine development in general. With these findings it would allow vaccine developers to understand which egg associated amino acid changes have a high likelihood of impacting viral fitness as well as increase our understanding of how the HA protein impacts viral fitness of LAIV.

PB1-F2 Protein Emergence with 245 NA Gly+ Isolates

Human H3N2 viruses encode the PB1-F2 protein, a 2nd protein generated from the PB1 vRNA. PB1-F2 is known to be involved in modulating the host immune response as well as modulating aspects of viral polymerase function [210, 337]. PB1-F2 antagonizes interferon production by interfering with the apoptotic pathway as well as

suppressing the mitochondrial anti-viral response (MAVS) pathway [338-344]. While not the focus of Chapter 3, H3N2 isolates with the 245 NA Gly+ genotype also had a mutation in PB1-F2 protein (H75P) during the 2014/15 season. Sequence analysis shows that the PB1-F2 H75P mutation fixed in the human H3N2 when the 245 NA Gly+ genotype emerged and fixed. All of the 3c.2a isolates from 2014/15 fell into two categories, 245 NA Gly- PB1-F2 75H or 245 NA Gly+ PB1-F2 75P, suggesting that these genes grouped together [234]. The combination of these genes should be further studied to understand the effect that the PB1-F2 75H genotype or PB1-F2 75P genotype has on viral replication. The 75th amino acid in PB1-F2 is involved in mitochondrial targeting and some reports suggest that a Histidine residue at position 75 of the PB1-F2 protein decreases cellular inflammation [345, 346]. Interestingly, the H75P mutation found in recent isolates could increase inflammation and response to viral infection. The significance of such remains to be studied. To address how PB1-F2 75 H/P impact virus fitness, I would assess how this protein impacts innate immune induction, viral RNA transcription, viral polymerase localization, and viral replication. Creating reverse genetics viruses with either PB1-F2 gene and then assessing markers of innate immune induction as well as host transcriptional response would address questions relating innate immune induction [347-350]. Levels of secreted IFN-λ as well as other cytokines and chemokines would be assessed in our hNEC model. Using these same recombinant viruses, I could assess the level of viral transcripts present in the cell and localization of viral polymerase components. PB1-F2 modulates viral polymerase activity and localization through direct interaction with the PB1 protein and this would be

a relatively straight forward way of understanding how this mutation impacts polymerase activity [344].

Additionally, while the previous suggested studies would uncover the mechanistic role of the PB1-F2 mutation, a panel of recombinant viruses differing in both 245 NA glycosylation and PB1-F2 genotype should be created. These four viruses (245 NA Gly+/- and PB1-F2 75 H/P) could illustrate how the PB1-F2 mutation impacts virus replication and potentially how this mutation works in synergy with the 245 NA glycosylation. For example, if the 245 NA Gly+ PB1-F2 75H virus is significantly attenuated compared to the 245 NA Gly+ PB1-F2 75P virus it would indicate that the PB1-F2 75P protein was a key factor in allowing this 245 NA Gly+ virus to emerge and dominate the population. On the other hand, if the PB1-F2 75P decreased replication of the 245 NA Gly- virus, it would suggest that only the combination of 245 NA Gly+ and PB1-F2P would create a virus fit enough emerge in the human H3N2 population. Taken together, this set of experiments would lead to a greater understanding of the interplay of different mutations and segments with the influenza genome. These experiments would either uncover the functional benefit that PB1-F2 75P gives to H3N2 viruses, or it would indicate that the PB1-F2 mutation was a passenger and the 245 NA Gly+ drove the dominance of that strain that descendants of which still circulate to this day.

Identifying the Mechanism that 245 NA Glycosylation Impacts Viral Replication

Neuraminidase removes sialic acid from respiratory mucins and removes sialic acid from both host and viral proteins when the virus is budding. In Chapter 3, I showed that the 245 NA Gly+ virus had a significantly decreased replication fitness on hNECs but not immortalized MDCK cells. Based on these findings we hypothesized that the presence of respiratory mucins is the driving cellular factor inhibiting virus replication.

To support this hypothesis, the first step would be to assess the ability of 245 NA Gly +/- to infect cells with or without respiratory mucins. Respiratory mucins would be collected from our hNEC cultures then applied to MDCK cultures. While theoretically possible, using hNECs devoid of respiratory mucins through genetic modification or another respiratory epithelial cell line without respiratory mucins would add additional variables. Removing secreted mucins from hNEC cultures and adding them to MDCK cultures would indicate if viral replication is inhibited by the presence of soluble mucins, without the presence of other host cell factors of cell membrane anchored mucins present in hNEC cultures. If soluble respiratory mucins were not substantially impacting virus replication in these studies, the next step would be to test whether or not anchored respiratory mucins or other secreted host cell factors are inhibiting virus replication for the 245 NA Gly+ virus. Some groups have looked at how viruses migrate through respiratory mucins, showing that NA is polarized to the forward part of the virion particle as it moves through the respiratory epithelial cell mucin layer. Influenza HA and NA act as viral motors and propel the virus through mucins to the target cell. [238, 351]. Conducting similar experiments and tracking viral movement through mucins would be an important experiment to understand how the 245 NA glycosylation impacts the entry phase of the viral life cycle as well as viral motility. This would highlight key points in the viral life cycle the 245 NA glycosylation impacts replication.

Addressing the Ability of 245 NA Gly +/- Proteins to Cleave Sialic Acid from Respiratory Mucins

In a similar vein, assessing how 245 NA Gly +/- proteins interact with respiratory mucins would uncover how this glycosylation directly impacts physiologically relevant NA function. In Chapter 3 and 4, I showed that the 245 NA Gly+ NA protein had a

decreased reactivity towards both soluble (NA-STAR) and fixed (ELLA) substrate. Additionally, the 245 NA glycosylation decreases maximum velocity and affinity for soluble substrate. Fetuin, the substrate for the ELLA assay, contains both α2,6 and α2,3 sialic acid and all n and o-linked sites utilize sialic in the glycan [352-355]. The o-linked glycans containing α2,3 sialic acid present in fetuin is not representative of the topology of respiratory mucins and the o-linked glycosylations on mucin proteins. Mucins in general contain numerous o-linked glycosylation sites adjacent to one another, which results in a highly glycosylated protein covered in a glycan shell [195, 198-201, 356, 357]. Respiratory mucins can be as much as 85% by weight o-linked glycosylations [195, 358, 359]. Fetuin contains sporadic o-linked glycosylation sites throughout the protein sequence [352, 353, 355]. Utilizing a similar enzymatic substrate, either whole respiratory mucins or o-linked glycans in an array-like format could address how the 245 NA Gly +/- proteins interact with physiologically relevant ligands oriented in a physiological relevant manner. This set of assays would highlight how the recent human H3N2 NA proteins interact with respiratory mucins and o-linked glycans.

Addressing Recent NA Protein Specificity for Sialic Acid Containing Ligands

Following the work in Chapters 3 and 4, one important question remaining is to address is the specificity of recent H3N2 NA proteins with the added 245 NA glycosylation. Glycosylations change the HA protein preference for different carbohydrates present in sialic acid containing receptors and this has implications of altering cell tropism and receptor activity [81, 82]. In recent years the composition of the ligand and not just α2,6 vs α2,3 sialic acid has becoming increasingly relevant in HA receptor function. At this time, little is known if the NA protein has a similar preference for the penultimate sugar in sialic acid containing molecules or the complexity of the

glycan that contains sialic acid moieties. Based on the glycan array data in Chapter 2 and 5, assessing the ability of these NA proteins to remove sialic acid from an array of sialic acid containing ligands could offer insight to the specificity of the 245 NA Gly+ and 245 NA Gly- proteins. These assays would likely have to be optimized to rule out the HA protein interfering with results, such as using virus like particles or a functionally defective HA protein. With this set of experiments, I could determine whether certain ligands are preferentially targeted for NA activity and whether or not the 245 NA glycosylation impacts the recognition of different sugars in a glycan chain. For example, I could determine if H3N2 NA proteins preferentially bind to single chain sialic acid containing ligands or multi-antennary ligands, and how glycosylations impact this preference. General characteristics of the complexity and composition of ligands preferred by recent human H3N2 NA proteins would be valuable information to determine how the 245 n-linked glycan changes the interaction between viral protein and substrate.

Neuraminidase Immunity Can Still be Utilized as a Universal Vaccine

Before the 245 NA glycosylation event that swept the circulating human H3N2 viruses, many groups had suggested the possibility of targeting the active site as a potent universal vaccine [88, 89, 241]. While this is likely no longer possible for H3N2 viruses, it is still possible for all H1N1 viruses and Influenza B viruses that circulate in the human population. Universal vaccines should be developed to target as many influenza strains as possible [215, 217, 360]. Comparing other influenza virus NA sequences to that of currently circulating H3N2 viruses, shows that no other isolates appear to have a putative n-linked glycosylation site near the active site of the NA enzyme. Therefore, targeting the active site of the highly conserved NA protein is still an

attractive candidate for a *nearly* universal influenza vaccine. As discussed in Chapter 3 the epitope targeted by the HCA-2 mAb inhibits all influenza A and B viruses, with the notable exception of post 2015 human H3N2 isolates. The ability of this antibody and others like it to be a quick line of defense against newly emerging zoonotic influenza viruses should not be overlooked, and in my opinion should be developed as part of the influenza pandemic threat preparedness [361, 362]. Since there is little to no immune pressure in animal reservoirs of influenza viruses, there will be no pressure on these animal reservoir influenza viruses to add glycosylations that would block anti-NA active site antibodies. The swine flu pandemic of 2009 originated from the human Spanish flu of 1918. In the nearly 100 years this virus was in swine the antigenicity of the strain changed very little. This highlights the fact that the antigenicity of influenza viruses, specifically the HA protein, changes significantly only under immune pressure [363]. Therefore, utilizing an immunization strategy that targets virtually all the animal reservoir influenza viruses is an attractive candidate for vaccine development. With this knowledge, the ability of whole NA protein or specific epitopes from the active site could be evaluated for inducing a broad nearly universal vaccine in mice or ferrets. The HCA-2 Ab, used in Chapter 4, recognizes a linear epitope. This antibody was first developed by immunizing rabbits and could be utilized in a similar manner to induce broad immunity in ferrets and mice.

Identifying Antigenic Epitopes of H3N2 neuraminidase protein and NA Immunity

Previous work has shown that treating mice with serum raised against a 245 NA Gly- virus could not protect against challenge with a 245 NA Gly+ virus, they did not look at an appropriate transmission model nor a vaccination challenge model [109]. At this point we don’t know how antibodies against the NA protein impact transmission of

the virus, we only know that they correlate with decreased disease severity in humans [89, 209, 240, 364]. Many studies have looked at using monoclonal NA specific antibodies in preventing viral infection but assessing the polyclonal response to NA is a logical next step. Questions such as age and sex differences in NA antibodies affinity, quantity or specific NA immune epitopes should be investigated as they have been with the HA protein. Neutralizing antibodies that target the HA protein have been well documented to decline based on age and sex and these same questions need to be addressed with NA antibodies [365-369]. The question remains how recent changes in the NA protein affect antigenicity. The HA protein regularly mutates antigenic sites in an effort to evade humoral immunity, and even minor point mutations in the HA protein can reduce neutralizing antibody reactivity [365]. Neuraminidase antigenic mutation can be addressed using human serum samples from numerous years and a panel of NA proteins. Assessing NA antibody binding and neutralization of virus infection would indicate how the human immune response recognizes various NA proteins and how viral evolution changes this response. Additionally, neuraminidase antibodies in nasal swab or nasal pharyngeal washes are correlates of protection against influenza [221]. The specificity and affinity of these neuraminidase mucosal antibodies (IgA and IgG) has yet to be determined and could be done with infected patients nasal wash samples or animal models. For example, do mucosal IgA antibodies target conserved regions of the NA protein (such as the enzymatic pocket) or are they broader and more diverse in recognition? There are numerous questions needed to be answered about how the antigenicity of the evolving NA protein can be utilized to effectively vaccinate individuals,

and these experiments would further our understanding of the systemic and local immune response to neuraminidase.

Neuraminidase Immunity and Antigenic Sin

Antigenic sin refers to the phenomenon where conserved epitopes within an antigen are boosted instead of developing a novel response [303, 308, 310, 311]. For example, patients that receive their first influenza vaccine or natural infection are more likely to repeatedly boost the response specific epitopes first encountered and not develop antibodies towards recently changed epitopes. For the NA protein, one would ask if antigenic sin has occurred in the human population and that is what drove the emergence of the 245 NA glycosylation genotype. Virtually all influenza A and B viruses that circulate in humans share a linear epitope within the NA protein active site as well as many other shared 3D epitopes on the NA protein [88, 89, 241]. The ability of patients to recognize these shared epitopes would indicate that humans have a tendency to focus on highly conserved epitopes across all influenza viruses, thus proving a version of NA antigenic sin. To test this, repeated infection in animal models with different HA/NA proteins would show the ability of the host immune system to boost the immune response to a specific NA epitope- and potentially develop a novel almost universal vaccine strategy. There are certain studies designed to induce HA stem antibodies by sequential vaccination with H1, H7, H9 and H11 proteins. These HA proteins all share similar epitopes on the stem of the molecule and not the head [370, 371]. This study could be redesigned by sequential vaccination with N1, N2, N3 (etc.) and then screen the resulting serum for epitopes that are recognized in the NA protein. The screen could be done with whole NA protein or a phage display experiment. While a phage display assay only tests linear epitopes, it would be a valuable tool to rapidly

screen many patients' serum for presence of conserved recognized epitopes [372-374]. I hypothesize that the enzymatic pocket would be the immunodominant epitope after such a study, and it would suggest that repeated infection with influenza predisposes people to boost the humoral immune response to this common epitope. Studies like this would show how the immune response to NA can be targeted at only specific epitopes and ignore other antigenic regions of the NA protein and would offer new insights into the immunodominant epitopes in the NA protein. Alternatively, if only the enzymatic site of the NA protein is targeted, it would suggest that this epitope is immunodominant and targeting other regions of the NA protein does not result in neutralizing protein function of virus infectivity. Additionally, it would offer evidence that continuous immune pressure lead to the emergence of the H3N2 245 NA glycosylation.

Evaluate NA Antibodies Contribution to Antibody Dependent Cellular Cytotoxicity (ADCC)

Neutralizing antibodies that target and neutralizing the influenza HA protein are the largest contributor to preventing infection and decreasing disease severity [375]. However, the ability of non-neutralizing antibodies to aid in viral clearance and bolster the immune response are an often-overlooked aspect of protective immunity [376]. The ability of NA specific antibodies to stimulate a non-neutralizing immune response pathway is largely unstudied. In this dissertation the NA immunity work was focused largely on monoclonal antibodies and specific epitopes. However, the immune response to the HA and NA of influenza A viruses is polyclonal in nature. Therefore, testing the ability of human serum samples from taken from patients with contemporary influenza infections to stimulate the ADCC pathway and assess the polyclonal non-neutralizing response to influenza NA would be an important experiment to fill this gap in our

understanding of influenza immunity. Many groups infect immortalized MDCK cells then use human serum and effector cells (e.g., Jurkat immortalized T cells) to test ADCC antibodies against HA proteins [376-379]. I would focus on NA specific antibodies by expressing NA proteins in the absence of any other influenza proteins. Studying how the 245 NA glycosylation impacts the ADCC response with human serum would further expand our knowledge how this NA glycosylation impacts another facet of the immune response. This experimental plan would add to our knowledge of how NA protein evolution evades non-neutralizing antibodies, and if NA specific non-neutralizing antibodies play a major role in the immune response to influenza infection.

Conclusion

Traditional influenza vaccines rely on a decades old manufacturing process, one which routinely leads to severe seasons and underperforming vaccine components. Current vaccination formulation procedures have been insufficient to respond quickly to a rapidly changing virus under constant immune pressure, and even when the correct strain is chosen the reliance on growing most influenza vaccines in eggs can lead to complete failure of a vaccine component. Even though the LAIV vaccine is a relatively new influenza vaccine, only being approved in the United States in September of 2003, there have been numerous documented issues with antigenicity and efficacy. While the work in this dissertation focused on one vaccine component in one influenza season, the same findings can apply to each year's LAIV vaccine. Egg adaptation and the unknown result of combining certain HA proteins with the LAIV vaccine platform can result in an over-attenuated low efficacy LAIV vaccine. The idea that HA protein plays a role in attenuation is not a novel concept, but the improvements outlined in the dissertation could alleviate the unpredictable efficacy of each years LAIV strain.

A common theme in studying influenza is the rapid evolution of each segment in response to a variety of host pressures. When glycosylation changes occur within the influenza HA protein, the vaccine has been shown to fail due to dramatic antigenicity changes. The finding that glycosylation changes that happen to the NA protein and dramatically impact humoral immunity and virus fitness is a novel finding presented in this dissertation. This dissertation shows that the influenza virus will incur a significant fitness advantage at the benefit of blocking the activity of NA specific neutralizing antibodies. Since nearly all H3N2 viruses have undergone this cost-benefit process, it suggests that NA immunity plays a large role in the human immune response and deserves further attention. NA immunity is not a recent finding in the influenza community however NA immunity deserves an equal consideration when developing influenza vaccines and evaluating NA focused universal influenza vaccines.

References

1. Ghebrehewet S, MacPherson P, Ho A. Influenza. BMJ. 2016;355:i6258.

2. Peteranderl C, Herold S, Schmoldt C. Human Influenza Virus Infections. Semin Respir Crit Care Med. 2016;37(4):487-500.

3. CDC. Disease Burden of Influenza 2020 [Available from: https://www.cdc.gov/flu/about/burden/index.html.

4. Webster RG, Bean WJ, Jr. Genetics of influenza virus. Annu Rev Genet. 1978;12:415-31.

5. Scholtissek C. Influenza virus genetics. Adv Genet. 1979;20:1-36.

6. Brown EG. Influenza virus genetics. Biomed Pharmacother. 2000;54(4):196-209.

7. Samji T. Influenza A: understanding the viral life cycle. Yale J Biol Med. 2009;82(4):153-9.

8. Noda T. [Orthomyxoviruses]. Uirusu. 2012;62(2):219-28.

9. Lamb RA, Zebedee SL, Richardson CD. Influenza virus M2 protein is an integral membrane protein expressed on the infected-cell surface. Cell. 1985;40(3):627-33.

10. Lamb RA, Lai CJ. Conservation of the influenza virus membrane protein (M1) amino acid sequence and an open reading frame of RNA segment 7 encoding a second protein (M2) in H1N1 and H3N2 strains. Virology. 1981;112(2):746-51.

11. Lamb RA, Choppin PW. Identification of a second protein (M2) encoded by RNA segment 7 of influenza virus. Virology. 1981;112(2):729-37.

12. Martin K, Helenius A. Nuclear transport of influenza virus ribonucleoproteins: the viral matrix protein (M1) promotes export and inhibits import. Cell. 1991;67(1):117-30.

13. Ito T, Gorman OT, Kawaoka Y, Bean WJ, Webster RG. Evolutionary analysis of the influenza A virus M gene with comparison of the M1 and M2 proteins. J Virol. 1991;65(10):5491-8.

14. Elster C, Larsen K, Gagnon J, Ruigrok RW, Baudin F. Influenza virus M1 protein binds to RNA through its nuclear localization signal. J Gen Virol. 1997;78 (Pt 7):1589-96.

15. Stubbs TM, Te Velthuis AJ. The RNA-dependent RNA polymerase of the influenza A virus. Future Virol. 2014;9(9):863-76.

16. Skehel JJ. RNA-dependent RNA polymerase activity of the influenza virus. Virology. 1971;45(3):793-6.

17. Hastie ND, Mahy BW. RNA-dependent RNA polymerase in nuclei of cells infected with influenza virus. J Virol. 1973;12(5):951-61.

18. Wu WW, Weaver LL, Pante N. Purification and visualization of influenza a viral ribonucleoprotein complexes. J Vis Exp. 2009(24).

19. Wu WW, Sun YH, Pante N. Nuclear import of influenza A viral ribonucleoprotein complexes is mediated by two nuclear localization sequences on viral nucleoprotein. Virol J. 2007;4:49.

20. Terrier O, Carron C, De Chassey B, Dubois J, Traversier A, Julien T, et al. Nucleolin interacts with influenza A nucleoprotein and contributes to viral ribonucleoprotein complexes nuclear trafficking and efficient influenza viral replication. Sci Rep. 2016;6:29006.

21. Couceiro JN, Paulson JC, Baum LG. Influenza virus strains selectively recognize sialyloligosaccharides on human respiratory epithelium; the role of the host cell in selection of hemagglutinin receptor specificity. Virus Res. 1993;29(2):155-65.

22. Matrosovich MN, Matrosovich TY, Gray T, Roberts NA, Klenk HD. Human and avian influenza viruses target different cell types in cultures of human airway epithelium. Proc Natl Acad Sci U S A. 2004;101(13):4620-4.

23. Schauer R. Achievements and challenges of sialic acid research. Glycoconj J. 2000;17(7-9):485-99.

24. Shelton H, Ayora-Talavera G, Ren J, Loureiro S, Pickles RJ, Barclay WS, et al. Receptor binding profiles of avian influenza virus hemagglutinin subtypes on human cells as a predictor of pandemic potential. J Virol. 2011;85(4):1875-80.

25. Shinya K, Ebina M, Yamada S, Ono M, Kasai N, Kawaoka Y. Avian flu: influenza virus receptors in the human airway. Nature. 2006;440(7083):435-6.

26. Dou D, Revol R, Ostbye H, Wang H, Daniels R. Influenza A Virus Cell Entry, Replication, Virion Assembly and Movement. Front Immunol. 2018;9:1581.

27. Sun X, Whittaker GR. Entry of influenza virus. Adv Exp Med Biol. 2013;790:72-82.

28. Luo M. Influenza virus entry. Adv Exp Med Biol. 2012;726:201-21.

29. Geisow MJ, Evans WH. pH in the endosome. Measurements during pinocytosis and receptor-mediated endocytosis. Exp Cell Res. 1984;150(1):36-46.

30. Cross KJ, Langley WA, Russell RJ, Skehel JJ, Steinhauer DA. Composition and functions of the influenza fusion peptide. Protein Pept Lett. 2009;16(7):766-78.

31. Skehel JJ, Daniels RS, Hay AJ, Ruigrok R, Wharton SA, Wrigley NG, et al. Structural changes in influenza virus haemagglutinin at the pH of membrane fusion. Biochem Soc Trans. 1986;14(2):252-3.

32. Beyer WE, Ruigrok RW, van Driel H, Masurel N. Influenza virus strains with a fusion threshold of pH 5.5 or lower are inhibited by amantadine. Brief report. Arch Virol. 1986;90(1-2):173-81.

33. Maeda T, Kawasaki K, Ohnishi S. Interaction of influenza virus hemagglutinin with target membrane lipids is a key step in virus-induced hemolysis and fusion at pH 5.2. Proc Natl Acad Sci U S A. 1981;78(7):4133-7.

34. Shtykova EV, Dadinova LA, Fedorova NV, Golanikov AE, Bogacheva EN, Ksenofontov AL, et al. Influenza virus Matrix Protein M1 preserves its conformation with pH, changing multimerization state at the priming stage due to electrostatics. Sci Rep. 2017;7(1):16793.

35. Fontana J, Steven AC. At low pH, influenza virus matrix protein M1 undergoes a conformational change prior to dissociating from the membrane. J Virol. 2013;87(10):5621-8.

36. Bui M, Whittaker G, Helenius A. Effect of M1 protein and low pH on nuclear transport of influenza virus ribonucleoproteins. J Virol. 1996;70(12):8391-401.

37. Fodor E, Te Velthuis AJW. Structure and Function of the Influenza Virus Transcription and Replication Machinery. Cold Spring Harb Perspect Med. 2019.

38. Boivin S, Hart DJ. Interaction of the influenza A virus polymerase PB2 C-terminal region with importin alpha isoforms provides insights into host adaptation and polymerase assembly. J Biol Chem. 2011;286(12):10439-48.

39. Gabriel G, Herwig A, Klenk HD. Interaction of polymerase subunit PB2 and NP with importin alpha1 is a determinant of host range of influenza A virus. PLoS Pathog. 2008;4(2):e11.

40. te Velthuis AJ, Turrell L, Vreede FT, Fodor E. Uncoupling of influenza A virus transcription and replication through mutation of the unpaired adenosine in the viral RNA promoter. J Virol. 2013;87(18):10381-4.

41. Pflug A, Lukarska M, Resa-Infante P, Reich S, Cusack S. Structural insights into RNA synthesis by the influenza virus transcription-replication machine. Virus Res. 2017;234:103-17.

42. Drake JW. Rates of spontaneous mutation among RNA viruses. Proc Natl Acad Sci U S A. 1993;90(9):4171-5.

43. Drake JW, Holland JJ. Mutation rates among RNA viruses. Proc Natl Acad Sci U S A. 1999;96(24):13910-3.

44. Kundu A, Nayak DP. Analysis of the signals for polarized transport of influenza virus (A/WSN/33) neuraminidase and human transferrin receptor, type II transmembrane proteins. J Virol. 1994;68(3):1812-8.

45. Kornfeld R, Kornfeld S. Assembly of asparagine-linked oligosaccharides. Annu Rev Biochem. 1985;54:631-64.

46. Reily C, Stewart TJ, Renfrow MB, Novak J. Glycosylation in health and disease. Nat Rev Nephrol. 2019;15(6):346-66.

47. Holsinger LJ, Lamb RA. Influenza virus M2 integral membrane protein is a homotetramer stabilized by formation of disulfide bonds. Virology. 1991;183(1):32-43.

48. Bauer CM, Pinto LH, Cross TA, Lamb RA. The influenza virus M2 ion channel protein: probing the structure of the transmembrane domain in intact cells by using engineered disulfide cross-linking. Virology. 1999;254(1):196-209.

49. Ye ZP, Pal R, Fox JW, Wagner RR. Functional and antigenic domains of the matrix (M1) protein of influenza A virus. J Virol. 1987;61(2):239-46.

50. Wakefield L, Brownlee GG. RNA-binding properties of influenza A virus matrix protein M1. Nucleic Acids Res. 1989;17(21):8569-80.

51. Ruigrok RW, Barge A, Durrer P, Brunner J, Ma K, Whittaker GR. Membrane interaction of influenza virus M1 protein. Virology. 2000;267(2):289-98.

52. Hu B, Hofer CT, Thiele C, Veit M. Cholesterol Binding to the Transmembrane Region of a Group 2 Hemagglutinin (HA) of Influenza Virus Is Essential for Virus Replication, Affecting both Virus Assembly and HA Fusion Activity. J Virol. 2019;93(15).

53. Elkins MR, Williams JK, Gelenter MD, Dai P, Kwon B, Sergeyev IV, et al. Cholesterol-binding site of the influenza M2 protein in lipid bilayers from solid-state NMR. Proc Natl Acad Sci U S A. 2017;114(49):12946-51.

54. Bajimaya S, Frankl T, Hayashi T, Takimoto T. Cholesterol is required for stability and infectivity of influenza A and respiratory syncytial viruses. Virology. 2017;510:234-41.

55. Ohkura T, Momose F, Ichikawa R, Takeuchi K, Morikawa Y. Influenza A virus hemagglutinin and neuraminidase mutually accelerate their apical targeting through clustering of lipid rafts. J Virol. 2014;88(17):10039-55.

56. Vahey MD, Fletcher DA. Influenza A virus surface proteins are organized to help penetrate host mucus. Elife. 2019;8.

57. Harris A, Cardone G, Winkler DC, Heymann JB, Brecher M, White JM, et al. Influenza virus pleiomorphy characterized by cryoelectron tomography. Proc Natl Acad Sci U S A. 2006;103(50):19123-7.

58. Paulino J, Pang X, Hung I, Zhou HX, Cross TA. Influenza A M2 Channel Clustering at High Protein/Lipid Ratios: Viral Budding Implications. Biophys J. 2019;116(6):1075-84.

59. Leser GP, Lamb RA. Influenza virus assembly and budding in raft-derived microdomains: a quantitative analysis of the surface distribution of HA, NA and M2 proteins. Virology. 2005;342(2):215-27.

60. Matrosovich MN, Matrosovich TY, Gray T, Roberts NA, Klenk HD. Neuraminidase is important for the initiation of influenza virus infection in human airway epithelium. J Virol. 2004;78(22):12665-7.

61. McAuley JL, Gilbertson BP, Trifkovic S, Brown LE, McKimm-Breschkin JL. Influenza Virus Neuraminidase Structure and Functions. Front Microbiol. 2019;10:39.

62. Millard PS. Review: Neuraminidase inhibitors reduce symptomatic influenza; oseltamivir does not reduce hospitalizations. Ann Intern Med. 2014;161(8):JC2.

63. McNicholl IR, McNicholl JJ. Neuraminidase inhibitors: zanamivir and oseltamivir. Ann Pharmacother. 2001;35(1):57-70.

64. Allen JD, Ross TM. H3N2 influenza viruses in humans: Viral mechanisms, evolution, and evaluation. Hum Vaccin Immunother. 2018;14(8):1840-7.

65. Wu NC, Wilson IA. Influenza Hemagglutinin Structures and Antibody Recognition. Cold Spring Harb Perspect Med. 2019.

66. Russell CJ, Hu M, Okda FA. Influenza Hemagglutinin Protein Stability, Activation, and Pandemic Risk. Trends Microbiol. 2018;26(10):841-53.

67. Klenk HD, Garten W, Rott R. Inhibition of proteolytic cleavage of the hemagglutinin of influenza virus by the calcium-specific ionophore A23187. EMBO J. 1984;3(12):2911-5.

68. Lazarowitz SG, Compans RW, Choppin PW. Proteolytic cleavage of the hemagglutinin polypeptide of influenza virus. Function of the uncleaved polypeptide HA. Virology. 1973;52(1):199-212.

69. Bertram S, Glowacka I, Steffen I, Kuhl A, Pohlmann S. Novel insights into proteolytic cleavage of influenza virus hemagglutinin. Rev Med Virol. 2010;20(5):298-310.

70. Bottcher E, Matrosovich T, Beyerle M, Klenk HD, Garten W, Matrosovich M. Proteolytic activation of influenza viruses by serine proteases TMPRSS2 and HAT from human airway epithelium. J Virol. 2006;80(19):9896-8.

71. An Y, McCullers JA, Alymova I, Parsons LM, Cipollo JF. Glycosylation Analysis of Engineered H3N2 Influenza A Virus Hemagglutinins with Sequentially Added Historically Relevant Glycosylation Sites. J Proteome Res. 2015;14(9):3957-69.

72. Alymova IV, York IA, Air GM, Cipollo JF, Gulati S, Baranovich T, et al. Glycosylation changes in the globular head of H3N2 influenza hemagglutinin modulate receptor binding without affecting virus virulence. Sci Rep. 2016;6:36216.

73. Rogers GN, Daniels RS, Skehel JJ, Wiley DC, Wang XF, Higa HH, et al. Host-mediated selection of influenza virus receptor variants. Sialic acid-alpha 2,6Gal-specific clones of A/duck/Ukraine/1/63 revert to sialic acid-alpha 2,3Gal-specific wild type in ovo. J Biol Chem. 1985;260(12):7362-7.

74. Pekosz A, Newby C, Bose PS, Lutz A. Sialic acid recognition is a key determinant of influenza A virus tropism in murine trachea epithelial cell cultures. Virology. 2009;386(1):61-7.

75. Kumlin U, Olofsson S, Dimock K, Arnberg N. Sialic acid tissue distribution and influenza virus tropism. Influenza Other Respir Viruses. 2008;2(5):147-54.

76. Ito T, Suzuki Y, Takada A, Kawamoto A, Otsuki K, Masuda H, et al. Differences in sialic acid-galactose linkages in the chicken egg amnion and allantois influence human influenza virus receptor specificity and variant selection. J Virol. 1997;71(4):3357-62.

77. Alford D, Ellens H, Bentz J. Fusion of influenza virus with sialic acid-bearing target membranes. Biochemistry. 1994;33(8):1977-87.

78. Rogers GN, Paulson JC. Receptor determinants of human and animal influenza virus isolates: differences in receptor specificity of the H3 hemagglutinin based on species of origin. Virology. 1983;127(2):361-73.

79. McQuillan AM, Byrd-Leotis L, Heimburg-Molinaro J, Cummings RD. Natural and Synthetic Sialylated Glycan Microarrays and Their Applications. Front Mol Biosci. 2019;6:88.

80. Kiss G, Chen X, Brindley MA, Campbell P, Afonso CL, Ke Z, et al. Capturing enveloped viruses on affinity grids for downstream cryo-electron microscopy applications. Microsc Microanal. 2014;20(1):164-74.

81. Byrd-Leotis L, Gao C, Jia N, Mehta AY, Trost J, Cummings SF, et al. Antigenic Pressure on H3N2 Influenza Virus Drift Strains Imposes Constraints on Binding to Sialylated Receptors but Not Phosphorylated Glycans. J Virol. 2019;93(22).

82. Byrd-Leotis L, Cummings RD, Steinhauer DA. The Interplay between the Host Receptor and Influenza Virus Hemagglutinin and Neuraminidase. Int J Mol Sci. 2017;18(7).

83. Streltsov VA, Schmidt PM, McKimm-Breschkin JL. Structure of an Influenza A virus N9 neuraminidase with a tetrabrachion-domain stalk. Acta Crystallogr F Struct Biol Commun. 2019;75(Pt 2):89-97.

84. Shtyrya YA, Mochalova LV, Bovin NV. Influenza virus neuraminidase: structure and function. Acta Naturae. 2009;1(2):26-32.

85. Suzuki T, Takahashi T, Saito T, Guo CT, Hidari KI, Miyamoto D, et al. Evolutional analysis of human influenza A virus N2 neuraminidase genes based on the transition of the low-pH stability of sialidase activity. FEBS Lett. 2004;557(1-3):228-32.

86. Baum LG, Paulson JC. The N2 neuraminidase of human influenza virus has acquired a substrate specificity complementary to the hemagglutinin receptor specificity. Virology. 1991;180(1):10-5.

87. Kobasa D, Kodihalli S, Luo M, Castrucci MR, Donatelli I, Suzuki Y, et al. Amino acid residues contributing to the substrate specificity of the influenza A virus neuraminidase. J Virol. 1999;73(8):6743-51.

88. Doyle TM, Li C, Bucher DJ, Hashem AM, Van Domselaar G, Wang J, et al. A monoclonal antibody targeting a highly conserved epitope in influenza B neuraminidase provides protection against drug resistant strains. Biochem Biophys Res Commun. 2013;441(1):226-9.

89. Doyle TM, Jaentschke B, Van Domselaar G, Hashem AM, Farnsworth A, Forbes NE, et al. The universal epitope of influenza A viral neuraminidase fundamentally contributes to enzyme activity and viral replication. J Biol Chem. 2013;288(25):18283-9.

90. Ives JA, Carr JA, Mendel DB, Tai CY, Lambkin R, Kelly L, et al. The H274Y mutation in the influenza A/H1N1 neuraminidase active site following oseltamivir phosphate treatment leave virus severely compromised both in vitro and in vivo. Antiviral Res. 2002;55(2):307-17.

91. Baz M, Abed Y, Simon P, Hamelin ME, Boivin G. Effect of the neuraminidase mutation H274Y conferring resistance to oseltamivir on the replicative capacity and virulence of old and recent human influenza A(H1N1) viruses. J Infect Dis. 2010;201(5):740-5.

92. Matsuoka Y, Swayne DE, Thomas C, Rameix-Welti MA, Naffakh N, Warnes C, et al. Neuraminidase stalk length and additional glycosylation of the hemagglutinin influence the virulence of influenza H5N1 viruses for mice. J Virol. 2009;83(9):4704-8.

93. Baigent SJ, McCauley JW. Glycosylation of haemagglutinin and stalk-length of neuraminidase combine to regulate the growth of avian influenza viruses in tissue culture. Virus Res. 2001;79(1-2):177-85.

94. Monto AS, Petrie JG, Cross RT, Johnson E, Liu M, Zhong W, et al. Antibody to Influenza Virus Neuraminidase: An Independent Correlate of Protection. J Infect Dis. 2015;212(8):1191-9.

95. Krammer F, Fouchier RAM, Eichelberger MC, Webby RJ, Shaw-Saliba K, Wan H, et al. NAction! How Can Neuraminidase-Based Immunity Contribute to Better Influenza Virus Vaccines? MBio. 2018;9(2).

96. Sylte MJ, Suarez DL. Influenza neuraminidase as a vaccine antigen. Curr Top Microbiol Immunol. 2009;333:227-41.

97. Mitnaul LJ, Matrosovich MN, Castrucci MR, Tuzikov AB, Bovin NV, Kobasa D, et al. Balanced hemagglutinin and neuraminidase activities are critical for efficient replication of influenza A virus. J Virol. 2000;74(13):6015-20.

98. Wagner R, Matrosovich M, Klenk HD. Functional balance between haemagglutinin and neuraminidase in influenza virus infections. Rev Med Virol. 2002;12(3):159-66.

99. Gaymard A, Le Briand N, Frobert E, Lina B, Escuret V. Functional balance between neuraminidase and haemagglutinin in influenza viruses. Clin Microbiol Infect. 2016;22(12):975-83.

100. Yang X, Steukers L, Forier K, Xiong R, Braeckmans K, Van Reeth K, et al. A beneficiary role for neuraminidase in influenza virus penetration through the respiratory mucus. PLoS One. 2014;9(10):e110026.

101. Scholtissek C. Stability of infectious influenza A viruses at low pH and at elevated temperature. Vaccine. 1985;3(3 Suppl):215-8.

102. Cohen M, Zhang XQ, Senaati HP, Chen HW, Varki NM, Schooley RT, et al. Influenza A penetrates host mucus by cleaving sialic acids with neuraminidase. Virol J. 2013;10:321.

103. Palese P, Tobita K, Ueda M, Compans RW. Characterization of temperature sensitive influenza virus mutants defective in neuraminidase. Virology. 1974;61(2):397-410.

104. Lai JCC, Karunarathna H, Wong HH, Peiris JSM, Nicholls JM. Neuraminidase activity and specificity of influenza A virus are influenced by haemagglutinin-receptor binding. Emerg Microbes Infect. 2019;8(1):327-38.

105. Matrosovich M, Zhou N, Kawaoka Y, Webster R. The surface glycoproteins of H5 influenza viruses isolated from humans, chickens, and wild aquatic birds have distinguishable properties. J Virol. 1999;73(2):1146-55.

106. Blumenkrantz D, Roberts KL, Shelton H, Lycett S, Barclay WS. The short stalk length of highly pathogenic avian influenza H5N1 virus neuraminidase limits transmission of pandemic H1N1 virus in ferrets. J Virol. 2013;87(19):10539-51.

107. Li Y, Bostick DL, Sullivan CB, Myers JL, Griesemer SB, Stgeorge K, et al. Single hemagglutinin mutations that alter both antigenicity and receptor binding avidity influence influenza virus antigenic clustering. J Virol. 2013;87(17):9904-10.

108. Doud MB, Lee JM, Bloom JD. How single mutations affect viral escape from broad and narrow antibodies to H1 influenza hemagglutinin. Nat Commun. 2018;9(1):1386.

109. Chen Y-Q, Lan LY-L, Huang M, Henry C, Wilson PC. 2018.

110. CDC. How Influenza (Flu) Vaccines are Made 2020 [Available from: https://www.cdc.gov/flu/prevent/how-fluvaccine-made.htm.

111. Gouma S, Weirick M, Hensley SE. Potential antigenic mismatch of the H3N2 component of the 2019 Southern Hemisphere influenza vaccine. Clin Infect Dis. 2019.

112. de Jong JC, Beyer WE, Palache AM, Rimmelzwaan GF, Osterhaus AD. Mismatch between the 1997/1998 influenza vaccine and the major epidemic A(H3N2) virus strain as the cause of an inadequate vaccine-induced antibody response to this strain in the elderly. J Med Virol. 2000;61(1):94-9.

113. Tricco AC, Chit A, Soobiah C, Hallett D, Meier G, Chen MH, et al. Comparing influenza vaccine efficacy against mismatched and matched strains: a systematic review and meta-analysis. BMC Med. 2013;11:153.

114. Buckland BC. The development and manufacture of influenza vaccines. Hum Vaccin Immunother. 2015;11(6):1357-60.

115. Baxter MD. Manufacturing a flu vaccine. N C Med J. 2007;68(1):49-50.

116. Chan MCW, Wang MH, Chen Z, Hui DSC, Kwok AK, Yeung ACM, et al. Frequent Genetic Mismatch between Vaccine Strains and Circulating Seasonal Influenza Viruses, Hong Kong, China, 1996-2012. Emerg Infect Dis. 2018;24(10):1825-34.

117. Suptawiwat O, Jeamtua W, Boonarkart C, Kongchanagul A, Puthawathana P, Auewarakul P. Effects of the Q223R mutation in the hemagglutinin (HA) of egg-adapted pandemic 2009 (H1N1) influenza A virus on virus growth and binding of HA to human- and avian-type cell receptors. Acta Virol. 2013;57(3):333-8.

118. Skowronski DM, Janjua NZ, De Serres G, Sabaiduc S, Eshaghi A, Dickinson JA, et al. Low 2012-13 influenza vaccine effectiveness associated with mutation in the egg-adapted H3N2 vaccine strain not antigenic drift in circulating viruses. PLoS One. 2014;9(3):e92153.

119. Rocha EP, Xu X, Hall HE, Allen JR, Regnery HL, Cox NJ. Comparison of 10 influenza A (H1N1 and H3N2) haemagglutinin sequences obtained directly from clinical specimens to those of MDCK cell- and egg-grown viruses. J Gen Virol. 1993;74 (Pt 11):2513-8.

120. Liu F, Tzeng WP, Horner L, Kamal RP, Tatum HR, Blanchard EG, et al. Influence of Immune Priming and Egg Adaptation in the Vaccine on Antibody Responses to Circulating A(H1N1)pdm09 Viruses After Influenza Vaccination in Adults. J Infect Dis. 2018;218(10):1571-81.

121. Gatherer D. Passage in egg culture is a major cause of apparent positive selection in influenza B hemagglutinin. J Med Virol. 2010;82(1):123-7.

122. Parker L, Wharton SA, Martin SR, Cross K, Lin Y, Liu Y, et al. Effects of egg-adaptation on receptor-binding and antigenic properties of recent influenza A (H3N2) vaccine viruses. J Gen Virol. 2016;97(6):1333-44.

123. Gambaryan AS, Tuzikov AB, Piskarev VE, Yamnikova SS, Lvov DK, Robertson JS, et al. Specification of receptor-binding phenotypes of influenza virus isolates from different hosts using synthetic sialylglycopolymers: non-egg-adapted human H1 and H3 influenza A and influenza B viruses share a common high binding affinity for 6'-sialyl(N-acetyllactosamine). Virology. 1997;232(2):345-50.

124. Gambaryan AS, Robertson JS, Matrosovich MN. Effects of egg-adaptation on the receptor-binding properties of human influenza A and B viruses. Virology. 1999;258(2):232-9.

125. Toback SL, Levin MJ, Block SL, Belshe RB, Ambrose CS, Falloon J. Quadrivalent Ann Arbor strain live-attenuated influenza vaccine. Expert Rev Vaccines. 2012;11(11):1293-303.

126. Sheldon EA, Jeanfreau R, Sliman JA, Charenkavanich S, Rousculp MD, Dubovsky F, et al. Immunogenicity of a quadrivalent Ann Arbor strain live attenuated influenza vaccine

delivered using a blow-fill-seal device in adults: a randomized, active-controlled study*. Influenza Other Respir Viruses. 2013;7(6):1142-50.

127. Zeneca A. FluMist Quadrivalent 2020 [Available from: https://www.flumistquadrivalent.com/.

128. Cox NJ, Kitame F, Kendal AP, Maassab HF, Naeve C. Identification of sequence changes in the cold-adapted, live attenuated influenza vaccine strain, A/Ann Arbor/6/60 (H2N2). Virology. 1988;167(2):554-67.

129. Wohlgemuth N, Ye Y, Fenstermacher KJ, Liu H, Lane AP, Pekosz A. The M2 protein of live, attenuated influenza vaccine encodes a mutation that reduces replication in human nasal epithelial cells. Vaccine. 2017;35(48 Pt B):6691-9.

130. Tomoda T, Morita H, Kurashige T, Maassab HF. Prevention of influenza by the intranasal administration of cold-recombinant, live-attenuated influenza virus vaccine: importance of interferon-gamma production and local IgA response. Vaccine. 1995;13(2):185-90.

131. Ambrose CS, Wu X, Jones T, Mallory RM. The role of nasal IgA in children vaccinated with live attenuated influenza vaccine. Vaccine. 2012;30(48):6794-801.

132. Fischer WA, 2nd, Chason KD, Brighton M, Jaspers I. Live attenuated influenza vaccine strains elicit a greater innate immune response than antigenically-matched seasonal influenza viruses during infection of human nasal epithelial cell cultures. Vaccine. 2014;32(15):1761-7.

133. Boyce TG, Gruber WC, Coleman-Dockery SD, Sannella EC, Reed GW, Wolff M, et al. Mucosal immune response to trivalent live attenuated intranasal influenza vaccine in children. Vaccine. 1999;18(1-2):82-8.

134. Mallory RM, Yu J, Kameo S, Tanaka M, Rito K, Itoh Y, et al. The safety and efficacy of quadrivalent live attenuated influenza vaccine in Japanese children aged 2-18 years: Results of two phase 3 studies. Influenza Other Respir Viruses. 2018;12(4):438-45.

135. Halasa N, Englund JA, Nachman S, Weinberg GA, Huber VC, Allison K, et al. Safety of live attenuated influenza vaccine in mild to moderately immunocompromised children with cancer. Vaccine. 2011;29(24):4110-5.

136. Krammer F, Smith GJD, Fouchier RAM, Peiris M, Kedzierska K, Doherty PC, et al. Influenza. Nat Rev Dis Primers. 2018;4(1):3.

137. von Itzstein M. The war against influenza: discovery and development of sialidase inhibitors. Nat Rev Drug Discov. 2007;6(12):967-74.

138. Fischer WA, 2nd, King LS, Lane AP, Pekosz A. Restricted replication of the live attenuated influenza A virus vaccine during infection of primary differentiated human nasal epithelial cells. Vaccine. 2015;33(36):4495-504.

139. Gould PS, Easton AJ, Dimmock NJ. Live Attenuated Influenza Vaccine contains Substantial and Unexpected Amounts of Defective Viral Genomic RNA. Viruses. 2017;9(10).

140. Martinez-Sobrido L, Peersen O, Nogales A. Temperature Sensitive Mutations in Influenza A Viral Ribonucleoprotein Complex Responsible for the Attenuation of the Live Attenuated Influenza Vaccine. Viruses. 2018;10(10).

141. Lanthier PA, Huston GE, Moquin A, Eaton SM, Szaba FM, Kummer LW, et al. Live attenuated influenza vaccine (LAIV) impacts innate and adaptive immune responses. Vaccine. 2011;29(44):7849-56.

142. Forero A, Fenstermacher K, Wohlgemuth N, Nishida A, Carter V, Smith EA, et al. Evaluation of the innate immune responses to influenza and live-attenuated influenza vaccine infection in primary differentiated human nasal epithelial cells. Vaccine. 2017;35(45):6112-21.

143. Shcherbik S, Pearce N, Kiseleva I, Larionova N, Rudenko L, Xu X, et al. Implementation of new approaches for generating conventional reassortants for live attenuated influenza vaccine based on Russian master donor viruses. J Virol Methods. 2016;227:33-9.

144. Kiseleva IV, Isakova IN, Larionova NV, Oleinik ES, Rudenko LG. [Efficacy of production of reassortant of epidemic strains and cold-adapted influenza viruses in chicken embryo and MDCK cells]. Zh Mikrobiol Epidemiol Immunobiol. 2007(6):40-5.

145. Wohlgemuth N, Lane AP, Pekosz A. Influenza A Virus M2 Protein Apical Targeting Is Required for Efficient Virus Replication. J Virol. 2018;92(22).

146. Ramanathan M, Jr., Lane AP. Innate immunity of the sinonasal cavity and its role in chronic rhinosinusitis. Otolaryngol Head Neck Surg. 2007;136(3):348-56.

147. WHO. Recommended composition of influenza virus vaccines for use in the 2013-14 northern hemisphere influenza season 2013 [Available from: https://www.who.int/influenza/vaccines/virus/recommendations/2013_14_north/en/.

148. Neumann G, Watanabe T, Ito H, Watanabe S, Goto H, Gao P, et al. Generation of influenza A viruses entirely from cloned cDNAs. Proc Natl Acad Sci U S A. 1999;96(16):9345-50.

149. Fodor E, Devenish L, Engelhardt OG, Palese P, Brownlee GG, Garcia-Sastre A. Rescue of influenza A virus from recombinant DNA. J Virol. 1999;73(11):9679-82.

150. Ibricevic A, Pekosz A, Walter MJ, Newby C, Battaile JT, Brown EG, et al. Influenza virus receptor specificity and cell tropism in mouse and human airway epithelial cells. J Virol. 2006;80(15):7469-80.

151. NIH. ImageJ 2020 [Available from: https://imagej.nih.gov/ij/.

152. Stevens J, Chen LM, Carney PJ, Garten R, Foust A, Le J, et al. Receptor specificity of influenza A H3N2 viruses isolated in mammalian cells and embryonated chicken eggs. J Virol. 2010;84(16):8287-99.

153. Mochalova L, Gambaryan A, Romanova J, Tuzikov A, Chinarev A, Katinger D, et al. Receptor-binding properties of modern human influenza viruses primarily isolated in Vero and MDCK cells and chicken embryonated eggs. Virology. 2003;313(2):473-80.

154. Takemae N, Ruttanapumma R, Parchariyanon S, Yoneyama S, Hayashi T, Hiramatsu H, et al. Alterations in receptor-binding properties of swine influenza viruses of the H1 subtype after isolation in embryonated chicken eggs. J Gen Virol. 2010;91(Pt 4):938-48.

155. Glycomics CfF. MAMMALIAN PRINTED ARRAY VERSION 5.2 2020 [Available from: http://www.functionalglycomics.org/static/consortium/resources/resourcecoreh8.shtml.

156. Nelson SW, Lorbach JN, Nolting JM, Stull JW, Jackwood DJ, Davis IC, et al. Madin-Darby canine kidney cell sialic acid receptor modulation induced by culture medium conditions: Implications for the isolation of influenza A virus. Influenza Other Respir Viruses. 2019;13(6):593-602.

157. de Courcey F, Zholos AV, Atherton-Watson H, Williams MT, Canning P, Danahay HL, et al. Development of primary human nasal epithelial cell cultures for the study of cystic fibrosis pathophysiology. Am J Physiol Cell Physiol. 2012;303(11):C1173-9.

158. Park DY, Kim S, Kim CH, Yoon JH, Kim HJ. Alternative Method for Primary Nasal Epithelial Cell Culture Using Intranasal Brushing and Feasibility for the Study of Epithelial Functions in Allergic Rhinitis. Allergy Asthma Immunol Res. 2016;8(1):69-78.

159. Muller L, Brighton LE, Carson JL, Fischer WA, 2nd, Jaspers I. Culturing of human nasal epithelial cells at the air liquid interface. J Vis Exp. 2013(80).

160. Guo Y, Zhao X, Yang Z. [Ciliogenesis in human nasal epithelial cells cultured at the air-liquid interface]. Lin Chuang Er Bi Yan Hou Ke Za Zhi. 2004;18(2):88-90.

161. Charles DD, Fisher JR, Hoskinson SM, Medina-Colorado AA, Shen YC, Chaaban MR, et al. Development of a Novel ex vivo Nasal Epithelial Cell Model Supporting Colonization With Human Nasal Microbiota. Front Cell Infect Microbiol. 2019;9:165.

162. Schagen J, Sly PD, Fantino E. Characterizing well-differentiated culture of primary human nasal epithelial cells for use in wound healing assays. Lab Invest. 2018;98(11):1478-86.

163. CDC. ACIP votes down use of LAIV for 2016-2017 flu season 2016 [Available from: https://www.cdc.gov/media/releases/2016/s0622-laiv-flu.html.

164. Sassaki GL, Elli S, Rudd TR, Macchi E, Yates EA, Naggi A, et al. Human (alpha2-->6) and avian (alpha2-->3) sialylated receptors of influenza A virus show distinct conformations and dynamics in solution. Biochemistry. 2013;52(41):7217-30.

165. Karakus U, Pohl MO, Stertz S. Breaking the Convention: Sialoglycan Variants, Coreceptors, and Alternative Receptors for Influenza A Virus Entry. J Virol. 2020;94(4).

166. Nicholls JM, Chan RW, Russell RJ, Air GM, Peiris JS. Evolving complexities of influenza virus and its receptors. Trends Microbiol. 2008;16(4):149-57.

167. Imai M, Kawaoka Y. The role of receptor binding specificity in interspecies transmission of influenza viruses. Curr Opin Virol. 2012;2(2):160-7.

168. Nobusawa E, Ishihara H, Morishita T, Sato K, Nakajima K. Change in receptor-binding specificity of recent human influenza A viruses (H3N2): a single amino acid change in hemagglutinin altered its recognition of sialyloligosaccharides. Virology. 2000;278(2):587-96.

169. Kumari K, Gulati S, Smith DF, Gulati U, Cummings RD, Air GM. Receptor binding specificity of recent human H3N2 influenza viruses. Virol J. 2007;4:42.

170. Belshe RB, Coelingh K, Ambrose CS, Woo JC, Wu X. Efficacy of live attenuated influenza vaccine in children against influenza B viruses by lineage and antigenic similarity. Vaccine. 2010;28(9):2149-56.

171. Rhorer J, Ambrose CS, Dickinson S, Hamilton H, Oleka NA, Malinoski FJ, et al. Efficacy of live attenuated influenza vaccine in children: A meta-analysis of nine randomized clinical trials. Vaccine. 2009;27(7):1101-10.

172. Lindsey BB, Jagne YJ, Armitage EP, Singanayagam A, Sallah HJ, Drammeh S, et al. Effect of a Russian-backbone live-attenuated influenza vaccine with an updated pandemic H1N1 strain on shedding and immunogenicity among children in The Gambia: an open-label, observational, phase 4 study. Lancet Respir Med. 2019;7(8):665-76.

173. Vincent AL, Ma W, Lager KM, Richt JA, Janke BH, Sandbulte MR, et al. Live attenuated influenza vaccine provides superior protection from heterologous infection in pigs with maternal antibodies without inducing vaccine-associated enhanced respiratory disease. J Virol. 2012;86(19):10597-605.

174. Matrosovich MN, Gambaryan AS, Teneberg S, Piskarev VE, Yamnikova SS, Lvov DK, et al. Avian influenza A viruses differ from human viruses by recognition of sialyloligosaccharides and gangliosides and by a higher conservation of the HA receptor-binding site. Virology. 1997;233(1):224-34.

175. Matrosovich M, Tuzikov A, Bovin N, Gambaryan A, Klimov A, Castrucci MR, et al. Early alterations of the receptor-binding properties of H1, H2, and H3 avian influenza virus hemagglutinins after their introduction into mammals. J Virol. 2000;74(18):8502-12.

176. AstraZeneca. Update: Live Attenuated Influenza Vaccine (LAIV) 2017 [Available from: https://www.izsummitpartners.org/content/uploads/2017/05/10e-1_Bandell_Update-on-LAIV.pdf.

177. Skehel JJ, Wiley DC. Receptor binding and membrane fusion in virus entry: the influenza hemagglutinin. Annu Rev Biochem. 2000;69:531-69.

178. Matrosovich MN, Gambaryan AS, Tuzikov AB, Byramova NE, Mochalova LV, Golbraikh AA, et al. Probing of the receptor-binding sites of the H1 and H3 influenza A and influenza B virus hemagglutinins by synthetic and natural sialosides. Virology. 1993;196(1):111-21.

179. Bradley KC, Galloway SE, Lasanajak Y, Song X, Heimburg-Molinaro J, Yu H, et al. Analysis of influenza virus hemagglutinin receptor binding mutants with limited receptor recognition properties and conditional replication characteristics. J Virol. 2011;85(23):12387-98.

180. Kilbourne ED, Johansson BE, Grajower B. Independent and disparate evolution in nature of influenza A virus hemagglutinin and neuraminidase glycoproteins. Proc Natl Acad Sci U S A. 1990;87(2):786-90.

181. Jang J, Bae SE. Comparative Co-Evolution Analysis Between the HA and NA Genes of Influenza A Virus. Virology (Auckl). 2018;9:1178122X18788328.

182. Altman MO, Angel M, Kosik I, Trovao NS, Zost SJ, Gibbs JS, et al. Human Influenza A Virus Hemagglutinin Glycan Evolution Follows a Temporal Pattern to a Glycan Limit. mBio. 2019;10(2).

183. Shih AC, Hsiao TC, Ho MS, Li WH. Simultaneous amino acid substitutions at antigenic sites drive influenza A hemagglutinin evolution. Proc Natl Acad Sci U S A. 2007;104(15):6283-8.

184. Kirkpatrick E, Qiu X, Wilson PC, Bahl J, Krammer F. The influenza virus hemagglutinin head evolves faster than the stalk domain. Sci Rep. 2018;8(1):10432.

185. Nakajima K, Nobusawa E, Nagy A, Nakajima S. Accumulation of amino acid substitutions promotes irreversible structural changes in the hemagglutinin of human influenza AH3 virus during evolution. J Virol. 2005;79(10):6472-7.

186. Koel BF, Mogling R, Chutinimitkul S, Fraaij PL, Burke DF, van der Vliet S, et al. Identification of amino acid substitutions supporting antigenic change of influenza A(H1N1)pdm09 viruses. J Virol. 2015;89(7):3763-75.

187. DeDiego ML, Chiem K, Topham DJ. Directed selection of amino acid changes in the influenza hemagglutinin and neuraminidase affecting protein antigenicity. Vaccine. 2018;36(43):6383-92.

188. Xie H, Wan XF, Ye Z, Plant EP, Zhao Y, Xu Y, et al. H3N2 Mismatch of 2014-15 Northern Hemisphere Influenza Vaccines and Head-to-head Comparison between Human and Ferret Antisera derived Antigenic Maps. Sci Rep. 2015;5:15279.

189. Jennings L, Huang QS, Barr I, Lee PI, Kim WJ, Buchy P, et al. Literature review of the epidemiology of influenza B disease in 15 countries in the Asia-Pacific region. Influenza Other Respir Viruses. 2018;12(3):383-411.

190. El Moussi A, Pozo F, Ben Hadj Kacem MA, Ledesma J, Cuevas MT, Casas I, et al. Virological Surveillance of Influenza Viruses during the 2008-09, 2009-10 and 2010-11 Seasons in Tunisia. PLoS One. 2013;8(9):e74064.

191. Sanicas M, Forleo E, Pozzi G, Diop D. A review of the surveillance systems of influenza in selected countries in the tropical region. Pan Afr Med J. 2014;19:121.

192. Kosik I, Ince WL, Gentles LE, Oler AJ, Kosikova M, Angel M, et al. Influenza A virus hemagglutinin glycosylation compensates for antibody escape fitness costs. PLoS Pathog. 2018;14(1):e1006796.

193. Prachanronarong KL, Canale AS, Liu P, Somasundaran M, Hou S, Poh YP, et al. Mutations in Influenza A Virus Neuraminidase and Hemagglutinin Confer Resistance against a Broadly Neutralizing Hemagglutinin Stem Antibody. J Virol. 2019;93(2).

194. Breitling J, Aebi M. N-linked protein glycosylation in the endoplasmic reticulum. Cold Spring Harb Perspect Biol. 2013;5(8):a013359.

195. Pamela Stanley HS, and Naoyuki Taniguchi. Essentials of Glycobiology, 3rd Edition. New York: Cold Spring Harbor; 2009.

196. Tretter V, Altmann F, Marz L. Peptide-N4-(N-acetyl-beta-glucosaminyl)asparagine amidase F cannot release glycans with fucose attached alpha 1----3 to the asparagine-linked N-acetylglucosamine residue. Eur J Biochem. 1991;199(3):647-52.

197. Maley F, Trimble RB, Tarentino AL, Plummer TH, Jr. Characterization of glycoproteins and their associated oligosaccharides through the use of endoglycosidases. Anal Biochem. 1989;180(2):195-204.

198. Hattrup CL, Gendler SJ. Structure and function of the cell surface (tethered) mucins. Annu Rev Physiol. 2008;70:431-57.

199. Rose MC, Voynow JA. Respiratory tract mucin genes and mucin glycoproteins in health and disease. Physiol Rev. 2006;86(1):245-78.

200. Woo HJ, Bae CH, Song SY, Lee HM, Kim YD. Expression of membrane-bound mucins in human nasal mucosa: different patterns for MUC4 and MUC16. Arch Otolaryngol Head Neck Surg. 2010;136(6):603-9.

201. Hang HC, Bertozzi CR. The chemistry and biology of mucin-type O-linked glycosylation. Bioorg Med Chem. 2005;13(17):5021-34.

202. Van den Steen P, Rudd PM, Dwek RA, Opdenakker G. Concepts and principles of O-linked glycosylation. Crit Rev Biochem Mol Biol. 1998;33(3):151-208.

203. McFadden ER, Jr., Pichurko BM, Bowman HF, Ingenito E, Burns S, Dowling N, et al. Thermal mapping of the airways in humans. J Appl Physiol (1985). 1985;58(2):564-70.

204. Regnard J. Cold and the airways. Int J Sports Med. 1992;13 Suppl 1:S182-4.

205. CDC. Summary of the 2014/15 Flu Season 2015 [Available from: https://www.cdc.gov/flu/pastseasons/1415season.htm.

206. Flannery B, Clippard J, Zimmerman RK, Nowalk MP, Jackson ML, Jackson LA, et al. Early estimates of seasonal influenza vaccine effectiveness - United States, January 2015. MMWR Morb Mortal Wkly Rep. 2015;64(1):10-5.

207. Flannery B, Zimmerman RK, Gubareva LV, Garten RJ, Chung JR, Nowalk MP, et al. Enhanced Genetic Characterization of Influenza A(H3N2) Viruses and Vaccine Effectiveness by Genetic Group, 2014-2015. J Infect Dis. 2016;214(7):1010-9.

208. Eichelberger MC, Monto AS. Neuraminidase, the Forgotten Surface Antigen, Emerges as an Influenza Vaccine Target for Broadened Protection. J Infect Dis. 2019;219(Supplement_1):S75-S80.

209. Walz L, Kays SK, Zimmer G, von Messling V. Neuraminidase-Inhibiting Antibody Titers Correlate with Protection from Heterologous Influenza Virus Strains of the Same Neuraminidase Subtype. J Virol. 2018;92(17).

210. Gocnikova H, Russ G. Influenza a virus PB1-F2 protein. Acta Virol. 2007;51(2):101-8.

211. Powell H, Pekosz A. Neuraminidase antigenic drift of Influenza A virus H3N2 clade 3c.2a viruses alters virus replication, enzymatic activity and inhibitory antibody binding. bioRxiv. 2020:2020.02.20.957399.

212. WHO. Influenza Seasonal Facts Sheet. Available online: https://wwwwhoint/news-room/fact-sheets/detail/influenza-(seasonal). 2019.

213. Neu KE, Henry Dunand CJ, Wilson PC. Heads, stalks and everything else: how can antibodies eradicate influenza as a human disease? Curr Opin Immunol. 2016;42:48-55.

214. Kim H, Webster RG, Webby RJ. Influenza Virus: Dealing with a Drifting and Shifting Pathogen. Viral Immunol. 2018;31(2):174-83.

215. Estrada LD, Schultz-Cherry S. Development of a Universal Influenza Vaccine. J Immunol. 2019;202(2):392-8.

216. Sautto GA, Kirchenbaum GA, Ross TM. Towards a universal influenza vaccine: different approaches for one goal. Virol J. 2018;15(1):17.

217. Jang YH, Seong BL. The Quest for a Truly Universal Influenza Vaccine. Front Cell Infect Microbiol. 2019;9:344.

218. Yang J, Liu S, Du L, Jiang S. A new role of neuraminidase (NA) in the influenza virus life cycle: implication for developing NA inhibitors with novel mechanism of action. Rev Med Virol. 2016;26(4):242-50.

219. Basak S, Tomana M, Compans RW. Sialic acid is incorporated into influenza hemagglutinin glycoproteins in the absence of viral neuraminidase. Virus Res. 1985;2(1):61-8.

220. Piepenbrink MS, Nogales A, Basu M, Fucile CF, Liesveld JL, Keefer MC, et al. Broad and Protective Influenza B Virus Neuraminidase Antibodies in Humans after Vaccination and their Clonal Persistence as Plasma Cells. MBio. 2019;10(2).

221. Gilbert PB, Fong Y, Juraska M, Carpp LN, Monto AS, Martin ET, et al. HAI and NAI titer correlates of inactivated and live attenuated influenza vaccine efficacy. BMC Infect Dis. 2019;19(1):453.

222. Chen YQ, Wohlbold TJ, Zheng NY, Huang M, Huang Y, Neu KE, et al. Influenza Infection in Humans Induces Broadly Cross-Reactive and Protective Neuraminidase-Reactive Antibodies. Cell. 2018;173(2):417-29 e10.

223. Kosik I, Angeletti D, Gibbs JS, Angel M, Takeda K, Kosikova M, et al. Neuraminidase inhibition contributes to influenza A virus neutralization by anti-hemagglutinin stem antibodies. J Exp Med. 2019;216(2):304-16.

224. Jiang L, Fantoni G, Couzens L, Gao J, Plant E, Ye Z, et al. Comparative Efficacy of Monoclonal Antibodies That Bind to Different Epitopes of the 2009 Pandemic H1N1 Influenza Virus Neuraminidase. J Virol. 2016;90(1):117-28.

225. Eichelberger MC, Wan H. Influenza neuraminidase as a vaccine antigen. Curr Top Microbiol Immunol. 2015;386:275-99.

226. Yasuhara A, Yamayoshi S, Kiso M, Sakai-Tagawa Y, Koga M, Adachi E, et al. Antigenic drift originating from changes to the lateral surface of the neuraminidase head of influenza A virus. Nat Microbiol. 2019;4(6):1024-34.

227. Gao J, Couzens L, Burke DF, Wan H, Wilson P, Memoli MJ, et al. Antigenic Drift of the Influenza A(H1N1)pdm09 Virus Neuraminidase Results in Reduced Effectiveness of A/California/7/2009 (H1N1pdm09)-Specific Antibodies. MBio. 2019;10(2).

228. Sandbulte MR, Westgeest KB, Gao J, Xu X, Klimov AI, Russell CA, et al. Discordant antigenic drift of neuraminidase and hemagglutinin in H1N1 and H3N2 influenza viruses. Proc Natl Acad Sci U S A. 2011;108(51):20748-53.

229. Wan H, Gao J, Yang H, Yang S, Harvey R, Chen YQ, et al. The neuraminidase of A(H3N2) influenza viruses circulating since 2016 is antigenically distinct from the A/Hong Kong/4801/2014 vaccine strain. Nat Microbiol. 2019;4(12):2216-25.

230. Zou S, Gao R, Zhang Y, Li X, Chen W, Bai T, et al. Molecular characterization of H6 subtype influenza viruses in southern China from 2009 to 2011. Emerg Microbes Infect. 2016;5(7):e73.

231. Couzens L, Gao J, Westgeest K, Sandbulte M, Lugovtsev V, Fouchier R, et al. An optimized enzyme-linked lectin assay to measure influenza A virus neuraminidase inhibition antibody titers in human sera. J Virol Methods. 2014;210:7-14.

232. Lambre CR, Terzidis H, Greffard A, Webster RG. Measurement of anti-influenza neuraminidase antibody using a peroxidase-linked lectin and microtitre plates coated with natural substrates. J Immunol Methods. 1990;135(1-2):49-57.

233. Marathe BM, Leveque V, Klumpp K, Webster RG, Govorkova EA. Determination of neuraminidase kinetic constants using whole influenza virus preparations and correction for spectroscopic interference by a fluorogenic substrate. PLoS One. 2013;8(8):e71401.

234. Blumenkrantz D, Mehoke T, Hardick J, Shaw-Saliba K, Powell H, Liu H, et al. Identification of H3N2 NA and PB1-F2 genetic variants and their association with disease symptoms in the 2014-15 influenza season. bioRxiv. 2020:2020.02.20.956979.

235. Matrosovich M, Matrosovich T, Carr J, Roberts NA, Klenk HD. Overexpression of the alpha-2,6-sialyltransferase in MDCK cells increases influenza virus sensitivity to neuraminidase inhibitors. J Virol. 2003;77(15):8418-25.

236. Kosik I, Yewdell JW. Influenza A virus hemagglutinin specific antibodies interfere with virion neuraminidase activity via two distinct mechanisms. Virology. 2017;500:178-83.

237. Jegaskanda S, Reading PC, Kent SJ. Influenza-specific antibody-dependent cellular cytotoxicity: toward a universal influenza vaccine. J Immunol. 2014;193(2):469-75.

238. Du R, Cui Q, Rong L. Competitive Cooperation of Hemagglutinin and Neuraminidase during Influenza A Virus Entry. Viruses. 2019;11(5).

239. Zanin M, Baviskar P, Webster R, Webby R. The Interaction between Respiratory Pathogens and Mucus. Cell Host Microbe. 2016;19(2):159-68.

240. Eichelberger MC, Morens DM, Taubenberger JK. Neuraminidase as an influenza vaccine antigen: a low hanging fruit, ready for picking to improve vaccine effectiveness. Curr Opin Immunol. 2018;53:38-44.

241. Stadlbauer D, Zhu X, McMahon M, Turner JS, Wohlbold TJ, Schmitz AJ, et al. Broadly protective human antibodies that target the active site of influenza virus neuraminidase. Science. 2019;366(6464):499-504.

242. Sultana I, Yang K, Getie-Kebtie M, Couzens L, Markoff L, Alterman M, et al. Stability of neuraminidase in inactivated influenza vaccines. Vaccine. 2014;32(19):2225-30.

243. Powers DC, Kilbourne ED, Johansson BE. Neuraminidase-specific antibody responses to inactivated influenza virus vaccine in young and elderly adults. Clin Diagn Lab Immunol. 1996;3(5):511-6.

244. An Y, Parsons LM, Jankowska E, Melnyk D, Joshi M, Cipollo JF. N-Glycosylation of Seasonal Influenza Vaccine Hemagglutinins: Implication for Potency Testing and Immune Processing. J Virol. 2019;93(2).

245. Zost SJ, Parkhouse K, Gumina ME, Kim K, Diaz Perez S, Wilson PC, et al. Contemporary H3N2 influenza viruses have a glycosylation site that alters binding of antibodies elicited by egg-adapted vaccine strains. Proc Natl Acad Sci U S A. 2017;114(47):12578-83.

246. CDC. Seasonal Influenza Vaccine Effectiveness, 2014-2015 2015 [Available from: https://www.cdc.gov/flu/vaccines-work/2014-2015.html.

247. Beer K, Dai M, Howell S, Rijal P, Townsend AR, Lin Y, et al. Characterization of neutralizing epitopes in antigenic site B of recently circulating influenza A(H3N2) viruses. J Gen Virol. 2018;99(8):1001-11.

248. Lazniewski M, Dawson WK, Szczepinska T, Plewczynski D. The structural variability of the influenza A hemagglutinin receptor-binding site. Brief Funct Genomics. 2018;17(6):415-27.

249. Richard M, Erny A, Care B, Traversier A, Barthelemy M, Hay A, et al. Rescue of a H3N2 influenza virus containing a deficient neuraminidase protein by a hemagglutinin with a low receptor-binding affinity. PLoS One. 2012;7(5):e33880.

250. Lin YP, Gregory V, Collins P, Kloess J, Wharton S, Cattle N, et al. Neuraminidase receptor binding variants of human influenza A(H3N2) viruses resulting from substitution of aspartic acid 151 in the catalytic site: a role in virus attachment? J Virol. 2010;84(13):6769-81.

251. Guo H, Rabouw H, Slomp A, Dai M, van der Vegt F, van Lent JWM, et al. Kinetic analysis of the influenza A virus HA/NA balance reveals contribution of NA to virus-receptor binding and NA-dependent rolling on receptor-containing surfaces. PLoS Pathog. 2018;14(8):e1007233.

252. She YM, Farnsworth A, Li X, Cyr TD. Topological N-glycosylation and site-specific N-glycan sulfation of influenza proteins in the highly expressed H1N1 candidate vaccines. Sci Rep. 2017;7(1):10232.

253. Sun X, Jayaraman A, Maniprasad P, Raman R, Houser KV, Pappas C, et al. N-linked glycosylation of the hemagglutinin protein influences virulence and antigenicity of the 1918 pandemic and seasonal H1N1 influenza A viruses. J Virol. 2013;87(15):8756-66.

254. Lednicky JA, Iovine NM, Brew J, Loeb JC, Sugimoto JD, Rand KH, et al. Hemagglutinin Gene Clade 3C.2a Influenza A(H3N2) Viruses, Alachua County, Florida, USA, 2014-15. Emerg Infect Dis. 2016;22(1):121-3.

255. Jorquera PA, Mishin VP, Chesnokov A, Nguyen HT, Mann B, Garten R, et al. Insights into the antigenic advancement of influenza A(H3N2) viruses, 2011-2018. Sci Rep. 2019;9(1):2676.

256. Takashima S, Ishida HK, Inazu T, Ando T, Ishida H, Kiso M, et al. Molecular cloning and expression of a sixth type of alpha 2,8-sialyltransferase (ST8Sia VI) that sialylates O-glycans. J Biol Chem. 2002;277(27):24030-8.

257. Chothe SK, Bhushan G, Nissly RH, Yeh YT, Brown J, Turner G, et al. Avian and human influenza virus compatible sialic acid receptors in little brown bats. Sci Rep. 2017;7(1):660.

258. Kasson PM, Pande VS. Structural basis for influence of viral glycans on ligand binding by influenza hemagglutinin. Biophys J. 2008;95(7):L48-50.

259. Aljurayyan A, Puksuriwong S, Ahmed M, Sharma R, Krishnan M, Sood S, et al. Activation and Induction of Antigen-Specific T Follicular Helper Cells Play a Critical Role in Live-Attenuated Influenza Vaccine-Induced Human Mucosal Anti-influenza Antibody Response. J Virol. 2018;92(11).

260. Lartey S, Zhou F, Brokstad KA, Mohn KG, Slettevoll SA, Pathirana RD, et al. Live-Attenuated Influenza Vaccine Induces Tonsillar Follicular T Helper Cell Responses That Correlate With Antibody Induction. J Infect Dis. 2020;221(1):21-32.

261. Kotomina T, Korenkov D, Matyushenko V, Prokopenko P, Rudenko L, Isakova-Sivak I. Live attenuated influenza vaccine viral vector induces functional cytotoxic T-cell immune response against foreign CD8+ T-cell epitopes inserted into NA and NS1 genes using the 2A self-cleavage site. Hum Vaccin Immunother. 2018;14(12):2964-70.

262. Li J, Arevalo MT, Chen Y, Chen S, Zeng M. T-cell-mediated cross-strain protective immunity elicited by prime-boost vaccination with a live attenuated influenza vaccine. Int J Infect Dis. 2014;27:37-43.

263. He XS, Holmes TH, Zhang C, Mahmood K, Kemble GW, Lewis DB, et al. Cellular immune responses in children and adults receiving inactivated or live attenuated influenza vaccines. J Virol. 2006;80(23):11756-66.

264. Mohn KGI, Zhou F, Brokstad KA, Sridhar S, Cox RJ. Boosting of Cross-Reactive and Protection-Associated T Cells in Children After Live Attenuated Influenza Vaccination. J Infect Dis. 2017;215(10):1527-35.

265. Cheng X, Zengel JR, Suguitan AL, Jr., Xu Q, Wang W, Lin J, et al. Evaluation of the humoral and cellular immune responses elicited by the live attenuated and inactivated influenza vaccines and their roles in heterologous protection in ferrets. J Infect Dis. 2013;208(4):594-602.

266. Hoft DF, Lottenbach KR, Blazevic A, Turan A, Blevins TP, Pacatte TP, et al. Comparisons of the Humoral and Cellular Immune Responses Induced by Live Attenuated Influenza Vaccine and Inactivated Influenza Vaccine in Adults. Clin Vaccine Immunol. 2017;24(1).

267. Chung JR, Flannery B, Thompson MG, Gaglani M, Jackson ML, Monto AS, et al. Seasonal Effectiveness of Live Attenuated and Inactivated Influenza Vaccine. Pediatrics. 2016;137(2):e20153279.

268. Rudenko L, Kiseleva I, Krutikova E, Stepanova E, Rekstin A, Donina S, et al. Rationale for vaccination with trivalent or quadrivalent live attenuated influenza vaccines: Protective vaccine efficacy in the ferret model. PLoS One. 2018;13(12):e0208028.

269. Ambrose CS, Levin MJ, Belshe RB. The relative efficacy of trivalent live attenuated and inactivated influenza vaccines in children and adults. Influenza Other Respir Viruses. 2011;5(2):67-75.

270. Brickley EB, Wright PF, Khalenkov A, Neuzil KM, Ortiz JR, Rudenko L, et al. The Effect of Preexisting Immunity on Virus Detection and Immune Responses in a Phase II, Randomized Trial of a Russian-Backbone, Live, Attenuated Influenza Vaccine in Bangladeshi Children. Clin Infect Dis. 2019;69(5):786-94.

271. Matrajt L, Halloran ME, Antia R. Successes and failures of the live-attenuated influenza vaccine: can we do better? Clin Infect Dis. 2019.

272. Parker L, Ritter L, Wu W, Maeso R, Bright H, Dibben O. Haemagglutinin stability was not the primary cause of the reduced effectiveness of live attenuated influenza vaccine against A/H1N1pdm09 viruses in the 2013-2014 and 2015-2016 seasons. Vaccine. 2019;37(32):4543-50.

273. Myers CA, Faix DJ, Blair PJ. Possible reduced effectiveness of the 2009 H1N1 component of live, attenuated influenza vaccine. Clin Infect Dis. 2011;53(2):207-8.

274. Pebody R, McMenamin J, Nohynek H. Live attenuated influenza vaccine (LAIV): recent effectiveness results from the USA and implications for LAIV programmes elsewhere. Arch Dis Child. 2018;103(1):101-5.

275. Neumann G, Kawaoka Y. Host range restriction and pathogenicity in the context of influenza pandemic. Emerg Infect Dis. 2006;12(6):881-6.

276. Peiris JS, Poon LL, Guan Y. Emergence of a novel swine-origin influenza A virus (S-OIV) H1N1 virus in humans. J Clin Virol. 2009;45(3):169-73.

277. Novel Swine-Origin Influenza AVIT, Dawood FS, Jain S, Finelli L, Shaw MW, Lindstrom S, et al. Emergence of a novel swine-origin influenza A (H1N1) virus in humans. N Engl J Med. 2009;360(25):2605-15.

278. England PH. Influenza vaccine effectiveness (VE) in adults and children in primary care in the United Kingdom (UK): provisional end-ofseason results 2017-18 2018 [Available from: https://assets.publishing.service.gov.uk/government/uploads/system/uploads/attachment_data/file/779474/Influenza_vaccine_effectiveness_in_primary_care_2017_2018.pdf.

279. Grohskopf LA, Sokolow LZ, Fry AM, Walter EB, Jernigan DB. Update: ACIP Recommendations for the Use of Quadrivalent Live Attenuated Influenza Vaccine (LAIV4) - United States, 2018-19 Influenza Season. MMWR Morb Mortal Wkly Rep. 2018;67(22):643-5.

280. Voeten JT, Kiseleva IV, Glansbeek HL, Basten SM, Drieszen-van der Cruijsen SK, Rudenko LG, et al. Master donor viruses A/Leningrad/134/17/57 (H2N2) and B/USSR/60/69

and derived reassortants used in live attenuated influenza vaccine (LAIV) do not display neurovirulent properties in a mouse model. Arch Virol. 2010;155(9):1391-9.

281. Talaat KR, Karron RA, Liang PH, McMahon BA, Luke CJ, Thumar B, et al. An open-label phase I trial of a live attenuated H2N2 influenza virus vaccine in healthy adults. Influenza Other Respir Viruses. 2013;7(1):66-73.

282. McCahon D, Beare AS, Stealey V. The production of live attenuated influenza A strains by recombination with A/Okuda/57 (H2N2). Postgrad Med J. 1976;52(608):389-94.

283. Klimov AI, Cox NJ, Yotov WV, Rocha E, Alexandrova GI, Kendal AP. Sequence changes in the live attenuated, cold-adapted variants of influenza A/Leningrad/134/57 (H2N2) virus. Virology. 1992;186(2):795-7.

284. Isakova-Sivak I, Stukova M, Erofeeva M, Naykhin A, Donina S, Petukhova G, et al. H2N2 live attenuated influenza vaccine is safe and immunogenic for healthy adult volunteers. Hum Vaccin Immunother. 2015;11(4):970-82.

285. Broadbent AJ, Santos CP, Paskel M, Matsuoka Y, Lu J, Chen Z, et al. Replication of live attenuated cold-adapted H2N2 influenza virus vaccine candidates in non human primates. Vaccine. 2015;33(1):193-200.

286. Jackson D, Pitcher M, Hudson C, Andrews N, Southern J, Ellis J, et al. Viral Shedding in Recipients of Live Attenuated Influenza Vaccine in the 2016-2017 and 2017-2018 Influenza Seasons in the United Kingdom. Clin Infect Dis. 2019.

287. Shcherbik S, Pearce N, Carney P, Bazhenova E, Larionova N, Kiseleva I, et al. Evaluation of A(H1N1)pdm09 LAIV vaccine candidates stability and replication efficiency in primary human nasal epithelial cells. Vaccine X. 2019;2:100031.

288. Organization WH. Influenza A(H1N1)pdm09 egg-derived candidate vaccine viruses for

development and production of vaccines for use in the 2017-2018 northern hemisphere influenza season 2018 [Available from: https://www.who.int/influenza/vaccines/virus/candidates_reagents/summary_a_h1n1pdm09_cvv-egg_nh1718.pdf?ua=1.

289. Korsun N, Angelova S, Gregory V, Daniels R, Georgieva I, McCauley J. Antigenic and genetic characterization of influenza viruses circulating in Bulgaria during the 2015/2016 season. Infect Genet Evol. 2017;49:241-50.

290. Stepanova EA, Kotomina TS, Matyushenko VA, Smolonogina TA, Shapovalova VS, Rudenko LG, et al. Amino Acid Substitutions N123D and N149D in Hemagglutinin Molecule Enhance Immunigenicity of Live Attenuated Influenza H7N9 Vaccine Strain in Experiment. Bull Exp Biol Med. 2019;166(5):631-6.

291. Rudenko L, Isakova-Sivak I, Naykhin A, Kiseleva I, Stukova M, Erofeeva M, et al. H7N9 live attenuated influenza vaccine in healthy adults: a randomised, double-blind, placebo-controlled, phase 1 trial. Lancet Infect Dis. 2016;16(3):303-10.

292. de Jonge J, Isakova-Sivak I, van Dijken H, Spijkers S, Mouthaan J, de Jong R, et al. H7N9 Live Attenuated Influenza Vaccine Is Highly Immunogenic, Prevents Virus Replication, and Protects Against Severe Bronchopneumonia in Ferrets. Mol Ther. 2016;24(5):991-1002.

293. Wu NC, Zost SJ, Thompson AJ, Oyen D, Nycholat CM, McBride R, et al. A structural explanation for the low effectiveness of the seasonal influenza H3N2 vaccine. PLoS Pathog. 2017;13(10):e1006682.

294. Mameli C, Cocchi I, Fumagalli M, Zuccotti G. Influenza Vaccination: Effectiveness, Indications, and Limits in the Pediatric Population. Front Pediatr. 2019;7:317.

295. Trombetta CM, Marchi S, Manini I, Lazzeri G, Montomoli E. Challenges in the development of egg-independent vaccines for influenza. Expert Rev Vaccines. 2019;18(7):737-50.

296. de Vries RP, Peng W, Grant OC, Thompson AJ, Zhu X, Bouwman KM, et al. Three mutations switch H7N9 influenza to human-type receptor specificity. PLoS Pathog. 2017;13(6):e1006390.

297. Dortmans JC, Dekkers J, Wickramasinghe IN, Verheije MH, Rottier PJ, van Kuppeveld FJ, et al. Adaptation of novel H7N9 influenza A virus to human receptors. Sci Rep. 2013;3:3058.

298. Wu NC, Lv H, Thompson AJ, Wu DC, Ng WWS, Kadam RU, et al. Preventing an Antigenically Disruptive Mutation in Egg-Based H3N2 Seasonal Influenza Vaccines by Mutational Incompatibility. Cell Host Microbe. 2019;25(6):836-44 e5.

299. Harding AT, Heaton BE, Dumm RE, Heaton NS. Rationally Designed Influenza Virus Vaccines That Are Antigenically Stable during Growth in Eggs. mBio. 2017;8(3).

300. Medeiros R, Escriou N, Naffakh N, Manuguerra JC, van der Werf S. Hemagglutinin residues of recent human A(H3N2) influenza viruses that contribute to the inability to agglutinate chicken erythrocytes. Virology. 2001;289(1):74-85.

301. Lu B, Zhou H, Chan W, Kemble G, Jin H. Single amino acid substitutions in the hemagglutinin of influenza A/Singapore/21/04 (H3N2) increase virus growth in embryonated chicken eggs. Vaccine. 2006;24(44-46):6691-3.

302. Li X, Kantola K, Hedman L, Arku B, Hedman K, Soderlund-Venermo M. Original antigenic sin with human bocaviruses 1-4. J Gen Virol. 2015;96(10):3099-108.

303. Webster RG, Kasel JA, Couch RB, Laver WG. Influenza virus subunit vaccines. II. Immunogenicity and original antigenic sin in humans. J Infect Dis. 1976;134(1):48-58.

304. Virelizier JL, Allison AC, Schild GC. Antibody responses to antigenic determinants of influenza virus hemagglutinin. II. Original antigenic sin: a bone marrow-derived lymphocyte memory phenomenon modulated by thymus-derived lymphocytes. J Exp Med. 1974;140(6):1571-8.

305. Rasmussen RA, Montefiori DC, Robinson HL, McClure HM, Ruprecht RM. Heterologous neutralizing antibody induction in a simian-human immunodeficiency virus primate model: lack of original antigenic sin. J Infect Dis. 2001;184(12):1603-7.

306. Deutsch S, Vinit MA, Bussard AE. Original antigenic sin at the cellular level--III. Importance of protein carrier in the stimulation process. Immunochemistry. 1975;12(3):191-7.

307. Deutsch S, Vinit MA, Bussard AE. Original antigenic sin at the cellular level. II. Specificity of the antibodies produced by individual cells. Eur J Immunol. 1973;3(4):235-40.

308. Angelova LA, Shvartsman Ya S. Original antigenic sin to influenza in rats. Immunology. 1982;46(1):183-8.

309. Singh RA, Rodgers JR, Barry MA. The role of T cell antagonism and original antigenic sin in genetic immunization. J Immunol. 2002;169(12):6779-86.

310. Pan K. Understanding original antigenic sin in influenza with a dynamical system. PLoS One. 2011;6(8):e23910.

311. Haaheim LR. Original antigenic sin. A confounding issue? Dev Biol (Basel). 2003;115:49-53.

312. Yewdell JW, Santos JJS. Original Antigenic Sin: How Original? How Sinful? Cold Spring Harb Perspect Med. 2020.

313. Worobey M, Plotkin S, Hensley SE. Influenza Vaccines Delivered in Early Childhood Could Turn Antigenic Sin into Antigenic Blessings. Cold Spring Harb Perspect Med. 2020.

314. Vatti A, Monsalve DM, Pacheco Y, Chang C, Anaya JM, Gershwin ME. Original antigenic sin: A comprehensive review. J Autoimmun. 2017;83:12-21.

315. Novartis. Flucelvax Quadrivalent 2020 [Available from: https://www.flucelvax.com/flucelvax-quadrivalent.

316. Buhler S, Ramharter M. Flucelvax Tetra: a surface antigen, inactivated, influenza vaccine prepared in cell cultures. ESMO Open. 2019;4(1):e000481.

317. Moro PL, Winiecki S, Lewis P, Shimabukuro TT, Cano M. Surveillance of adverse events after the first trivalent inactivated influenza vaccine produced in mammalian cell culture (Flucelvax((R))) reported to the Vaccine Adverse Event Reporting System (VAERS), United States, 2013-2015. Vaccine. 2015;33(48):6684-8.

318. Manini I, Domnich A, Amicizia D, Rossi S, Pozzi T, Gasparini R, et al. Flucelvax (Optaflu) for seasonal influenza. Expert Rev Vaccines. 2015;14(6):789-804.

319. Lamb YN. Cell-Based Quadrivalent Inactivated Influenza Virus Vaccine (Flucelvax((R)) Tetra/Flucelvax Quadrivalent((R))): A Review in the Prevention of Influenza. Drugs. 2019;79(12):1337-48.

320. Yang H, Carney PJ, Chang JC, Guo Z, Villanueva JM, Stevens J. Structure and receptor binding preferences of recombinant human A(H3N2) virus hemagglutinins. Virology. 2015;477:18-31.

321. Monamele GC, Vernet MA, Njankouo MR, Victoir K, Akoachere JF, Anong D, et al. Genetic and antigenic characterization of influenza A(H3N2) in Cameroon during the 2014-2016 influenza seasons. PLoS One. 2017;12(9):e0184411.

322. Herve PL, Lorin V, Jouvion G, Da Costa B, Escriou N. Addition of N-glycosylation sites on the globular head of the H5 hemagglutinin induces the escape of highly pathogenic avian influenza A H5N1 viruses from vaccine-induced immunity. Virology. 2015;486:134-45.

323. Al Khatib HA, Al Thani AA, Gallouzi I, Yassine HM. Epidemiological and genetic characterization of pH1N1 and H3N2 influenza viruses circulated in MENA region during 2009-2017. BMC Infect Dis. 2019;19(1):314.

324. Abdelwhab EM, Veits J, Tauscher K, Ziller M, Grund C, Hassan MK, et al. Progressive glycosylation of the haemagglutinin of avian influenza H5N1 modulates virus replication, virulence and chicken-to-chicken transmission without significant impact on antigenic drift. J Gen Virol. 2016;97(12):3193-204.

325. Tsuchiya E, Sugawara K, Hongo S, Matsuzaki Y, Muraki Y, Nakamura K. Role of overlapping glycosylation sequons in antigenic properties, intracellular transport and biological activities of influenza A/H2N2 virus haemagglutinin. J Gen Virol. 2002;83(Pt 12):3067-74.

326. Sugawara K, Kitame F, Nishimura H, Nakamura K. Operational and topological analyses of antigenic sites on influenza C virus glycoprotein and their dependence on glycosylation. J Gen Virol. 1988;69 (Pt 3):537-47.

327. Saito T, Nakaya Y, Suzuki T, Ito R, Saito T, Saito H, et al. Antigenic alteration of influenza B virus associated with loss of a glycosylation site due to host-cell adaptation. J Med Virol. 2004;74(2):336-43.

328. Gu C, Zeng X, Song Y, Li Y, Liu L, Kawaoka Y, et al. Glycosylation and an amino acid insertion in the head of hemagglutinin independently affect the antigenic properties of H5N1 avian influenza viruses. Sci China Life Sci. 2019;62(1):76-83.

329. Basak S, Compans RW. Studies on the role of glycosylation in the functions and antigenic properties of influenza virus glycoproteins. Virology. 1983;128(1):77-91.

330. Skowronski DM, Sabaiduc S, Chambers C, Eshaghi A, Gubbay JB, Krajden M, et al. Mutations acquired during cell culture isolation may affect antigenic characterisation of influenza A(H3N2) clade 3C.2a viruses. Euro Surveill. 2016;21(3):30112.

331. Nakowitsch S, Waltenberger AM, Wressnigg N, Ferstl N, Triendl A, Kiefmann B, et al. Egg- or cell culture-derived hemagglutinin mutations impair virus stability and antigen content of inactivated influenza vaccines. Biotechnol J. 2014;9(3):405-14.

332. Bloom JD, Glassman MJ. Inferring stabilizing mutations from protein phylogenies: application to influenza hemagglutinin. PLoS Comput Biol. 2009;5(4):e1000349.

333. Phillips AM, Doud MB, Gonzalez LO, Butty VL, Lin YS, Bloom JD, et al. Enhanced ER proteostasis and temperature differentially impact the mutational tolerance of influenza hemagglutinin. Elife. 2018;7.

334. Chen W, Helenius J, Braakman I, Helenius A. Cotranslational folding and calnexin binding during glycoprotein synthesis. Proc Natl Acad Sci U S A. 1995;92(14):6229-33.

335. Daniels R, Kurowski B, Johnson AE, Hebert DN. N-linked glycans direct the cotranslational folding pathway of influenza hemagglutinin. Mol Cell. 2003;11(1):79-90.

336. Klein EY, Blumenkrantz D, Serohijos A, Shakhnovich E, Choi JM, Rodrigues JV, et al. Stability of the Influenza Virus Hemagglutinin Protein Correlates with Evolutionary Dynamics. mSphere. 2018;3(1).

337. Zell R, Krumbholz A, Wutzler P. Influenza A virus PB1-F2 gene. Emerg Infect Dis. 2006;12(10):1607-8; author reply 8-9.

338. Zaraket H, Kondo H, Hibino A, Yagami R, Odagiri T, Takemae N, et al. Full Genome Characterization of Human Influenza A/H3N2 Isolates from Asian Countries Reveals a Rare Amantadine Resistance-Conferring Mutation and Novel PB1-F2 Polymorphisms. Front Microbiol. 2016;7:262.

339. Wei P, Luo P, Li W, Zi H, Qi X, Deng F, et al. Emergence of truncated PB1-F2 protein of H3N2 influenza virus during its epidemic period in Jiangsu Province, China. Chin Med J (Engl). 2014;127(8):1487-92.

340. Pena L, Vincent AL, Loving CL, Henningson JN, Lager KM, Li W, et al. Strain-dependent effects of PB1-F2 of triple-reassortant H3N2 influenza viruses in swine. J Gen Virol. 2012;93(Pt 10):2204-14.

341. McAuley J, Deng YM, Gilbertson B, Mackenzie-Kludas C, Barr I, Brown L. Rapid evolution of the PB1-F2 virulence protein expressed by human seasonal H3N2 influenza viruses reduces inflammatory responses to infection. Virol J. 2017;14(1):162.

342. Deventhiran J, Kumar SR, Raghunath S, Leroith T, Elankumaran S. PB1-F2 Protein Does Not Impact the Virulence of Triple-Reassortant H3N2 Swine Influenza Virus in Pigs but Alters Pathogenicity and Transmission in Turkeys. J Virol. 2016;90(1):222-31.

343. Alymova IV, Green AM, van de Velde N, McAuley JL, Boyd KL, Ghoneim HE, et al. Immunopathogenic and antibacterial effects of H3N2 influenza A virus PB1-F2 map to amino acid residues 62, 75, 79, and 82. J Virol. 2011;85(23):12324-33.

344. Mazur I, Anhlan D, Mitzner D, Wixler L, Schubert U, Ludwig S. The proapoptotic influenza A virus protein PB1-F2 regulates viral polymerase activity by interaction with the PB1 protein. Cell Microbiol. 2008;10(5):1140-52.

345. Yoshizumi T, Ichinohe T, Sasaki O, Otera H, Kawabata S, Mihara K, et al. Influenza A virus protein PB1-F2 translocates into mitochondria via Tom40 channels and impairs innate immunity. Nat Commun. 2014;5:4713.

346. Yamada H, Chounan R, Higashi Y, Kurihara N, Kido H. Mitochondrial targeting sequence of the influenza A virus PB1-F2 protein and its function in mitochondria. FEBS Lett. 2004;578(3):331-6.

347. Varga ZT, Ramos I, Hai R, Schmolke M, Garcia-Sastre A, Fernandez-Sesma A, et al. The influenza virus protein PB1-F2 inhibits the induction of type I interferon at the level of the MAVS adaptor protein. PLoS Pathog. 2011;7(6):e1002067.

348. Varga ZT, Grant A, Manicassamy B, Palese P. Influenza virus protein PB1-F2 inhibits the induction of type I interferon by binding to MAVS and decreasing mitochondrial membrane potential. J Virol. 2012;86(16):8359-66.

349. Park ES, Byun YH, Park S, Jang YH, Han WR, Won J, et al. Co-degradation of interferon signaling factor DDX3 by PB1-F2 as a basis for high virulence of 1918 pandemic influenza. EMBO J. 2019;38(10).

350. Dudek SE, Wixler L, Nordhoff C, Nordmann A, Anhlan D, Wixler V, et al. The influenza virus PB1-F2 protein has interferon antagonistic activity. Biol Chem. 2011;392(12):1135-44.

351. Sakai T, Nishimura SI, Naito T, Saito M. Influenza A virus hemagglutinin and neuraminidase act as novel motile machinery. Sci Rep. 2017;7:45043.

352. Guttman M, Lee KK. Site-Specific Mapping of Sialic Acid Linkage Isomers by Ion Mobility Spectrometry. Anal Chem. 2016;88(10):5212-7.

353. Cointe D, Leroy Y, Chirat F. Determination of the sialylation level and of the ratio alpha-(2-->3)/alpha-(2-->6) sialyl linkages of N-glycans by methylation and GC/MS analysis. Carbohydr Res. 1998;311(1-2):51-9.

354. Green ED, Adelt G, Baenziger JU, Wilson S, Van Halbeek H. The asparagine-linked oligosaccharides on bovine fetuin. Structural analysis of N-glycanase-released oligosaccharides by 500-megahertz 1H NMR spectroscopy. J Biol Chem. 1988;263(34):18253-68.

355. Wu ZL, Huang X, Burton AJ, Swift KA. Probing sialoglycans on fetal bovine fetuin with azido-sugars using glycosyltransferases. Glycobiology. 2016;26(4):329-34.

356. Guzman-Aranguez A, Argueso P. Structure and biological roles of mucin-type O-glycans at the ocular surface. Ocul Surf. 2010;8(1):8-17.

357. Bergstrom KS, Xia L. Mucin-type O-glycans and their roles in intestinal homeostasis. Glycobiology. 2013;23(9):1026-37.

358. Jia N, Barclay WS, Roberts K, Yen HL, Chan RW, Lam AK, et al. Glycomic characterization of respiratory tract tissues of ferrets: implications for its use in influenza virus infection studies. J Biol Chem. 2014;289(41):28489-504.

359. Walther T, Karamanska R, Chan RW, Chan MC, Jia N, Air G, et al. Glycomic analysis of human respiratory tract tissues and correlation with influenza virus infection. PLoS Pathog. 2013;9(3):e1003223.

360. Nachbagauer R, Palese P. Is a Universal Influenza Virus Vaccine Possible? Annu Rev Med. 2020;71:315-27.

361. Roose K, Fiers W, Saelens X. Pandemic preparedness: toward a universal influenza vaccine. Drug News Perspect. 2009;22(2):80-92.

362. Crank MC, Mascola JR, Graham BS. Preparing for the Next Influenza Pandemic: The Development of a Universal Influenza Vaccine. J Infect Dis. 2019;219(Supplement_1):S107-S9.

363. Easterbrook JD, Kash JC, Sheng ZM, Qi L, Gao J, Kilbourne ED, et al. Immunization with 1976 swine H1N1- or 2009 pandemic H1N1-inactivated vaccines protects mice from a lethal 1918 influenza infection. Influenza Other Respir Viruses. 2011;5(3):198-205.

364. Weiss CD, Wang W, Lu Y, Billings M, Eick-Cost A, Couzens L, et al. Neutralizing and neuraminidase antibodies correlate with protection against influenza during a late season A/H3N2 outbreak among unvaccinated military recruits. Clin Infect Dis. 2019.

365. Fink AL, Engle K, Ursin RL, Tang WY, Klein SL. Biological sex affects vaccine efficacy and protection against influenza in mice. Proc Natl Acad Sci U S A. 2018;115(49):12477-82.

366. Potluri T, Fink AL, Sylvia KE, Dhakal S, Vermillion MS, Vom Steeg L, et al. Age-associated changes in the impact of sex steroids on influenza vaccine responses in males and females. NPJ Vaccines. 2019;4:29.

367. Vom Steeg LG, Klein SL. Sex and sex steroids impact influenza pathogenesis across the life course. Semin Immunopathol. 2019;41(2):189-94.

368. Nunez IA, Carlock MA, Allen JD, Owino SO, Moehling KK, Nowalk P, et al. Impact of age and pre-existing influenza immune responses in humans receiving split inactivated influenza vaccine on the induction of the breadth of antibodies to influenza A strains. PLoS One. 2017;12(11):e0185666.

369. Suzuki M, Saito N. Influenza Vaccine Effectiveness and Age. Clin Infect Dis. 2018;67(4):647.

370. Nachbagauer R, Salaun B, Stadlbauer D, Behzadi MA, Friel D, Rajabhathor A, et al. Pandemic influenza virus vaccines boost hemagglutinin stalk-specific antibody responses in primed adult and pediatric cohorts. NPJ Vaccines. 2019;4:51.

371. Krammer F, Palese P. Influenza virus hemagglutinin stalk-based antibodies and vaccines. Curr Opin Virol. 2013;3(5):521-30.

372. Yu L, Bloem LJ. Use of polymerase chain reaction to screen phage libraries. Methods Mol Biol. 1996;58:335-9.

373. Park HY, Kim J, Cho JH, Moon JY, Lee SJ, Yoon MY. Phage display screen for peptides that bind Bcl-2 protein. J Biomol Screen. 2011;16(1):82-9.

374. Li J, Feng L, Jiang X. In vivo phage display screen for peptide sequences that cross the blood-cerebrospinal-fluid barrier. Amino Acids. 2015;47(2):401-5.

375. Knossow M, Skehel JJ. Variation and infectivity neutralization in influenza. Immunology. 2006;119(1):1-7.

376. Von Holle TA, Moody MA. Influenza and Antibody-Dependent Cellular Cytotoxicity. Front Immunol. 2019;10:1457.

377. Valkenburg SA, Fang VJ, Leung NH, Chu DK, Ip DK, Perera RA, et al. Cross-reactive antibody-dependent cellular cytotoxicity antibodies are increased by recent infection in a household study of influenza transmission. Clin Transl Immunology. 2019;8(11):e1092.

378. Vanderven HA, Jegaskanda S, Wines BD, Hogarth PM, Carmuglia S, Rockman S, et al. Antibody-Dependent Cellular Cytotoxicity Responses to Seasonal Influenza Vaccination in Older Adults. J Infect Dis. 2017;217(1):12-23.

379. Jones JF, Segal DM. Antibody-dependent cell-mediated cytolysis (ADCC) with antibody-coated effectors: new methods for enhancing antibody binding and cytolysis. J Immunol. 1980;125(2):926-33.

Curriculum Vitae

Harrison R. Powell
434 South Patterson Park Ave Baltimore, MD 21231
Cell Phone: 978-621-0422
Email: hpowell7@jhu.edu

Education

Ph.D. in Molecular Microbiology and Immunology *Johns Hopkins University, Baltimore, MD*
Expected 4/2020
Bloomberg School of Public Health W. Harry Feinstone Department of Molecular Microbiology and Immunology. GPA 3.8
Honors and Awards: NIH T32 Grant 2016-2018, Harry J. Lawler Academic Scholarship 2016-2019

B.S. in Biology, Concentration in Neuroscience *Emmanuel College, Boston, MA* 2013
College of Arts and Science Biology Department. GPA 3.8
Honors and Awards: *cum laude*, Graduated with Distinction, Dean's list for academic achievement (2009-2013)

Academic Research

Johns Hopkins Bloomberg School of Public Health PhD Candidate, Ph.D. Candidate
2015-present

- *Dissertation:* Influenza A neuraminidase evolution impact on viral enzyme function, virus fitness, and immunity
- Identified how novel influenza variants in the human population evade human immunity
- Created new collaborations with multiple outside research labs for data acquisition and materials sharing
- Developed novel assay to test process improvement of manufacturing live attenuated influenza A vaccine
- Collaborated with Johns Hopkins Hospital clinical coordinators to mine existing data sets for patient samples
- Established and validated assays to test viral fitness of human clinical isolates of influenza A virus
- Mentored masters students in statistical data analysis, writing, and slide deck preparation and presentation

Professional Experience

Massachusetts General Hospital Transplantation Biology Research Center, Research Technician
2013-2015

- Senior research technician working with a pre-clinical model of hematopoietic stem cell and organ transplantation
- Developed novel assays to assess immunological tolerance of organ transplants in non-human primates
- Identified key biomarkers of immunological tolerance and rejection in swine model of hand and face transplant
- Assisted surgical cadaver team to pioneer new procedures to procure donor tissue at human cadaver lab
- Presented research at international plastic surgery conferences to leaders in field of reconstructive plastic surgery
- Mentored undergraduate research assistants for easy integration into the workspace and how to analyze and present research data

Merck Future Talent Program, Intern at Merck Pharmaceuticals Respiratory and Immunology R&D 2012

- Developed standard operating procedures for pre-clinical model of rheumatoid arthritis
- Identified biomarkers of disease progression in inducible model of rheumatoid arthritis
- Validated in-vivo model to screen pre-clinical small molecular compounds from synthetic libraries for bioactivity

- Presented research findings to key Merck shareholders
-

Leadership Experience

- Volunteer coach at Baltimore City ice hockey rink to mentor inner city youth on teamwork and communication through the sport of hockey. 2016-Present
- *Member at Large.* Johns Hopkins Student Assembly Social Committee officer tasked with planning student events and organizing vendors. 2016-2017
- Member of Student recruitment team for Molecular Microbiology and Immunology Program to aid in event planning and interview process. 2015 to Present
- *EMT-Basic and Training Assistant.* Mentored students on written and practical exam certification 2007-2013

Publications

Harrison R. Powell and Andrew Pekosz. 2020. Neuraminidase antigenic drift of influenza A virus H3N2 clade 3c.2a viruses alters virus replication, enzymatic activity and inhibitory antibody binding. Submitted to PLOS Pathogens. DOI 10.1101/2020.02.20.957399

Blumenkrantz D, Mehoke T, Hardick J, Shaw-Saliba K, **Powell H**, Liu H, et al. 2020. Identification of H3N2 NA and PB1-F2 genetic variants and their association with disease symptoms in the 2014-15 influenza season. bioRxiv. 2020:2020.02.20.956979.

Rebecca L. Ursin, Hsuan Liu, **Harrison R. Powell**, Jason Westerbeck, Kathryn Shaw-Saliba, Kristyn E. Sylvia, Katherine J. Fenstermacher, Tom Mehoke, Peter Thielen, Richard E. Rothman, Andrew Pekosz and Sabra L. Klein: Differential antibody recognition of H3N2 vaccine and seasonal influenza virus strains based on age, vaccine status, and gender in the 2017-18 season Submitted to Journal of Infectious Diseases

K. Shanmugarajah, H**. Powell**, D. A. Leonard, C. Mallard, A. Albritton, E. Harrington1 M. A. Randolph, E. Farkash, D. H. Sachs, J. M. Kurtz,and C. L. Cetrulo Jr.: The Effect of MHC Antigen Matching Between Donors and Recipients on Skin Tolerance of Vascularized Composite Allografts. American Journal of Transplantation doi: 10.1111/ajt.14189

David A Leonard, **Harrison Powell**, Alexander Albritton, Kumaran Shanmugarajah, Melissa Mastroianni, Sarah Lofgren, James Winter, Josef M Kurtz & Curtis L Cetrulo Jr (2015) Upper Extremity Transplantation in Non-Human Primates: An Orthotopic Model for Translational Research, Vascularized Composite Allotransplantation, doi:10.1080/23723505.2015.1072261

M. L. Madariaga, S. G. Michel, G. M. La Muraglia II, M. Sekijima, V. Villani, D. A. Leonard, **H. Powell**, J. M. Kurtz E. A. Farkash, R. B. Colvin, J. S. Allan, C. L. Cetrulo Jr, C. A. Huang, D. H. Sachs, K. Yamada, and J. C. Madsen: Kidney-induced cardiac allograft tolerance in miniature swine is dependent on MHC-matching of donor cardiac and renal parenchyma. American Journal of Transplantation doi:10.1111/ajt.13131

Presentations

Harrison Powell, Hsuan Liu and Andrew Pekosz. 07/2019. Novel neuraminidase glycosylation genotype in clade 3c.2a H3N2 2014-2015 Isolates impacts viral growth on human nasal epithelial cells and inhibitory antibody binding. American Society for Virology. Minneapolis, Minnesota Oral Presentation at 2019 Annual Meeting

Harrison Powell and Andrew Pekosz. 06/2019. Novel neuraminidase glycosylation genotype in clade 3c.2a H3N2 2014-2015 Isolates impacts viral growth on human nasal epithelial cells and inhibitory antibody binding. Oral Presentation Keynote at 2019 CEIRS Annual Meeting

Harrison Powell and Andrew Pekosz. Novel Neuraminidase Glycosylation Genotype in Clade 3c.2a H3N2 2014-2015 Isolates Impacts Viral Growth on Human Nasal Epithelial Cells, Neuraminidase Function and Inhibitory Antibody Binding. American Society for Virology. College Park, Maryland. Oral Presentation at 2018 American Society for Virology.

Harrison Powell, Deena Blumenkrantz, Hsuan Liu and Andrew Pekosz 11/2017. JH CEIRS H3N2 2014-2015 Human Surveillance: Functional significance of a new NA glycosylation site. Bergen, The Netherlands. Oral presentation. CEIRS Annual Surveillance Meeting.

Harrison Powell, Hsuan Liu, Nicholas Wohlgemuth Katherine J. Fenstermacher, and Andrew Pekosz. 06/2017. Egg Adaptation Associated Receptor Changes in Live Attenuated Influenza Virus Decrease Viral Replication in Human Nasal Epithelial Cell Cultures. American Society for Virology. Madison, WI. Poster Presentation